UNIVERSIDADE FEDERAL DE MINAS GERAIS
Escola de Engenharia
Programa de Pós-Graduação em Saneamento, Meio Ambiente e Recursos Hídricos

Flávia Cristina Rodrigues Costa

ASSESSMENT OF A HYBRID MEMBRANE DISTILLATION-LED-UV PROCESS: focus on fouling mitigation

Belo Horizonte
2021

Flávia Cristina Rodrigues Costa

ASSESSMENT OF A HYBRID MEMBRANE DISTILLATION-LED-UV PROCESS: focus on fouling mitigation

Dissertação apresentada ao Programa de Pós-Graduação em Saneamento, Meio Ambiente e Recursos Hídricos do Departamento de Engenharia Sanitária e Ambiental da Universidade Federal de Minas Gerais, como requisito parcial à obtenção do título de Mestre em Saneamento, Meio Ambiente e Recursos Hídricos.

Área de Concentração: Meio Ambiente

Linha de Pesquisa: Caracterização, prevenção e controle da poluição

Orientadora: Profª. Drª. Míriam Cristina Santos Amaral

Coorientadora: Profª. Drª. Bárbara Caroline Ricci

Belo Horizonte

2021

Costa, Flávia Cristina Rodrigues.
C837a Assessment of a hybrid membrane distillation-LED-UV process [recurso eletrônico] : focus on fouling mitigation / Flávia Cristina Rodrigues Costa. - 2021.
1 recurso online (152 f. : il., color.) : pdf.

Orientadora: Míriam Cristina Santos Amaral.
Coorientadora: Bárbara Caroline Ricci.

Dissertação (mestrado) - Universidade Federal de Minas Gerais, Escola de Engenharia.

Inclui bibliografia.

1. Engenharia sanitária - Teses. 2. Meio ambiente - Teses. 3. Biofilme - Teses. 4. Esgotos - Tratamento - Teses. I. Amaral, Míriam Cristina Santos. II. Ricci, Bárbara Caroline. III. Universidade Federal de Minas Gerais. Escola de Engenharia. IV. Título.

CDU: 628(043)

Ficha catalográfica elaborada pela bibliotecária Roseli Alves de Oliveira CRB/6 2121
Biblioteca Prof. Mário Werneck, Escola de Engenharia da UFMG

UNIVERSIDADE FEDERAL DE
MINAS GERAIS [ESCOLA DE
ENGENHARIA]
COLEGIADO DO CURSO DE GRADUAÇÃO / PÓS-GRADUAÇÃO EM
[SANEAMENTO, MEIO AMBIENTE E RECURSOS HÍDRICOS]

FOLHA DE APROVAÇÃO

["ASSESSMENT OF A HYBRID MEMBRANE DISTILLATION-LED-UV PROCESS: FOCUS ON FOULING MITIGATION "]

[Flávia Cristina Rodrigues Costa]

Dissertação de Mestrado] defendida e aprovada, no dia **[** 18 de junho de 2021**]**, pela Banca Examinadora designada pelo [Colegiado do Programa de Pós-Graduação **EM SANEAMENTO, MEIO AMBIENTE E RECURSOS HÍDRICOS**] da Universidade Federal de Minas Gerais constituída pelos seguintes professores:

[Prof. Dr. Frederico de Araujo Kronemberger**] - Membro Externo]**
[UFRJ]

[Profa. Vera Lúcia dos Santos**] - Membro Interno]**
[UFMG]

[Profa. Bárbara Caroline Ricci Nunes **- Coorientador]**
[UFMG]

[Profa. Míriam Cristina Santos Amaral Moravia **- Orientador]**
[UFMG]

APROVADA PELO COLEGIADO DO PPG SMARH

Sonaly Cristina Rezende Borges de Lima – Coordenadora

Belo Horizonte, 18 de junho de 2021.

Documento assinado eletronicamente por **Frederico de Araujo Kronemberger**, **Usuário Externo**, em 18/06/2021, às 09:48, conforme horário oficial de Brasília, com fundamento no art. 5º do Decreto nº 10.543, de 13 de novembro de 2020.

Documento assinado eletronicamente por **Miriam Cristina Santos Amaral Moravia**, **Professora do Magistério Superior**, em 17/08/2021, às 08:06, conforme horário oficial de Brasília, com fundamento no art. 5º do Decreto nº 10.543, de 13 de novembro de 2020.

Documento assinado eletronicamente por **Bárbara Caroline Ricci Nunes**, **Usuário Externo**, em 27/09/2021, às 09:36, conforme horário oficial de Brasília, com fundamento no art. 5º do Decreto nº 10.543, de 13 de novembro de 2020.

Documento assinado eletronicamente por **Eduardo Coutinho de Paula**, **Coordenador(a) de curso de pós-graduação**, em 11/12/2025, às 13:11, conforme horário oficial de Brasília, com fundamento no art. 5º do Decreto nº 10.543, de 13 de novembro de 2020.

A autenticidade deste documento pode ser conferida no site https://sei.ufmg.br/sei/controlador_externo.php?acao=documento_conferir&id_orgao_acesso_externo=0, informando o código verificador **0791143** e o código CRC **9B485BDD**.

Referência: Processo nº 23072.231731/2021-90

SEI nº 0791143

AGRADECIMENTOS

Agradeço primeiramente a Deus, pois do seu amor que foi possível o sustento em todas as dificuldades. Obrigada, Senhor, por guiar o meu caminho, por fazê-lo mais belo e por cuidar de mim através de tantas pessoas.

Agradeço de todo coração minha família: meus pais, Vicente e Sandra, aos quais dedico essa conquista; e meus irmãos, Daniel e Samuel. Obrigada por todo amor, carinho, incentivo, alegria, pela paciência e por entenderem que nem sempre pude estar presente.

Agradeço ao meu noivo, Diego, pela companhia, pelo amor, por acreditar em mim e sempre me incentivar. E por todas as ajudas logísticas e tecnológicas para a realização deste trabalho.

Agradeço aos amigos de CL, minha companhia para a vida, e a todos os amigos com os quais fui presenteada ao longo desses anos,

Agradeço a todos os professores que passaram em minha vida, que com empenho e dedicação, foram essenciais na minha trajetória.

Agradeço a minha orientadora, Profa. Dra. Míriam Amaral, por toda experiência e conhecimento compartilhados, pela condução da pesquisa, por todo o apoio, compreensão, atenção, paciência e confiança.

Agradeço a minha coorientadora, Profa. Dra. Bárbara Ricci, que caminha comigo desde a graduação, por todo conhecimento, atenção, conselhos, disponibilidade e pela amizade que foi sendo construída nesse período.

Agradeço a todos os colegas do GEAPS pelo convívio, experiências compartilhadas, ajudas e risadas. Obrigada por tornarem esse caminho mais leve e alegre.

Agradeço à UFMG, ao DESA e ao PPG SMARH pela oportunidade e recursos oferecidos para a desenvolvimento da pesquisa e para minha formação. Agradeço à CAPES pela bolsa concedida.

Agradeço à companhia de saneamento de Minas Gerais – COPASA-MG pelo fornecimento das amostras de esgoto tratado.

Agradeço ao professor Frederico e à professora Vera por gentilmente aceitarem o convite para compor a banca de avaliação deste trabalho.

Agradeço ao CEFET-MG, em especial ao Prof. Dr. Wagner Moravia, por disponibilizar o laboratório e seus recursos para a realização dos experimentos. Isso foi essencial para a realização dos ensaios de forma segura neste momento de pandemia. Meus sinceros agradecimentos. Agradeço também ao pessoal dos serviços gerais, manutenção e portaria do CEFET-MG, sempre disponíveis e solícitos.

Agradeço a PUC-MINAS, em especial ao Prof. Leonardo Mitre e a Edilene, por possibilitarem a realização das análises de MEV.

Agradeço a UFV, em especial a prof Dra. Ann Mounteer, por possibilitar as análises de YES. Também agradeço especialmente à Gemima, pelas análises e pela amizade que foi tão importante nessa caminhada.

Agradeço às minhas alunas de iniciação científica, Clarissa e Amanda, por terem abraçado o projeto com tanta dedicação.

Por fim, agradeço a todos que, de alguma maneira, foram importantes para a minha formação e para a realização dessa pesquisa. A vocês, minha sincera gratidão.

"Por vezes sentimos que aquilo que fazemos não é senão uma gota de água no mar. Mas o mar seria menor se lhe faltasse uma gota".

Madre Teresa de Calcut

RESUMO

Este estudo teve como principal objetivo a avaliação do desempenho de um módulo hibrido de destilação por membranas e LED ultravioleta (DM-LED-UV) com foco no controle da incrustação. O módulo proposto possui uma placa de quartzo no compartimento da alimentação, o que permitiu a radiação UVC atingir o concentrado e a camada de incrustação. Primeiramente, foi avaliada a performance do módulo construído no tratamento de esgoto secundário proveniente de tratamento anaeróbio. Verificou-se uma grande contribuição do fouling para a redução do fluxo de permeado. O desempenho do módulo híbrido foi similar ao desempenho da DM em termos de remoção de poluentes. Houve uma menor extensão de fouling no sistema DM-LED-UV e a camada incrustante ficou muito menos aderida à superfície da membrana, sendo facilmente removida mecanicamente. Isso foi atribuído ao maior caráter hidrofílico da camada formada no sistema híbrido, resultando em uma ligação mais fraca com a membrana hidrofóbica. Houve uma menor concentração de SMP/EPS no biofilme formado no sistema híbrido, sugerindo uma ação de inativação de microorganismos. Em seguida, foi avaliado o efeito do sistema híbrido na remoção de 17 α-Etinilestadiol (EE2). O módulo híbrido novamente teve uma performance similar à DM. O fluxo de permeado na DM-LED-UV foi maior do que na DM, apesar do maior efeito da polarização de pressão de vapor na DM-LED-UV. Não houve diferença significativa no incremento da condutividade da alimentação e do permeado dos dois testes. As eficiências de remoção de hormônios foram de 97,7 e 97,9% para DM e DM-LED-UV, respectivamente, e as remoções de efeito estrogênico de 99,2 e 99,0% para DM e DM-LED-UV, respectivamente. Assim, ao aplicar o módulo híbrido para mitigar a incrustação em DM tratando águas residuais reais e tratamento de água do mar, é improvável que a radiação diminua o desempenho do sistema em relação à remoção de micropoluentes. Por fim, foi realizada uma avaliação, por meio de uma extensa revisão da literatura, sobre a formação do biofilme na DM, suas consequências e possíveis métodos de mitigação. Concluiu-se que o biofilme na DM leva à diversos prejuízos e decaimento de performance, devendo haver esforços para mitigá-lo.

Palavras-chave: destilação assistida por membranas; led-uv; biofilme; incrustação; tratamento de esgoto; 17 α-Etinilestadiol (EE2).

ABSTRACT

The main objective of this study was to evaluate the performance of a hybrid module of membrane distillation and LED-UV (MD-LED-UV) focusing on fouling control. The newly built module has a quartz plate in the feed compartment, allowing the irradiation of the concentrate and the fouling layer. First, the module's performance in the treatment of secondary wastewater from anaerobic treatment was evaluated. There was an outstanding contribution of fouling in permeate flux decrease. The hybrid system's performance was similar to the MD's. Analysis of the membrane surfaces revealed a smaller extension of fouling in the MD-LED-UV system. The fouling layer was much less adhered to the membrane surface, being easily removed mechanically. It was attributed to the higher hydrophilic character of the layer formed in the hybrid system, resulting in a weaker bond with the hydrophobic membrane. A lower concentration of SMP/EPS in the biofilm formed in the hybrid system was observed, suggesting an inactivation action of microorganisms. Then, the effect of the hybrid system on the removal of 17 α-Ethinylstadiol (EE2) was evaluated. The hybrid module and MD had very similar performances. The permeate flux in MD-LED-UV was higher than in MD, although MD-LED-UV had a higher vapor pressure polarization effect. There was no significant difference between the increment in the feed and the permeate conductivities in both tests. However, the hormone removal efficiencies (97.7 and 97.9% for MD and MD-LED-UV, respectively) and the estrogenic effect removals (99.2 and 99.0% for MD and MD-LED-UV, respectively) were not impaired. Thus, when applying the MD-LED-UV module to mitigate fouling in real wastewater and seawater treatment, radiation is unlikely to lead to performance decline regarding micropollutants removal. Finally, a careful literature review on biofilm formation in MD, its consequences, and possible mitigation methods was carried out. It was concluded that the biofilm in MD leads to several damages and MD performance decay, and there should be efforts to mitigate it.

Keywords: membrane distillation; led-uv; biofilm; fouling; wastewater treatment; 17 α-Ethinylstadiol (EE2).

LIST OF FIGURES

Chapter 2

Chapter 3

Chapter 4

LIST OF TABLES

Chapter 2

Chapter 3

Chapter 4

TABLE OF CONTENTS

CHAPTER 1

Introduction

1 BACKGROUND AND JUSTIFICATION

While population growth is a concern as the demand for water increases, water quality has been deteriorating quickly. The annual generation of municipal wastewater has already reached 380 billion cubic meters globally (QADIR et al., 2020). Thus, water reuse becomes an attractive alternative. The planned reuse of water has been carried out around the world for years. For example, more than 200 water reuse projects are implemented in the EU with a volume of about 750 $Mm^3.yr^{-1}$. Water reuse volume in the EU is expected to be about 3,222 $Mm^3.yr^{-1}$ in 2025. In some states as Malta and Cyprus, reused water may satisfy up to 26% and 7.6% of their future water demand. The amount of reused water in the USA was approximately 3,850 $Mm^3.yr^{-1}$ in 2014. Besides, notable plenty of water reuse projects are being developed (ANGELAKIS; GIKAS, 2014).

In 2017, 21.3 mi $m^3.day^{-1}$ of domestic wastewater was generate in Brazil (approximately 246.5 $m^3.s^{-1}$) (IBGE, 2017) and almost 2 $m^3.s^{-1}$ of water was reused for direct non-potable in Brazil. It is expected to increase to 13 $m^3.s^{-1}$ by 2030 (medium-term), representing 4% of the total reused water globally. In the long term, 175 $m^3.s^{-1}$ can be achieved. It would greatly increase supply sources in the country (ANA, 2018). Aquapolo Project (SABESP/BRK Ambiental), which supplies, by contract, 650 $L.s^{-1}$ of reuse water to the Petrochemical Complex in the ABC Paulista Region (OLIVEIRA, 2016), and ETE Capivari II (SANASA) (28.9 $L.s^{-1}$ of reuse water (OBRACZKA et al., 2019)) are successful examples of reuse practice in Brazil.

Since conventional treatment processes cannot effectively remove nutrients, salts, and micropollutants (MP), it is necessary to apply advanced technologies to enable water reuse (GRANDCLÉMENT et al., 2017). Furthermore, the consequences of this kind of pollutant for health and the environment have been discussed but are not yet fully understood (REUNGOAT et al., 2009; FERNANDES et al., 2011; PARK, 2013). Thus, removing these pollutants is imperative for reuse and safe disposal since one of the main routes for MP to reach water bodies is through wastewaters (LUO et al., 2014).

Membrane distillation is a technology capable of providing 100% theoretical rejection to non-volatile compounds and has high MP rejection (SILVA et al., 2018). It has a low thermal energy requirement compared to other processes, enabling coupling to renewable energy sources or residual heat, being an alternative promising for the generation of high-quality water and pertinent to the water and energy nexus (BAKER, 2004; ALKHUDHIRI et al., 2012). Coupling

with solar energy is convenient to the Brazilian context since it has a large part of its territory in the solar belt.

However, as in other membrane separation processes, fouling formation is one of the leading causes of performance decrease. Organic fouling when treating real matrices as domestic wastewaters may be a great problem (TIJING et al., 2015). Biofouling may also be a problem. Previously, MD biofouling did not receive much attention since MD typically operates in temperatures higher than most microorganisms can survive. Then, it was thought that the consequences of the microbial community development on the surface of the MD membrane would not be so dramatic for the MD performance (GRYTA et al., 2002). However, recent studies have shown that MD conditions select the most adapted microorganisms over time. The selected organisms can form the biofilm, generating several losses to MD performance, such as flux and rejection decay, aside from reducing the membrane lifetime (BOGLER et al., 2017; LIU et al., 2019; LIU et al., 2020).

UV lamps are effective as bactericidal agents (AL-ABRI et al., 2019); have simple installation and maintenance, do not involve chemicals, and effectively mitigate biofouling (MATIN et al., 2011). Its performance is related to feed quality since water with higher turbidity limits light penetration (AL-ABRI et al., 2019). UV radiation reduces EPS in fouling, promotes thinner biofilms, and more limited microbial diversity (MARCONNET et al., 201).

Thus, the construction of a hybrid MD module coupled to the LED-UV is an opportunity for mitigating organic and biological fouling. The use of LED-UV is in line with the national (BRASIL, 2018) and the worldwide trend of reducing the use of mercury lamps, since these, among other disadvantages, generate hazardous waste and have a shorter lifetime (MATAFONOVA; BATOEV, 2018). Thus, the development of a hybrid MD-LED-UV module, whose evaluation was not found in the literature, appears as a promising alternative for pos-treating domestic effluent from secondary treatment, enabling water reuse.

Therefore, the present work contributes to the scientific and technological development of fouling control strategies that can be applied in MD and other already consolidated membrane processes. It is also a contribution to expanding the horizons of membranes technologies applications. Given the problem of water and energy, it is expected that this study may contribute to the development of technologies that promote greater social and environmental security.

2 OBJECTIVES

1.1 General objective

This study aimed to develop a hybrid membrane distillation and LED-UV module and to investigate its performance in terms of fouling control and pollutant removal.

1.2 Specific objectives

1) To develop a hybrid MD-LED-UV module;
2) To evaluate the efficiency of the MD-LED-UV system in treating secondary wastewater and in the fouling control;
3) To evaluate the removal of EE2 in the hybrid MD-LED-UV system;
4) To carry out a study concerning biofouling in MD membranes by conducting an in-depth literature review.

3 DOCUMENT STRUCTURE

For a better organization of the work developed, this document has been divided into five chapters, namely:

i. Chapter 1- Introduction
ii. Chapter 2 – Assessment of a new Hybrid Membrane Distillation-LED-UV System Treating Secondary Wastewater: Focusing on Fouling Control
iii. Chapter 3 –Removal of 17α-ethinylestradiol and Estrogenicic Activity by a Novel Hybrid Membrane Distillation-LED-UV System
iv. Chapter 4 - Biofouling in Membrane Distillation
v. Chapter 5 – Final Considerations

The first chapter presents a brief background on the dissertation theme, contextualizing the biofilm problem in MD. It also presents the objectives of this study and the justifications that demonstrate the relevance of the study. Chapter 2 presents the evaluation of the performance of the MD-LED-UV coupling, investigating the system in the treatment of secondary wastewater, focusing on fouling mitigation. During this stage of the study, it was perceived the need to assess whether the coupling with the LED-UV causes damage to the membrane surface in the first moment of the operation, while it is not yet covered by fouling, which could lead to less rejection of micropollutants. Thus, in Chapter 3, the evaluation of the MD-LED-UV coupling performance in micropollutants removal is done. Investigation on the removal of 17α-ethinylestradiol and its estrogenic effect was chosen for the study. The second and third chapters refer to specific objectives 2 and 3, respectively.

In order to understand if it is worth conducting more profound studies regarding the performance of the hybrid module in the specific mitigation of biofouling, Chapter 4 provides a comprehensive literature review on what is known at the time concerning MD biofouling, addressing: (1) what a biofilm is, its biotic and abiotic components, its development stages, with a focus on MD, and the role of the microbial community succession in the MD biofilm development; (2) how MD operational factors affect the biofouling formation; (3) consequences of biofilm for MD performance; (4) possibilities of mitigating biofouling in MD; (5) conclusion by highlighting the gaps, indicating possible directions for future efforts. This chapter refers to specific objective 4. Finally, in Chapter V, the main conclusions of the previous chapters are presented in an integrative approach to this research's conclusions and recommendations.

REFERENCES

AL-ABRI, M.; AL-GHAFRI, B.; BORA, T.; DOBRETSOV, S.; DUTTA, J.; CASTELLETTO, S.; ROSA, L.; BORETTI, A. Chlorination disadvantages and alternative routes for biofouling control in reverse osmosis desalination. *Npj Clean Water*, v. 2, 2019.

ALKHUDHIRI, A.; DARWISH, N.; HILAL, N. Membrane distillation : A comprehensive review. *Desalination*, v. 287, p. 2–18, 2012.

ANA - Agência Nacional de Águas. (2018). Conjuntura dos recursos hídricos no Brasil: informe 2018. Ed. Brasília.

ANGELAKIS, A. N.; GIKAS, P. Water reuse: overview of current practices and trends in the world with emphasis on EU states. *Water Utility Journal*, v. 8, n. 67, p. e78, 2014.

BAKER, R.W. *Membrane technology and applications.* John Wiley & Sons, 2012.

BOGLER, A.; BAR-ZEEV, E. Membrane distillation biofouling : Impact of feed water temperature on biofilm characteristics and membrane performance Membrane distillation biofouling : Impact of feed water temperature on biofilm character. *Environmental science & technology*, v. 52, n. 17, p. 10019-10029, 2018.

BRASIL. Decreto n. 9.470, de 14 de ago. de 2018. Promulgação da Convenção de Minamata sobre Mercúrio, firmada pela República Federativa do Brasil, em Kumamoto, em 10 de outubro de 2013., Brasília,DF, ago 2018.

FERNANDES, A. N; GIOVANELA, M.; ALMEIDA, C. A. P; ESTEVES, V. I.; SIERRA, M. M. D.; GRASSI, M. T.. Remoção dos hormônios 17β-estradiol e 17α-etinilestradiol de soluções aquosas empregando turfa decomposta como material adsorvente. *Química Nova*, v. 34, n. 9, p.1526-1533, 4 abr. 2011.

GRANDCLÉMENT, C.; SEYSSIECQ, I.; PIRAM, A.; WONG-WAH-CHUNG, P.; VANOT, G.; TILIACOS, N.; ROCHE, N.; DOUMENQ, P. From the conventional biological wastewater treatment to hybrid processes, the evaluation of organic micropollutant removal: A review. *Water Research*, v. 111, p. 297–317, 2017.

GRYTA, M. The assessment of microorganism growth in the membrane distillation system, *Desalination*, v. 142, p. 79–88, 2002.

GWI (Global Water Intelligence). Municipal water reuse markets 2010. Oxford, UK: Media Analytics Ltd1 2009.

IBGE. Pesquisa Nacional de Saneamento Básico 2017. Instituto Nacional de Geografia e Estatística, 2017. Available in: <https://www.ibge.gov.br/estatisticas/multidominio/meio-ambiente/9073-pesquisa-nacional-de-saneamento-basico.html?=&t=o-que-e>. Accessed 08/10/2021.

LIU, C.; CHEN, L.; ZHU, L.; WU, Z.; HU, Q.; PAN, M. The effect of feed temperature on biofouling development on the MD membrane and its relationship with membrane performance : An especial attention to the microbial community succession. *Journal of Membrane Science*, v. 573, p. 377–392, 2019.

LIU, C.; ZHU, L.; CHEN, L. Effect of salt and metal accumulation on performance of membrane distillation system and microbial community succession in membrane biofilms. *Water Research*, v. 177, p.115805, 2020.

LUO, Y.; GUO, W.; NGO, H. H.; NGHIEM, L. D.; HAI, F. I.; ZHANG, J.; LIANG, S.; WANG, X. C. A review on the occurrence of micropollutants in the aquatic environment and their fate and removal during wastewater treatment. Science of the total environment, 473, 619-641.MANSOURI, J.; CHEN, V. Strategies for controlling biofouling in membrane filtration systems : challenges and opportunities. *Journal of Materials Chemistry*, p. 4567–4586, 2014.

MARCONNET, C.; HOUARI, A.; SEYER, D.; DJAFER, M.; CORITON, G.; HEIM, V.; MARTINO, P. Di. Membrane biofouling control by UV irradiation. *Desalination*, v. 276, p. 75–81, 2011.

MATAFONOVA, G.; BATOEV, V. Recent advances in application of UV light-emitting diodes for degrading organic pollutants in water through advanced oxidation processes : A review. *Water Research*, v. 132, p. 177–189, 2018.

MATIN, A.; KHAN, Z.; ZAIDI, S.M.J.; BOYCE, M.C. Biofouling in reverse osmosis membranes for seawater desalination: Phenomena and prevention, *Desalination*, v. 281, p. 1–16, 2011.

OBRACZKA, M.; SILVA, D.; CAMPOS, A.; MURICY, B. Reuso de efluentes de tratamento secundário como alternativa de fonte de abastecimento de água no município do Rio de Janeiro. *Sistemas & Gestão*, v. 14(3), p. 291-309, 2019.

OLIVEIRA, Sheila. Membranas filtrantes – Estudo de caso Aquapolo, In XI Seminário Estadual de Saneamento e Meio Ambiente, ABES-ES, Espírito Santo, 2016.

PARK, Jun-beom. Effects of 17-α ethynyl estradiol on proliferation, differentiation & mineralization of osteoprecursor cells. *Indian Journal Of Medical Research*, v. 136, n. 3, p. 466, 2012.

QADIR, M.; DRECHSEL P.; CISNEROS B.J.; KIM, Y. A.Pramanik, P.Mehta, O.Olaniyan, Global and regional potential of wastewater as a water, nutrient and energy source, in Natural Resources Forum, Blackwell Publishing Ltd, Oxford, 40-51, 2020.

REUNGOAT, J.; MACOVÁ, M.; ESCHER, B. I.; CARSWELL, S.; MUELLER, J.; KELLER, J. Removal of micropollutants and reduction of biological activity in a full scale reclamation plant using ozonation and activated carbon filtration. *Water Research*, Coopers Plains, v. 44, n. 2, p.625-637, 1 out. 2009.

SILVA, T. L.; MORALES-TORRES, S.; ESTEVES, C. M.; RIBEIRO, A. R.; NUNES, O. C.; FIGUEIREDO, J. L.; SILVA, A. M. Desalination and removal of organic micropollutants and microorganisms by membrane distillation. Desalination, 437, 121-132, 2018.

TIJING, L.D.; WOO, Y.C.; CHOI, J.-S.; LEE, S.; KIM, S.-H.; SHON, H. K. Fouling and its control in membrane distillation - A review. *Journal of Membrane Science*, v. 475, p. 215-244, 2015.

CHAPTER 2

Assessment of a new Hybrid Membrane Distillation-LED-UV System Treating Secondary Wastewater: Focusing on Fouling Control

1 INTRODUCTION

Water quality has been deteriorating quickly due to human activities. Besides, population growth is a concern as the demand for water increases. In this context, it is relevant to consider alternative treatments that guarantee high-quality water to meet human needs. Desalination processes are interesting, as more than 95% of the world's water is in the seas or oceans. However, the annual generation of municipal wastewater has already reached 380 billion cubic meters globally, and an increase of 24% is expected by 2030 (QADIR et al., 2020). Thus, effluents' reuse becomes an attractive option, as it is a more viable technique for non-coastal areas and avoids more contamination of aquatic environments (SHANNON et al., 2008).

In this context, several technologies have been studied for the effective treatment of water. Among advanced technologies, membrane separation processes (PSM) have become cost-competitive with traditional treatment processes, as they provide high separation efficiency and are suitable for various applications. Among PSM, membrane distillation (MD) is a technology that enables sustainable water production. MD is a thermally driven separation process, in which a hydrophobic microporous membrane separates a hot phase (feed) from a cold phase (permeate), causing a temperature gradient across the membrane and inducing the formation of a gradient vapor pressure between the two phases (BAKER, 2004; ALKHUDHIRI et al., 2012). Typically, a temperature difference between the feed and the permeate of 10 to 20ºC can promote the steam's permeation. Thus, MD is a promising technology for the water nexus, as it is capable of promoting the reuse of wastewater; and for the energy nexus, as it operates at low temperatures, which allows it to be coupled to renewable energy sources or residual heat available in industries (ALKHUDHIRI et al., 2012). The possibility of coupling with solar energy is convenient to the Brazilian context since the country has a large part of its territory in the so-called solar belt, with the potential to generate 2,281 $KWh.m^{-2}.year^{-1}$ (PEREIRA et al., 2017).

Due to the MD membrane's hydrophobic character, only volatile substances can permeate the pores, making the process have 100% theoretical rejection of non-volatile contaminants. DM is also more resistant to concentration polarization than other PSM, an advantage to treat high salinity solutions (LAWSON et al., 1997). Besides, the operation is carried out without the application of hydraulic pressure, which increases the safety of the system and reduces equipment costs when compared to other PSMs such as reverse osmosis (RO) and nanofiltration (NF) (MANNA; PAL, 2016).

Like other PSM, MD is subject to fouling. It consists of the deposition of unwanted material on the membrane surface and leads to the deterioration of the MD's performance (WARSINGER et al., 2014). MD is susceptible to all fouling types: inorganic, organic, and biological (TIJING et al., 2015). Several authors have investigated inorganic and organic fouling in MD, its mechanisms, and control techniques (GRYTA, 2009; ZHANG et al., 2015; NAIDU et al., 2015). The biofilm formation, which has proven to be one of the most difficult fouling types to control, has recently gained prominence. Biofouling is formed due to the deposition, growth, and execution of microorganisms' metabolic activity on the membrane. The microorganisms secrete a polymeric matrix forming a complex layer covering the membrane, making the bacteria in a biofilm more protected than isolated organisms (MANSOURI et al., 2010).

MD biofouling consequences were noticed over time. Biofouling significantly decreases vapor pressure, increases temperature polarization, provides additional resistance to heat and mass transfer (GOH et al., 2013), and facilitates pore wetting. Therefore, there is a reduction in the permeate flux and quality (MANSOURI et al., 2010), increasing energy demand. Recently, some researchers have studied biofouling in MD (BOGLER et al., 2018; LIU et al., 2019; LIU et al., 2020b).

When treating wastewater, the main concern must be with organic and biological fouling. MD fouling depends on many factors as foulant and microorganisms features (as concentration, size, hydrophobicity, and charge); membrane characteristics (as hydrophobicity, pore size, surface charges); operational conditions (as temperature, flux, flow velocity); and feed properties (CHOUDHURY et al., 2019). In seconds, inorganic and organic compounds, such as proteins and polysaccharides present in the feed, attach to the membrane surface. This primary organic fouling layer forms a conditioning film (TIJING et al., 2015) that favors the attachment of the pioneering microorganisms (JIANG et al., 2019). After that, the fouling layer will develop over the operation under the conditions mentioned above.

Thus, it is necessary to investigate methods to control fouling and biofouling for better MD performance. To date, most studies with MD have focused on chemical modifications in the membrane, such as the introduction of silver nanoparticles (NTHUNYA et al., 2020); and the coupling of these modifications with other techniques, such as the introduction of air (WARSINGER et al., 2015). Although there is evidence that chemical modifications can mitigate fouling, many of the techniques are complex, time-consuming, and expensive (WANG et al., 2019). Also, the consequences for the environment and health of these nanoparticles are not fully known (BATLEY et al., 2013).

The inactivation of bacterial metabolism using biocides, such as chlorine and ozone, is the main method of biofouling control used in PSM. Oxidizing biocides generate reactive oxygen species (SWARAJ et al., 2013) and chemicals and these species affect the cell membrane (FAN et al., 2013), metabolic pathway enzymes (VELÁSQUEZ et al., 2017), and DNA structures (CHO et al., 2010). However, chlorine can damage polymeric membranes. Chlorination also forms carcinogenic by-products, such as trihalomethanes (AL-ABRI et al., 2019). The effect of ozone on MD fouling mitigation was studied in a hybrid catalytic ozonation membrane reactor. While in the MD test, the flux decreased 39.6% due to organic fouling, in the hybrid system, the reduction was 9.5% (ZHANG et al., 2016). However, as disadvantages, it is necessary to generate ozone in situ, it can damage the membrane surface (MATIN et al., 2011), and as higher temperatures decrease the ozone solubility (AL-ABRI et al., 2019), the efficiency of the process can be compromised coupled with MD.

Another technique is using UV lamps, which is effective as a bactericide (AL-ABRI et al., 2019); has simple installation and maintenance; and does not involve chemicals (MATIN et al., 2011). UV radiation penetrates the cell and damages the genetic material. Its efficiency is related to feed quality since water with higher turbidity limits light penetration (AL-ABRI et al., 2019). UV treatment reduces the amount of extracellular polymeric substances (EPS) on the membrane surface, favors the formation of thinner biofilms with less cell density and less microbial diversity. The coupling of UV irradiation with PSM can be done as pretreatment with irradiation (MARCONNET et al., 2011) or in a hybrid way (GUO et al., 2015). Marconnet et al. (2011) proposed a UV and NF irradiation treatment, focusing on biofouling control. With irradiation, a slight decrease in fouling extension was observed, in addition to a smaller decrease in the permeate flux Mofidi et al. (2000) carried out a pilot-scale study of the effect of introducing an irradiation step with a mercury lamp in the control of RO membrane fouling. It was observed that the adherence to the membrane of the irradiated bacteria decreased by 50%, which promoted the reduction of fouling and greater permeate flux.

The disadvantage of UV pre-treatment is that it has no residual effect. Therefore, microorganisms can develop again if the time between UV treatment and permeation is long and if some bacteria receive a radiation dose below that necessary for inactivation (MARCONNET et al., 2011). The hybrid system can overcome this risk through direct irradiation of the membrane. Another advantage of the hybrid system is the greater robustness to reach microorganisms when the treated matrix has high turbidity (GUO et al., 2015). Although there are studies on UV-MD radiation modules, they have been used for other

applications, such as photocatalytic membrane regeneration (GUO et al., 2019). Therefore, it is still necessary to evaluate the mitigation of biofilm by UV and investigate whether the membrane's integrity is impaired.

In water and effluent treatment studies by irradiated processes, mercury radiation sources are usually used (MATAFONOVA; BATOEV, 2018). However, these lamps have disadvantages, such as the risk of mercury exposure, the high energy demand for the operation, and a relatively short lifetime, around 100 to 1000 hours (BOTON; COTTON, 2011; JO; TAYADE, 2014). Also, 128 countries have signed the Minamata Convention on Mercury, which aims to promote the gradual elimination of the use of mercury sources in processes and products (MATAFONOVA; BATOEV, 2018). In Brazil, the Convention was promulgated through Decree No. 9,470 of August 14, 2018, causing the Minamata Convention to enter into force in the national territory (BRASIL, 2018).

In this context, the light-emitting diode (LED) is an alternative radiation source studied for various environmental applications lately. It has several advantages over mercury lamps, such as greater environmental safety; greater robustness; immediate activation, since no previous heating is necessary; less toxic components; and longer lifetime (JO; TAYADE, 2014). LEDs have been explored to control fouling in the study by Lee et al. (2019). They evaluated fouling mitigation in ultrafiltration caused by organic matter by oxidation with persulfate/LED-UV. With UV radiation alone, an increase in permeate flux of 32.9% has already been obtained, against an improvement of 34.9% promoted by the persulfate/UV system. Sperler et al. (2020) evaluated the performance of a LED-UVC-RO system for biofilm control and found a 15% delay in biofilm formation. However, no studies have been found to assess the performance of coupling UV-LEDs and MD to mitigate fouling. Thus, this study aims to investigate the performance of a new hybrid module for membrane distillation and UV-LED in the post-treatment of wastewater, focusing on fouling control.

2 MATERIALS AND METHODS

2.1 Experimental apparatus

The system scheme used in the study is shown in Fig 2.1. The experimental apparatus consists of: a feed tank; a heat exchanger automatically activated by a thermostat controller (MT520E fast, Full Gauge Controls, Canoas, Brazil); a distillate tank; a chiller (Chiller Gelaqua 1/8 hp., Santos, Brazil); a digital scale (L10001, BEL Engineering, Monza, Italy); the hybrid module; four thermometers inserted at the module inlets and outlets (TD08, Tecmak, Belo Horizonte, Brazil); and four diaphragm pumps (SFDP1-012-035-21, Seaflo, Fujian Liancheng County, China) coupled with circulation speed controllers to recirculate, feed, distillate, and both heating and cooling water. The scale was connected to a computer for automatic monitoring of the distillate mass variation. The feed temperature was set at 40ºC to favor microbial growth and relative community stability (LIU et al., 2019).

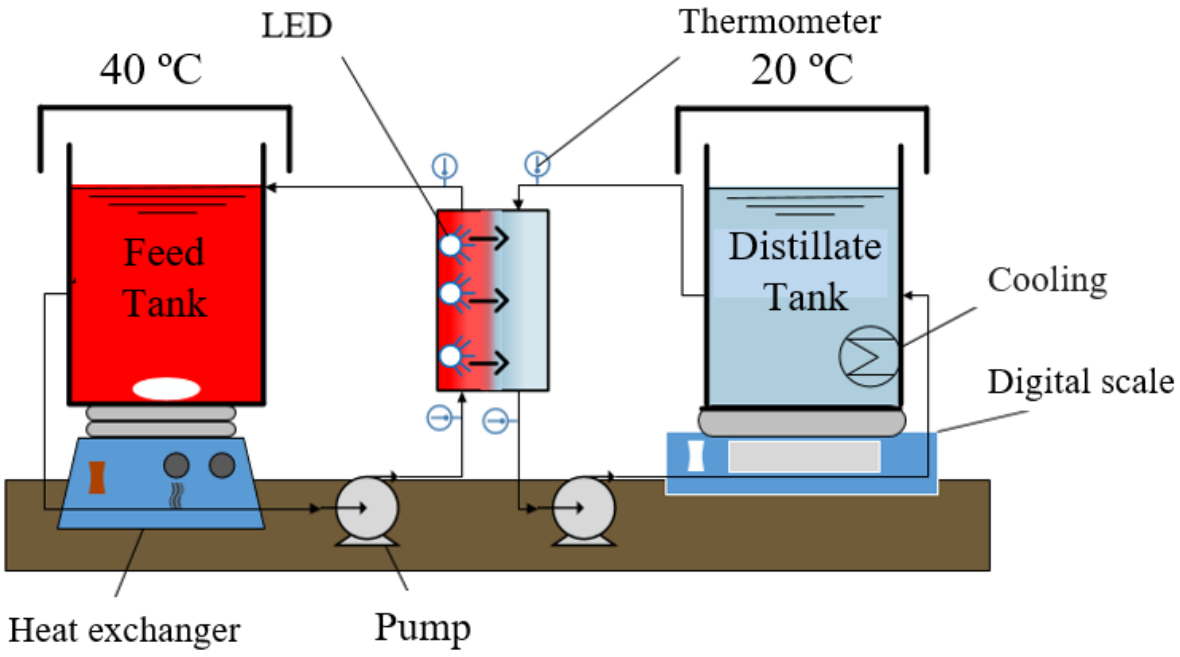

Fig. 2. 1 - Scheme of the experimental apparatus used in all tests

2.1.1 Hybrid MD-LED-UV module

The hybrid MD-LED-UV module was manufactured in acrylic in the DCMD configuration. It has a window in the feed compartment in which a quartz plate was fitted, as shown in Fig 3.2. Quartz is necessary to prevent emitted radiation absorption and allow it to reach both fouling

and solution. Thus, treated wastewater (described in 2.2), previously heated, is recirculated in the feed compartment, where the LED can be coupled so that UV irradiation occurs. In this same compartment, water vapor will permeate the hydrophobic membrane's pores due to the temperature gradient.

The flat-sheet MD membrane was obtained from Sterlitech Corporation (Kent, USA) and was made of polytetrafluoroethylene (PTFE) in non-woven polypropylene. It has an average pore size of 0.2 μm. The effective membrane area was 89.25 cm^2. The quartz plate area and, therefore, the effective irradiation area was 24.4 cm^2. The UVC-LED wavelength range is 260-280 nm, and it is the 59S brand, model X1.

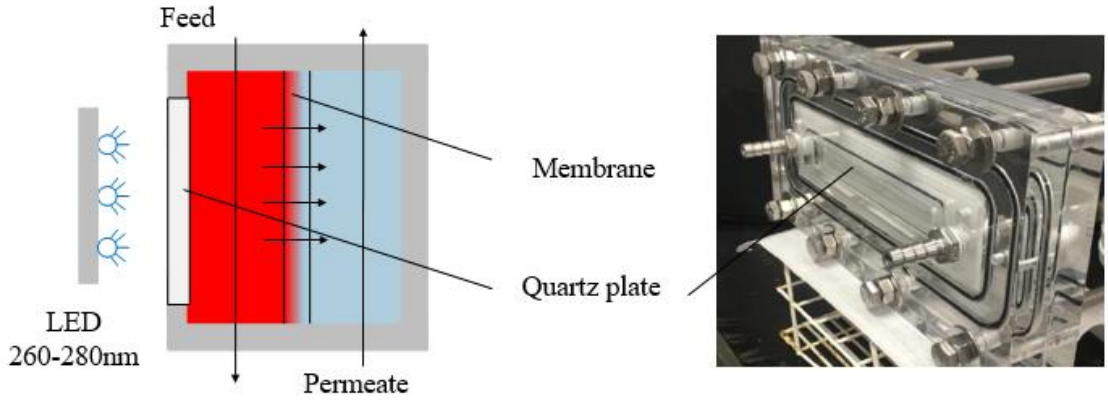

Fig. 2. 2 - On the left, the MD-LED-UV hybrid module (Top view). On the right, a photo of the built module.

2.2 Wastewater feed

The domestic wastewater used to feed the hybrid module in all experiments performed in this chapter was collected at the wastewater treatment plant (WWTP) Onça, in the metropolitan region of Belo Horizonte, Minas Gerais. This WWTP treats the Belo Horizonte municipal wastewater at a flow of 1.8 $m^3.s^{-1}$. Treatment comprises a preliminary stage involving screens and grit chambers, upflow anaerobic sludge blanket (UASB) reactors, trickling filters, and secondary sedimentation. Sampling was done at the WWTP's outlet, and in this work, it will be referred to as "secondary wastewater". The physicochemical characterization of the secondary wastewater is presented in Table 3.1. The sample was maintained refrigerated at 4°C until use.

Table 2. 1 - Physicochemical characterization of the secondary wastewater feed from MD and MD-LED-UV tests

Parameter	**Value**	
	MD	MD-LED-UV
pH	7.8 ± 0.1	7.7 ± 0.1
Electrical conductivity ($\mu S.cm^{-1}$)	1596 ± 13	1518 ± 50
Chemical oxygen demand (COD) ($mg.L^{-1}$)	150 ± 13	163 ± 11
Total suspended solids (TSS) ($mg.L^{-1}$)	18.6 ± 0.5	15.4 ± 4.1
Turbity (NTU)	15.9 ± 1.6	9.0 ± 0.3
Color (uH)	338 ± 9	347 ± 18
$N\text{-}NH_4^+$ ($mg.L^{-1}$)	93.0 ± 3.2	82.3 ± 1.1
NO_2^- ($mg.L^{-1}$)	Nd*	8.640 ± 0.006
NO_3^- ($mg.L^{-1}$)	0.6 ± 0.1	0.5 ± 0.2
$P\text{-}PO_4^{-3}$ ($mg.L^{-1}$)	12.2 ± 0.2	6.4 ± 0.1

*Nd: Not detected

In the context of MD and LED-UV coupling to treat secondary wastewater, the high concentration of suspended solids and turbidity can be a challenge for mitigating biofilm; however, it is known that the efficiency of disinfection of secondary wastewater with SST above 30 $mg.L^{-1}$ is compromised (EPA, 2006). Besides, it is expected that the irradiation in the developed hybrid module can promote a more effective inactivation of the microorganisms present in the biofilm with a higher dose of radiation (GUO et al., 2015).

2.3 Experimental procedure

Two MD experiments were carried out using the secondary wastewater as feed for 260 hours - without (referenced here as "MD teste") and with the coupling with the LED-UV (referenced as "MD-LED-UV test"). In MD test, MD was operated in closed system mode until approximately 66% recovery was obtained. Then, the system was supplied with secondary wastewater to maintain this recovery rate. The MD-LED-UV test was carried out with the activation of the LED-UV with an Arduino microcontroller, that automatically activated the LED. For every 3.5 min of irradiation, the LED remained off for 1.5 min, totaling 182 hours of radiation during the experiment. The study was conducted with periods without irradiation since it was previously evaluated that the performance of LED-UV for degradation of organic compounds and inactivation of microorganisms is similar under continuous irradiation and

pulse irradiation. In addition, with inactive periods, the LED's overheating or even its burning out is avoided, increasing its useful life and avoiding energy expenditure (LIANG et al., 2019; SONG et al., 2019).

In all experiments, the initial distillate was 3.5 L of distilled water. The recirculating flow rates for feed and distillate were 1.25 L min^{-1} (a cross-flow velocity of 47.2 $cm.s^{-1}$), indicating a laminar flow regime (Re ≅ 700). All tests were conducted under atmospheric pressure. The heating and cooling systems were adjusted to maintain approximately 40 and 20ºC in the feed and permeate. Periodically, the conductivity and temperature of the feed and distillate tanks were monitored. The feed and distillate temperature in the module outlet were also registered. The distillate weight variations were regularly recorded to calculate MD flux.

Before all tests, after the membrane was removed for further analysis, the system was cleaned by successively recirculating the following solutions for 30 min each: 10% hypochlorite solution, 5 mM EDTA solution at pH = 9, and 90% ethanol solution. Between each cleaning solution, distilled water was recirculated for 5 min. Finally, distilled water was recirculated 5 times for 5 min (BOGLER et al., 2018; ZODROW et al., 2014).

2.4 Analytical methods

The wastewater, concentrate, and distillate samples were characterized by the quantification of COD (5220 D), total suspended solids (2540 D), color (2120 C), turbidity (2130 B, Hach 2100Q turbidimeter), TOC (5310 B, TOC-VCPN, Shimadzu, Kyoto, Japan), electrical conductivity (2510, HI763100 Hanna Instruments conductivity meter), and pH (4500-H^+ B, MS TECNOPON mPA210 pH meter) in accordance with the Standard Methods for the Examination of Water and Wastewater. The analyzes of nitrite (LR, method 8507), nitrate (MR, method 8171), ammoniacal nitrogen (method 8038), and phosphate (method 8048) were performed with kits from Hach and the spectrophotometer Hach DR3900.

2.4.1 Fouling evaluation

The membrane samples from the irradiated area were cut into previously determined dimensions and sonicated to evaluate fouling. Then the fouling layer was gently scraped and diluted in a known volume of distilled water. This fouling solution was evaluated in terms of COD according to the methodology previously described.

To evaluate the soluble microbial products (SMP) and total extracellular polymeric substances (EPS) present in fouling samples, membrane samples were collected at the modules' inlet and outlet. They were extracted with the following steps: the samples of fouling solution were centrifuged at 4500 rpm for 10 min. The supernatants (SMP) were removed and separated. To extract the EPS, the sedimented material was resuspended in 50 mL of 0.05% NaCl solution and subsequently heated in a water bath until it reached 80 °C, a temperature maintained for 10 min (HE et al., 2017). The solution was centrifuged at 4500 rpm for 10 min, and the supernatant (EPS) was removed and separated. The supernatants of SMP and EPS were filtered (0.45 μm membranes) and characterized concerning proteins (LOWRY et al., 1951).

Membrane samples were also analyzed by Scanning Electron Microscopy (SEM), Dispersive Energy Spectroscopy (EDS), Fourier Transform Infrared Spectroscopy (FTIR), and Contact angle (AC). The heterotrophic plate count analysis was carried out to evaluate alive heterotrophic bacteria in the biofilm according to the Standard Methods for the Examination of Water and Wastewater.

2.5 Calculus

The MD permeate flux (J) was calculated by Eq 2.1

$$J = \frac{M_t - M_{t,i}}{A \times t} \quad (2.1)$$

Where J is given in $Kg.h^{-1}m^{-2}$, M_t is the mass of the permeate tank (Kg) at time t (h), $M_{t,i}$ is the initial mass of the permeate tank, and A is the effective area of the membrane (m^2).

The overall removal efficiency of the evaluated parameters (R) was calculated using equation 2.2.

$$R\ (\%) = \frac{C_f - C_p}{C_f} \times 100\% \quad (2.2)$$

Where C_f is the concentration of the compound present in the initial feed and C_p is the concentration of the compound that permeated the membrane, considering the mass of the compound and the volume of water that permeated it.

2.5.1 Temperature polarization

Temperature polarization was assessed in accordance with Srisurichan et al. (2006). Heat transfer is divided: (i) in convective heat transfer, which occurs from the bulk heated feed to the membrane surface boundary layer at the feed side (Eq. 2.3), (ii) conduction and latent heat transfer across membrane pores (Eq. 2.4) and convective heat transfer from the membrane surface boundary layer at the permeate side to the bulk permeate (Eq. 2.5).

$$Q = h_f\ (T_f - T_1) \tag{2.3}$$

Where Q is the heat flux; h_f is the heat transfer coefficient in the boundary layer at the feed side; T_f is the mean of the temperatures at the feed inlet and outlet of the module, considered as the MD feed bulk temperature; and T_1 is the temperature at the feed membrane surface.

$$Q = J\Delta H_v + \frac{k_T}{\delta}\ (T_1 - T_2) \tag{2.4}$$

Where ΔHv is the vaporization heat of water (2456 kJ.Kg^{-1} at 20 °C (RICCI et al., 2019)); k_T is the membrane thermal conductivity, calculated according to Ricci et al. (2019) and equals to 90.4 kW.m^{-1}.K^{-1}; δ is the membrane thickness (170 μm (MANAWI et al., 2014)); and T_2 is the temperature in the membrane surface at the permeate side.

$$Q = h_p\ (T_2 - T_p) \tag{2.5}$$

Where h_P is the heat transfer coefficient in the permeate boundary, and TP is the mean of the temperatures measured at the cold entrance and the cold exit of the module, considered as the MD permeate bulk temperature.

h_f and h_p were calculated with Eq. 2.6.

$$h = \frac{Nu\ k_f}{L} \tag{2.6}$$

Where k_f is the fluid thermal conductivity, L is the characteristic length, and Nu is the dimensionless Nusselt number, calculated with the Graetz-Lévêque Equation (Eq. 2.7) for laminar flux.

$$Nu = 1.86\ (Re\ \mathrm{Pr}\ \frac{d_h}{L_c})^{0.33} \tag{2.7}$$

Where d_h is the hydraulic diameter, L_c is the channel length, Re is the Reynolds number (Eq 2.8), and Pr is the Prandtl number (Eq 2.9).

$$Re = \frac{d_h \nu \rho}{\mu} \tag{2.8}$$

$$Pr = \frac{C_p \mu}{k_f} \tag{2.9}$$

Where ν, ρ, μ, and C_p are, respectively, the average fluid velocity, density, dynamic viscosity, and heat capacity.

From equations 2.3, 2.4, and 2.5, and heat balance, temperatures at the membranes' surface can be determined with Eq. (2.10) and (2.11).

$$T_1 = \frac{\frac{k_T}{\delta}\left[T_P + \left(\frac{h_f}{h_P}\right)T_F\right] + h_f T_f - J\Delta H_v}{\frac{k_T}{\delta} + h_f\left[1 + \left(\frac{k_T}{\delta h_f}\right)\right]} \tag{2.10}$$

$$T_2 = \frac{\frac{k_T}{\delta}\left[T_f + \left(\frac{h_P}{h_f}\right)T_P\right] + h_P T_P + J\Delta H_v}{\frac{k_T}{\delta} + h_P\left[1 + \left(\frac{k_T}{\delta h_{Af}}\right)\right]} \tag{2.11}$$

Finally, the temperature polarization coefficient (τ) was calculated by Eq. 2.12

$$\tau = \frac{T_1 - T_2}{T_f - T_p} \tag{2.12}$$

2.6.2 Concentration polarization

Concentration polarization occurs when concentration at the membrane surface at the feed side ($C_{m,f}$) is higher than the concentration in bulk ($C_{b,f}$). Both concentrations are related by the Nernst film model (RASTOGI et al., 2015) (Eq. 2.13).

$$C_{m,f} = C_{b,f}\, exp\left(\frac{J}{K_m}\right) \tag{2.13}$$

Where Km is the solute coefficient of mass transfer, estimated through Eq. 2.16, with Sherwood (Sh) (Eq. 2.14) and Schmidt (Sc) numbers (Eq. 2.15).

$$Sh = 1.86\left(Re\, Sc \frac{d_h}{L_c}\right)^{0.33} \tag{2.14}$$

$$Sc = \frac{\mu}{\rho D_T} \quad (2.15)$$

$$k_m = \frac{Sh\, D_T}{d_h} \quad (2.16)$$

The coefficient of concentration polarization (ζ) was obtained through Eq. 2.17.

$$\zeta = \frac{C_{m,f}}{C_{b,f}} \quad (2.17)$$

2.6.3 Vapor pressure polarization

The temperature polarization coefficient (ψ) is given by equation 2.18 and represents the fraction of the applied vapor pressure that effectively promotes permeation.

$$\psi = \frac{\Delta P_m}{\Delta P_b} \quad (2.18)$$

Where ΔP_m e ΔP_b are, respectively, the difference in vapor pressure on both sides of the membrane surface and the difference in vapor pressure between the bulk solutions. Vapor pressure without salinity (P), but dependent on temperature, was calculated using the Antoine relation. The activity coefficient (a) was calculated to obtain the vapor pressures in the feed compartment considering salinity ($P_{s,f}$).

$$P_{s,f} = P \times a \quad (2.19)$$

The calculation of the theoretical flux (J_t), considering the effects of temperature variations and the equivalent concentration of NaCl in the feed on the vapor pressure polarization ($P_{T_1,C_{m,f}}$) was performed with Eq. 2.20.

$$J_t = C \times (P_{T_1,C_{m,f}} - P_{T_2,C_0}) \quad (2.20)$$

Where C is the MD coefficient, and in this study calculated considering the point of highest flux in the tests, and P_{T_2,C_0} is the vapor pressure on the permeate side.

3 RESULTS AND DISCUSSION

3.1 Permeate flux and temperature

In the MD-LED-UV test, although it was conducted for the same time as the MD test, the volume that permeated the membrane at the end of the test was smaller. This is due to the lower permeate fluxes observed in the MD-LED-UV system (Fig 2.3).

The permeate flux (J) profile was divided into three periods, according to MD-LED0UV operation: (I) flux increase and stabilization, (II) flux pronounced decrease in the MD-LED-UV test, and (III) flux rate stabilization.

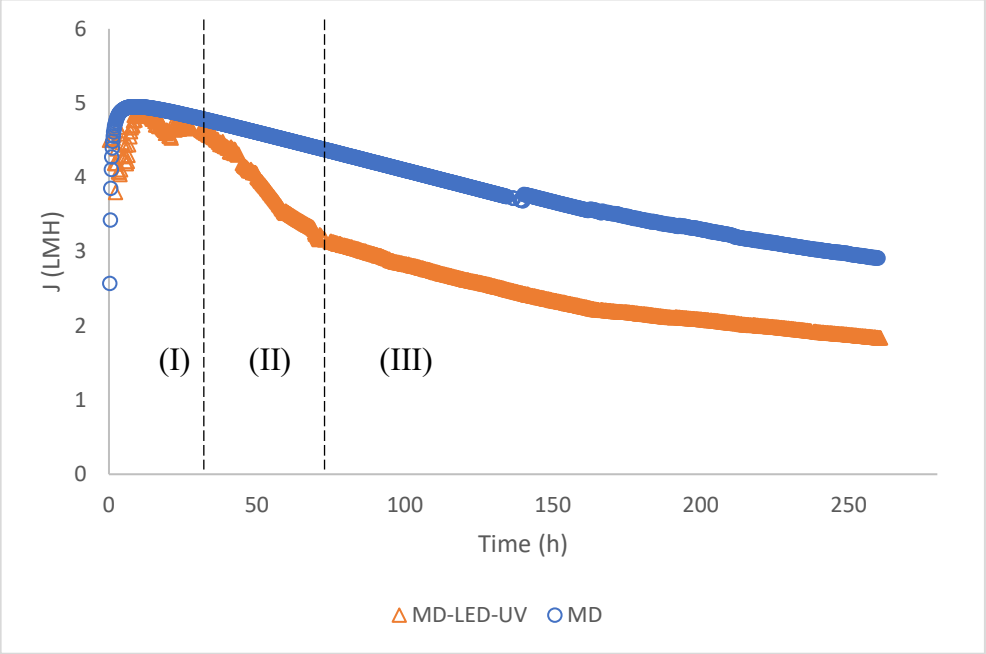

Fig. 2. 3 – Permeate flux in MD and MD-LED-UV

At the moment (I), flux increased rapidly in the first hours for the all tests. In that first moment, there was an increase in the feed tank temperature immediately after a rapid initial decrease when the heat exchange with the permeate began. Then, with the establishment of the polarization layers, gradual flux stabilization was observed. There is a decline in J at the moment (II) due to forming a thicker fouling layer on the membrane surface, increasing the mass and heat resistances (GOH et al., 2013). The photographic records of the membrane surfaces confirmed that when the fouling became more severe, the permeate flux decreased in

in MD test. Fig 2.4 shows the fouling over the membrane and spacer. It is possible to verify that the most extensive fouling layer observed after 30 hours coincides with the beginning of the drop in the permeate flux in this test.

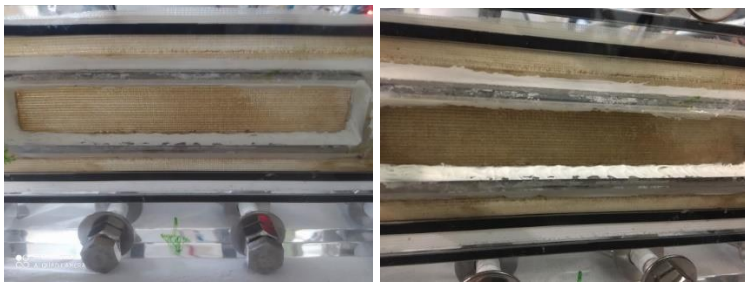

Fig. 2. 4 – Fouling after 24 (a) and 30 (b) hours in MD test

MD-LED-UV and MD tests exhibited similar permeate flux profiles during the moment (I). However, in stage (II), between 30 and 70 hours of operation, flux decline in MD-LED-UV was much faster. A more likely explanation for this is that UV radiation led to modifications in organic matter characteristics. As shown in Fig. 2.9, there was permeation of organic matter in the first hours of operation of the MD-LED-UV, which did not happen in the MD tests. This is a notable indication that the organic matter characteristics have changed by becoming, for example, more volatile. Therefore, it could permeate MD pores and, over time, may have accumulated into them, causing pore blockage, which would explain the increased flux decline.

In Fig. 2.5, it is possible to discriminate the effect of progressive fouling layer formation on flux decline. J_t considers the contribution of vapor pressure polarization - due to temperature and concentration polarization. J_t has similar variations to driving force variations, mainly due to temperature fluctuations in the feed (at night, the temperatures were lower). It is possible to observe that, in the MD test, J_t and J had close values for more than 150 hours. After this period, the fouling effect on flux was evident.

At the beginning of stage II, in the MD-LED-UV test, J_t and J had closer values. The observed fluxes were reduced throughout the operation, revealing the pore blockage effect in flux decline already in this stage. Considering only the driving force, a higher flux was expected. In stage III, during the MD-LED-UV test, there was a sharp drop in feed temperature between 120 and 160 hours due to an operational problem. As soon as the temperature was maintained at 40°C again, the theoretical flux returns to a high plateau. Theoretical fluxes became higher at the end of the tests because of higher temperatures.

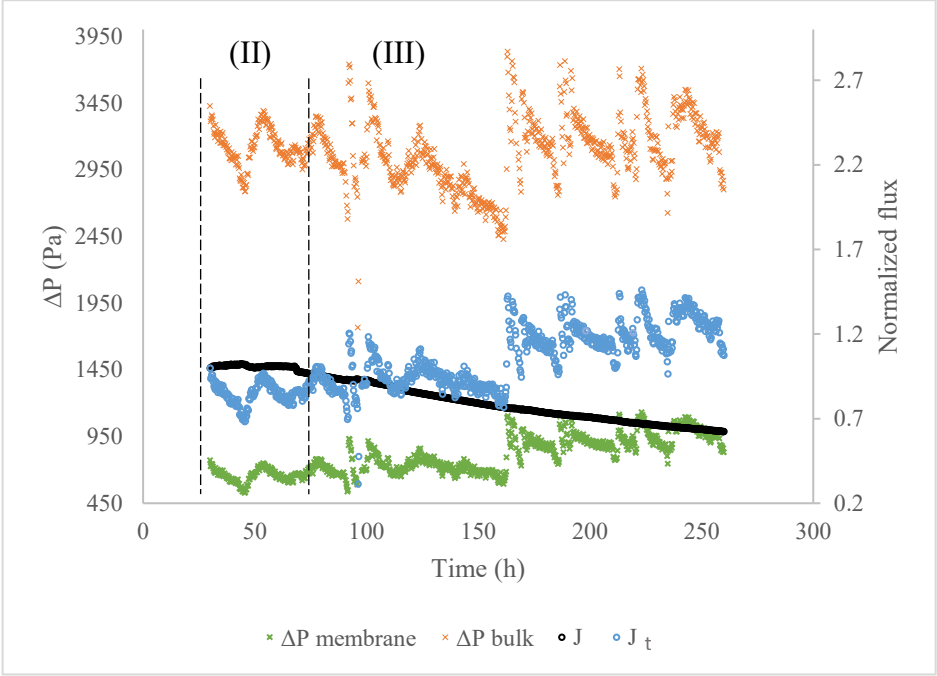

(a)

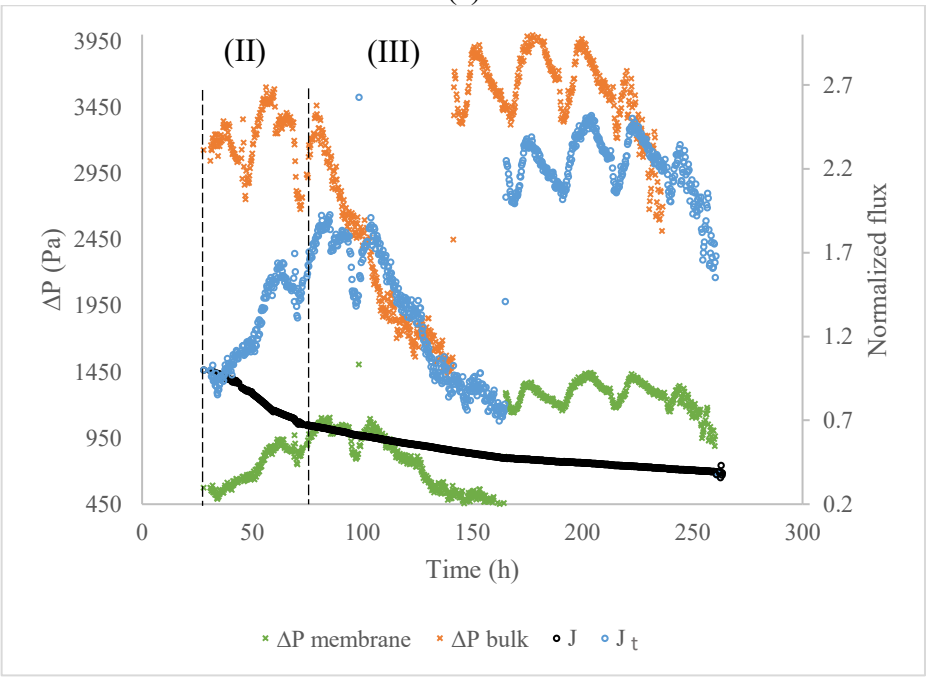

(b)

Fig. 2. 5 – Theoretical fluxes and effect of vapor pressure polarization on (a) MD and (b) MD-LED-UV

The polarization coefficients of temperature (τ), concentration (ζ) and vapor pressure (ψ) were calculated and are shown in Fig. 2.6

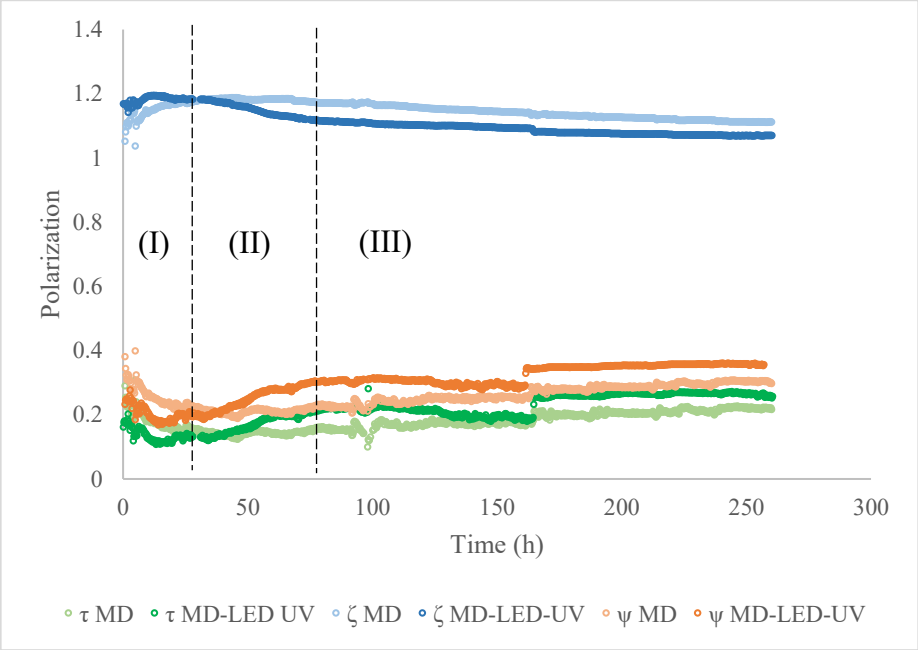

Fig. 2. 6 – Polarization coefficients

The higher concentration polarization in the MD test during stage (II) may be due to the higher permeate flux. Although temperature and vapor pressure polarization had a greater effect on the MD-LED-UV test during the first stage, in the second stage, it is inverted, becoming more pronounced in the MD test.

3.2 MD performance

In the beginning, an increase in permeate conductivity and a slight decrease in feed conductivity in all tests were observed (Fig 2.7). It can be explained by the permeation of ammonia (SHI et al., 2020), a component present in wastewater from anaerobic treatment. Permeation is explained by the higher temperature of the feed, favoring the gaseous form of ammonia (HUANG; SHANG, 2006). The pH of the feed can be adjusted to control the permeation of ammonia (JACOB et al., 2015) and enable its subsequent recovery. Another attempt to recover the ammonia is, in a first step, using an acidic solution as a cooling fluid to favor ammonia removal. Subsequently, in a second step, to proceed as in this study to recover water.

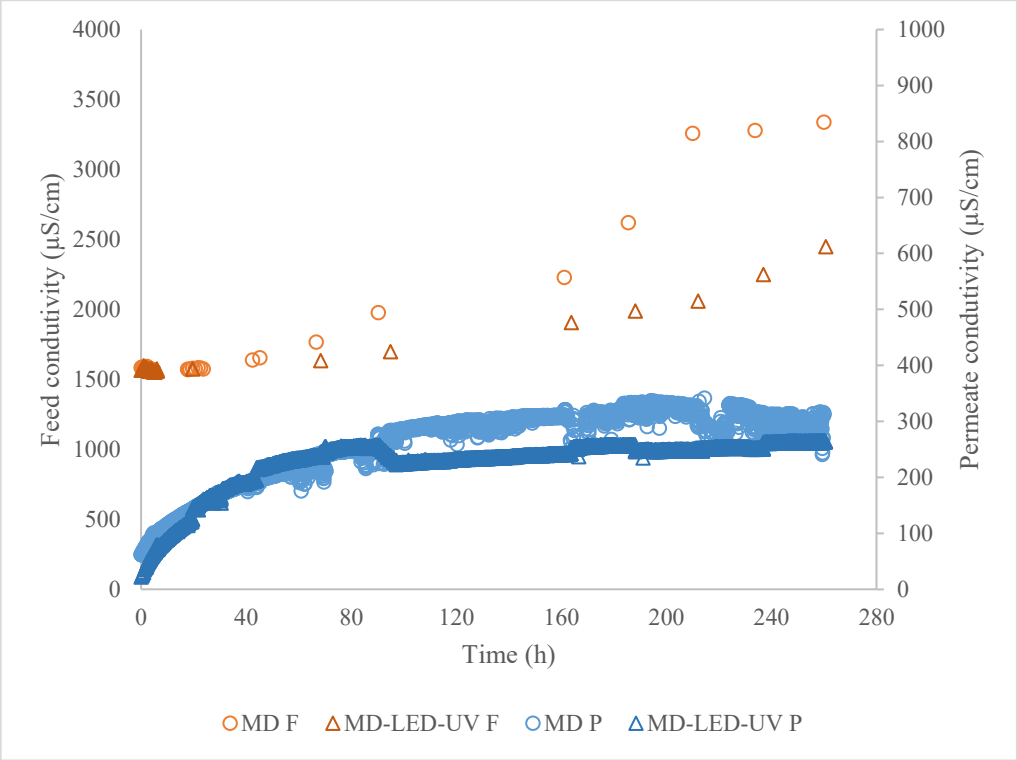

Fig. 2. 7 - Currents conductivity during operations

The permeate conductivity in the MD-LED-UV test stabilized at similar values as in the MD test. Stability could be achieved in the permeates after the volatile component had already permeated the membrane. Besides, the more developed fouling may have provided another barrier to the permeation of the compound. The lower permeate conductivity in the MD-LED-UV system observed over time is mainly due to the lower recovery. When comparing equivalent recovery rates, conductivities in both systems are very close.

Concentrate conductivity in the MD test increased until it was stabilized due to the addition of new feed after 210 hours of operation. In the MD-LED-UV test, the conductivity of the feed tank took longer to increase. The lower permeate fluxes can explain this. Comparing the conductivities at similar recovery rates, the values were close, as in permeate conductivity, with no significant difference between the data.

As the temperature increased at the beginning of the operation and the gaseous form of ammonia was favored, the pH of the feed had a progressively stronger base character until it tended to stabilize after 40 hours of operation in both systems (Fig. 2.8). With ammonia permeation (evidenced in item 3.22), the pH of permeate and concentrate tended to equalize over time, with no significant difference in pH increase through LED coupling. Thus, with the adjustment of feed pH and the predominance of ammonia in its ionic form (HUANG; SHANG,

2006), the pH of the permeate would have values closer to that of the initial distilled water in both systems.

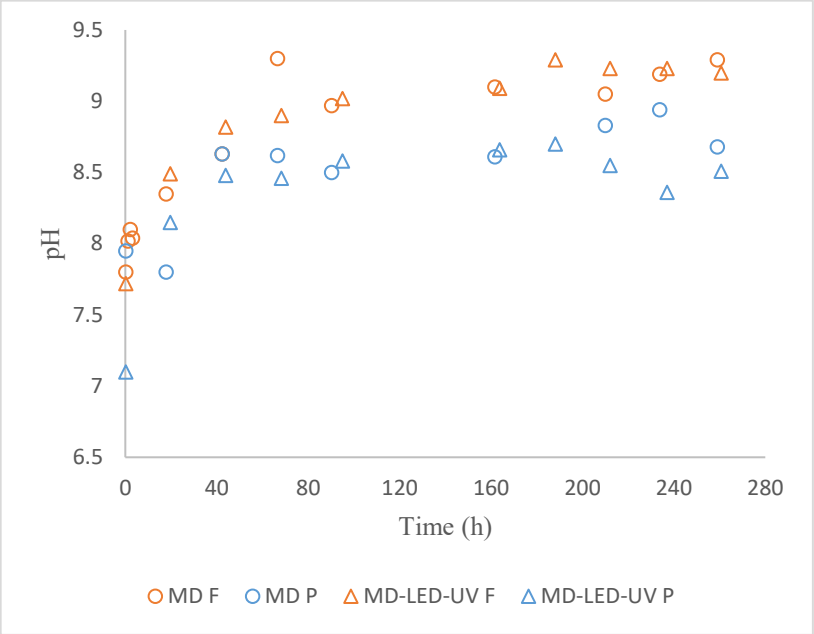

Fig. 2. 8- pH variations during MD and MD-LED-UV tests

3.2.1 Removal efficiencies

Fig 2.9 shows the COD concentration in the permeate and the concentrate of MD and MD-LED-UV. Organic matter was not detected in permeate in MD tests. In the MD-LED-UV test, it was initially observed the passage of organic matter into the permeate. However, after 90 hours of operation, COD permeation decreased, and the overall removal was over 96% after 200 h of operation. The LED operation was replicated up to 96 hours, and the same behaviour was observed concerning the COD concentration. Since there was no lesser rejection of the other parameters evaluated, the hypothesis of pore wetting was discarded.

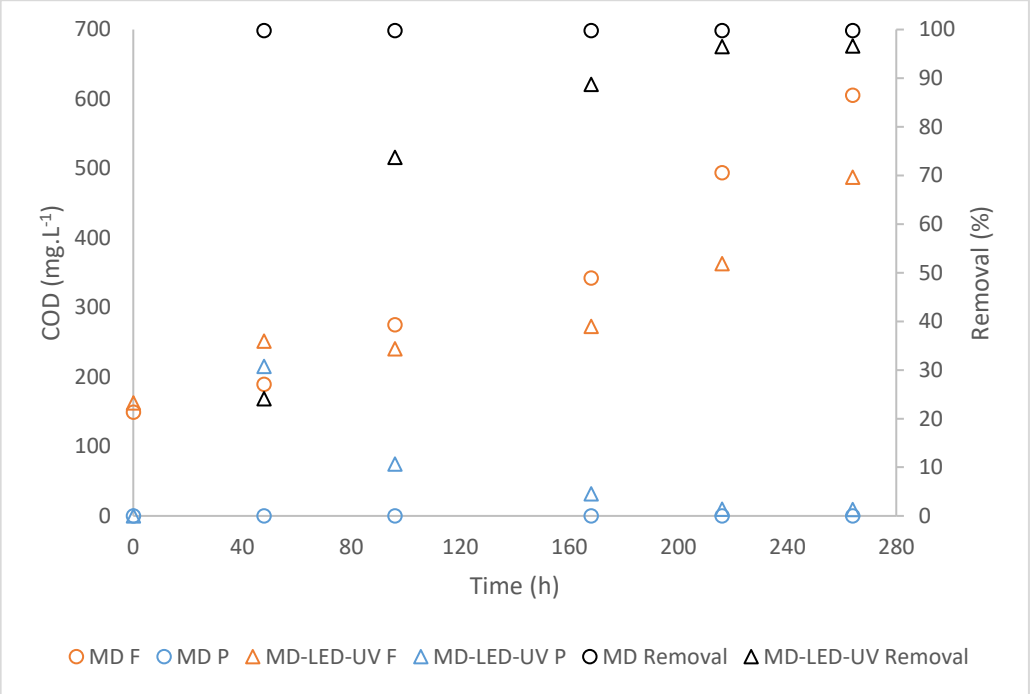

Fig. 2. 9 – COD concentration in MD and MD-LED-UV tests

Thus, two hypotheses deserve further study: (i) whether UV radiation promotes the degradation of organic molecules into volatile compounds; (ii) if the UV radiation modifies the membrane surface since initially, when the fouling does not cover the membrane is directly irradiated. Both hypotheses are consistent with the increase in rejection over time. After forming a denser fouling layer, there is an additional barrier to permeation and protecting the membrane from radiation. Concerning total organic carbon (TOC), in MD, the concentration was from 41 in the initial feed to 174 $mg.L^{-1}$ in the final concentrate, while in the MD-LED-UV test, the concentration increased from 75 to 150 $mg.L^{-1}$.

Regarding turbidity (Table 2.2), the overall removals were always greater than 90% in MD tests. During the MD-LED-UV test, there was a decrease in turbidity removal, which was 71% in the same period in which there was the least COD removal. When COD removals increased, turbidity also increased, ending at 73.6%, but, considering the high turbidity of the concentrate, instantaneous removal (R_i) (considering the turbidity value of the feed tank at that time), of 94.1% was obtained.

Table 2. 2 - Color and turbidity characterization of final currents from MD and MD-LED-UV tests

	MD			MD-LED-UV		
Parameter	**Concentrate**	**Permeate**	**R (%)**	**Concentrate**	**Permeate**	**R (%)**
Turbity (NTU)	78.7 ± 2.4	0.6 ± 0	93.4	117.3 ± 2.2	2.4 ± 0.4	73.6
Color (uH)	1351 ± 4	16 ± 1	99	1234 ± 25	28 ± 2	98

The color removal was very similar to both systems, superior to 98%, and suspended solids were not detected in permeate samples from any test.

3.2.2 Phosphorus and nitrogen removal

Fig 2.10 shows the variation of the phosphate concentration. The variation in the feed tank concentration was similar for MD-LED-UV and MD tests. For the first, the overall removals were consistently higher than 99.8%, and for the second, 95.7%. The results of phosphate removal indicate that the presence of the LED did not contribute to pore wetting since the removal was superior to that in the MD tests. Besides, these results also indicate that the membrane surface has not been modified to the point of reducing efficiency. Thus, the lower organic matter removal must have occurred due to the molecules' photolysis and decomposition (WETZEL et al., 1995) into volatile compounds.

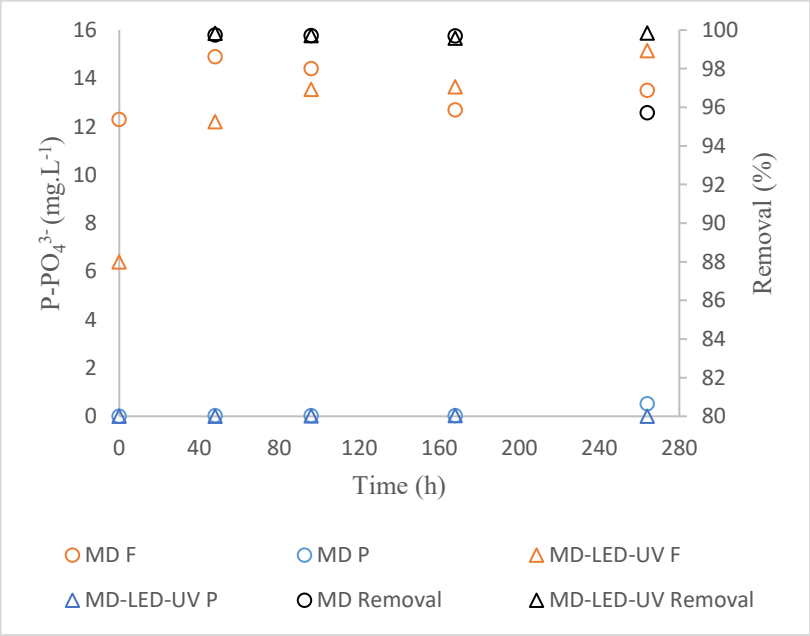

Fig. 2. 10 – $P\text{-}PO_4^{3-}$ concentration during MD and MD-LED-UV tests

Fig. 2.11 shows the variations in ammonia, nitrite, and nitrate concentrations in the concentrate and the permeate of the MD and MD-LED-UV tests. The ammonia concentration in the feed tanks decreased progressively. In addition to ammonia transport across the membrane, it was also possible to verify through nitrogen balance a loss of ammonia to the environment through evaporation. The vapor pressure of ammonia is higher than water vapor pressure and ammonia permeation was previously observed to be proportional to the feed temperature (JACOB et al., 2015).

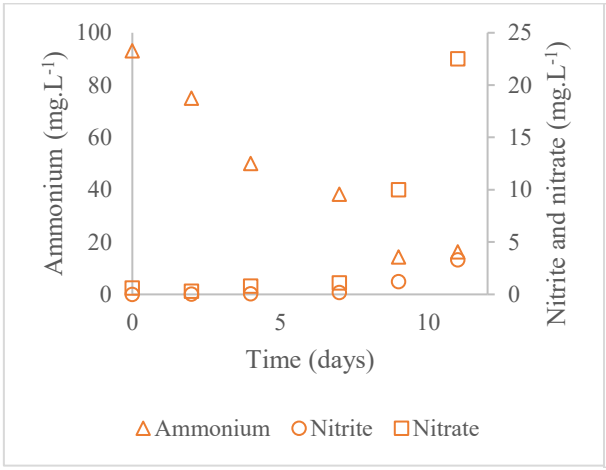
Ammonium (mg.L-1)
Nitrite and nitrate (mg.L-1)
Time (days)
Ammonium
Nitrite
Nitrate

(a)

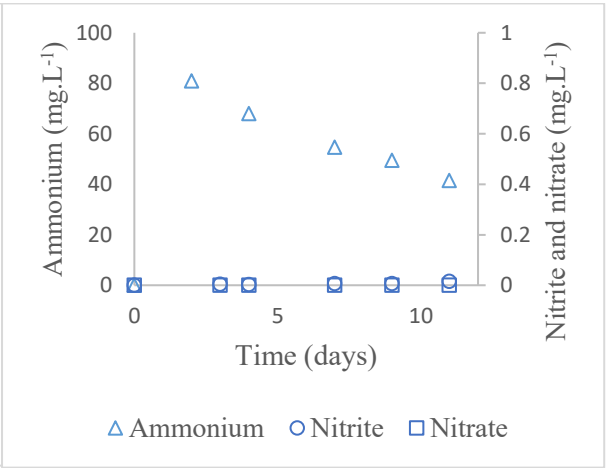
Ammonium (mg.L-1)
Nitrite and nitrate (mg.L-1)
Time (days)
Ammonium
Nitrite
Nitrate

(b)

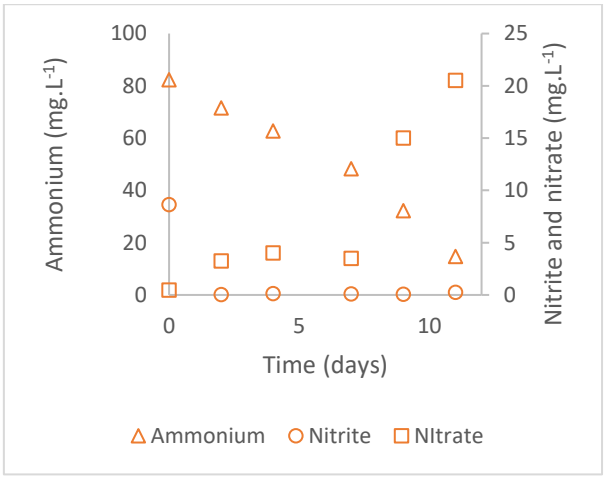
Ammonium (mg.L-1)
Nitrite and nitrate (mg.L-1)
Time (days)
Ammonium
Nitrite
NItrate

(c)

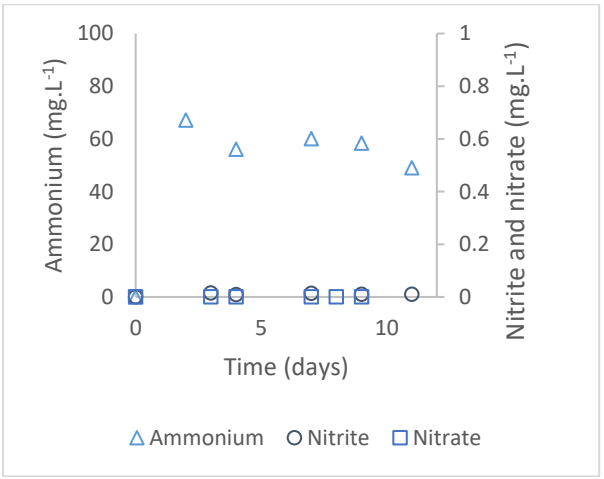
Ammonium (mg.L-1)
Nitrite and nitrate (mg.L-1)
Time (days)
Ammonium
Nitrite
Nitrate

(d)

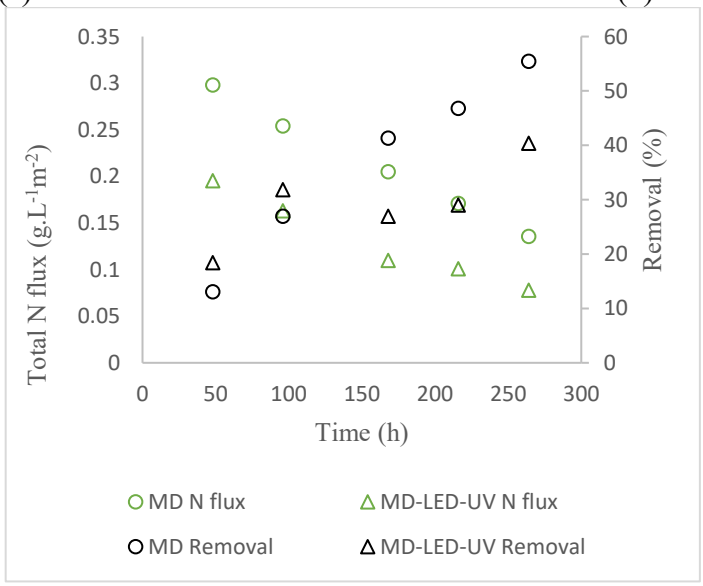
Total N flux (g.L-1m-2)
Removal (%)
Time (h)
MD N flux
MD-LED-UV N flux
MD Removal
MD-LED-UV Removal

(e)

Fig. 2. 11 – Variation of the nitrogen series from (a) MD_{Feed}, (b) $MD_{Permeate}$, (c) MD-LED-UV_{Feed}, (d) MD-LED-$UV_{Permeate}$, and (e)Total nitrogen flux and removal

As discussed in item 3.2, the low ammoniacal nitrogen removal due to its volatile character increased the permeate conductivity. The permeate of the MD test had a greater decrease in ammonia concentration over time. This is due to the greater permeate flux, which diluted the compound. Less removal of ammonia when treating feeeds rich in this compound by MD has been observed in other studies (YAN et al., 2019). Jacob et al. (2015), for example, observed, in some conditions, the increase of ammonia concentration in permeate from 0 to more than 100 $mg.L^{-1}$ in 18 hours of operation.

However, nitrite removals were greater than 99.98% in both systems and no nitrate was detected in any permeate sample.

3.3 Membrane and fouling evaluation

After the tests, membrane photographs and SEM images (Fig. 2.12) were taken to compare the effect of the LED on the fouling visually.

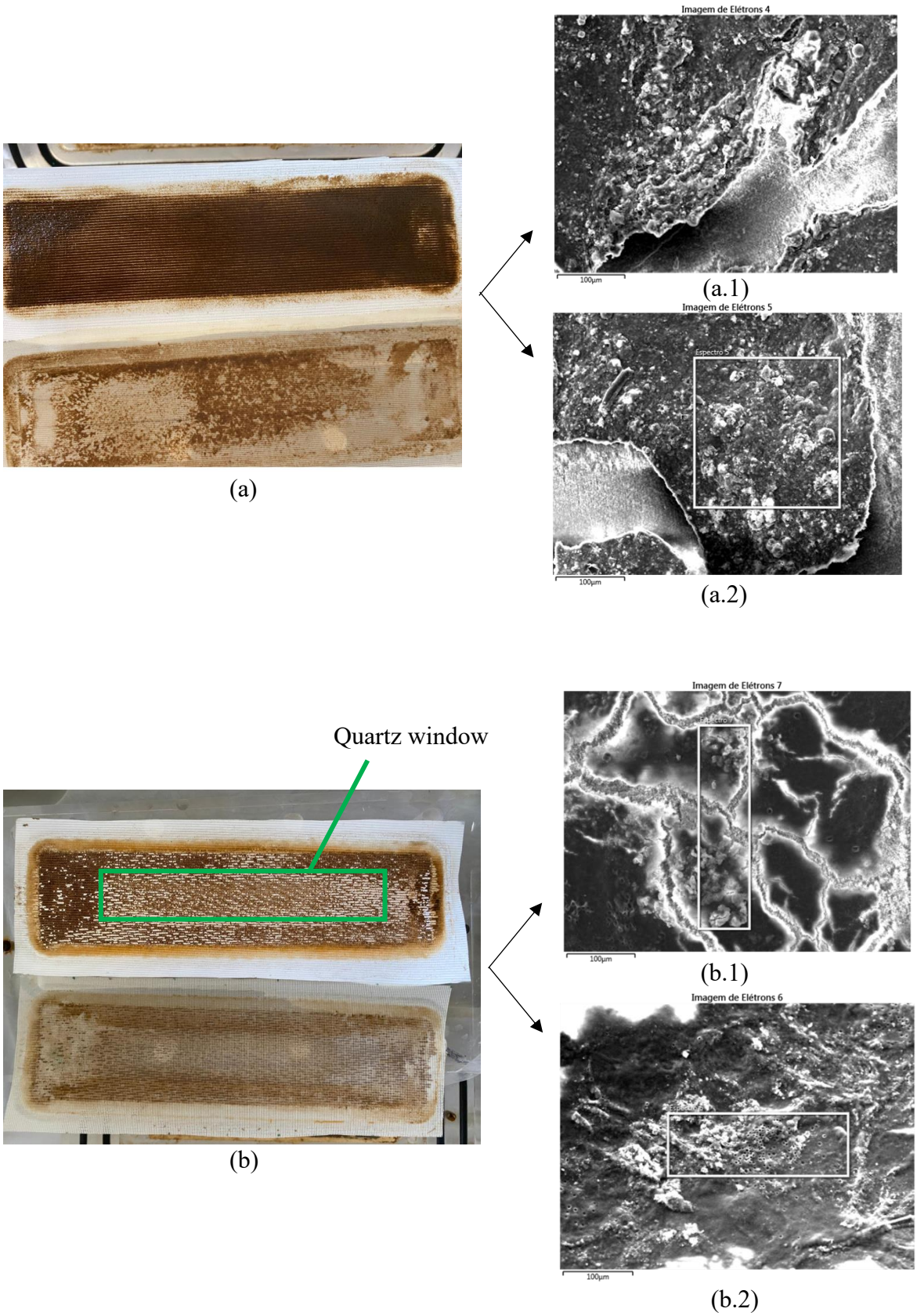

Fig. 2. 12 – MD fouling after tests: (a) MD and (b) MD-LED-UV and SEM images of membranes samples from (a.1) MD inlet, (a.2), (b.1) MD-LED-UV inlet, and (b.2) MD-LED-UV outlet. Images of the respective membranes (above) and spacers (below)

The images reveal that the MD-LED-UV test membrane and its respective spacer were visually less fouled, with much less fouling in the region of the quartz window (Fig. 2.12 (b) compared to the MD test (Fig. 2.12 (a)). Besides, the membrane fouling of this test was much less adhered to the membrane and was much more easily removed mechanically. In Fig 2.12 (b.2), the irradiated fouling is seen to have a more spongy texture with pores. The membrane from the MD test was more fouled, which can be explained by the greater recovery in this operation and that no mitigation method was applied.

In all membranes, it can be seen in pictures and SEM images that the part closest to the modules' outlet (on the left) is visibly more fouled than the part closest to the modules' inlet (on the right). A similar situation was observed by Krivorot et al. (2011), who attributed the smallest fouling extension close to the module inlet due to more turbulent hydrodynamic conditions. The authors also attributed the greater extent of fouling in the outlet to lower temperatures, which favors biofilm development.

The analysis of the elements present in new and fouled membrane surfaces are shown in Table 2.3. The new membrane has a predominance of fluorine and carbon, PTFE components. Fouling layers formed in MD and MD-LED-UV tests in the modules' inlet and outlet are remarkably distinct. In the outlet, there is a greater relative presence of carbon and oxygen. The similarity in the composition profile of the two tests suggests that the time of exposure to the foulant medium is more determinant for the relative composition of the layer than the recovery rate. The intensity of inorganics was lower over operations. In contrast, when evaluating fouling in MD, Liu et al. (2019) observed increased inorganics on the membrane surface with time. This difference is probably due to the effect of the feed composition on the formation of fouling since the researchers treated lake water. In this study, wastewater rich in organic matter and microorganisms was treated.

Furthermore, fluorine can be detected only in MD and MD-LED-UV inlets, which indicates that they are the samples with the greatest similarity to the new membrane and corroborates the effect of more turbulent hydrodynamic conditions on the mitigation of fouling.

Table 2. 3 - Energy counts analysis

Element	**Sample (% energy count)**				
	New membrane	MD inlet	MD outlet	MD-LED-UV inlet	MD-LED-UV outlet
C	25.7	34.7	45	38	53.9

F	74.3	22	-	25.8	-
O	-	24.5	35	23	38.7
Ca	-	12.3	12.6	12.2	2.8
P	-	2.8	3	-	-
Fe	-	1.1	13	-	0.4
Si	-	1.4	1.7	-	2.3
Mg	-	0.4	0.4	0.4	0.2
Al	-	0.8	0.8	-	1.2
Mn	-	-	0.1	-	-
K	-	-	0.1	0,5	-

The total count of heterotrophic bacteria on the membrane surfaces was superior to 3.0 x 10^3 UFC.mL^{-1} for all tests. The existence of organic matter (Table 2.4) and phosphorus (Table 2.3) in a membrane surface, together with the lower temperature in the feed compartment, may have made the membrane surface the most suitable place from the feed compartment for microorganisms to survive, as observed for other researchers (LIU et al., 2019).

Table 2. 4 - MD fouling characteristics

Test	COD (mg.cm^{-2})
MD	1.682
MD-LED-UV	2.795

Despite being less fouled, the fouling over the irradiated membrane was the one with the highest concentration of COD (Table 2.4). However, it is essential to emphasize that the fouling of the MD-LED-UV system was much less adhered to the membrane, allowing a better characterization. In tests without LED, fouling was much more adhered to, making complete extraction for analysis through sonication and mechanical removal not possible. Thus, the concentration of COD presented in the MD assays corresponds only to the reversible fraction of the fouling, which is easily physically removed.

Regarding specific biofilm mitigation in membranes with LED-UV coupling, Sperle et al. (2020) evaluated an RO-LED-UV system. The LEDs were positioned at the module entrance as an in situ pre-treatment. They observed that there was a delay in biofilm build-up in the coupled system, which was attributed to three main factors: the LED-UV disinfection power, reducing the amount of viable organisms; radiation changing the properties related to the adhesion of microorganisms to the membrane, as radiation has the potential to affect cell

proteins, which may have led to depolarization of cells present in the membrane surface; and bacteria's DNA damage leading to a slower cell cycle. As Mofidi et al. (2000) observed a lowest adherence of bacteria to RO membranes after irradiation, the hybrid module can have good anti-biofouling action with optimizing parameters such as irradiation time.

Previously, MD biofouling did not receive much attention since the process occurs at temperatures higher than many microorganisms can support, which would inhibit biofilm (GRYTA et al., 2002). However, the results found in this study go against the grain. Figure 2.13 shows SMP and EPS characterization in terms of proteins in the biological fouling formed over the membranes.

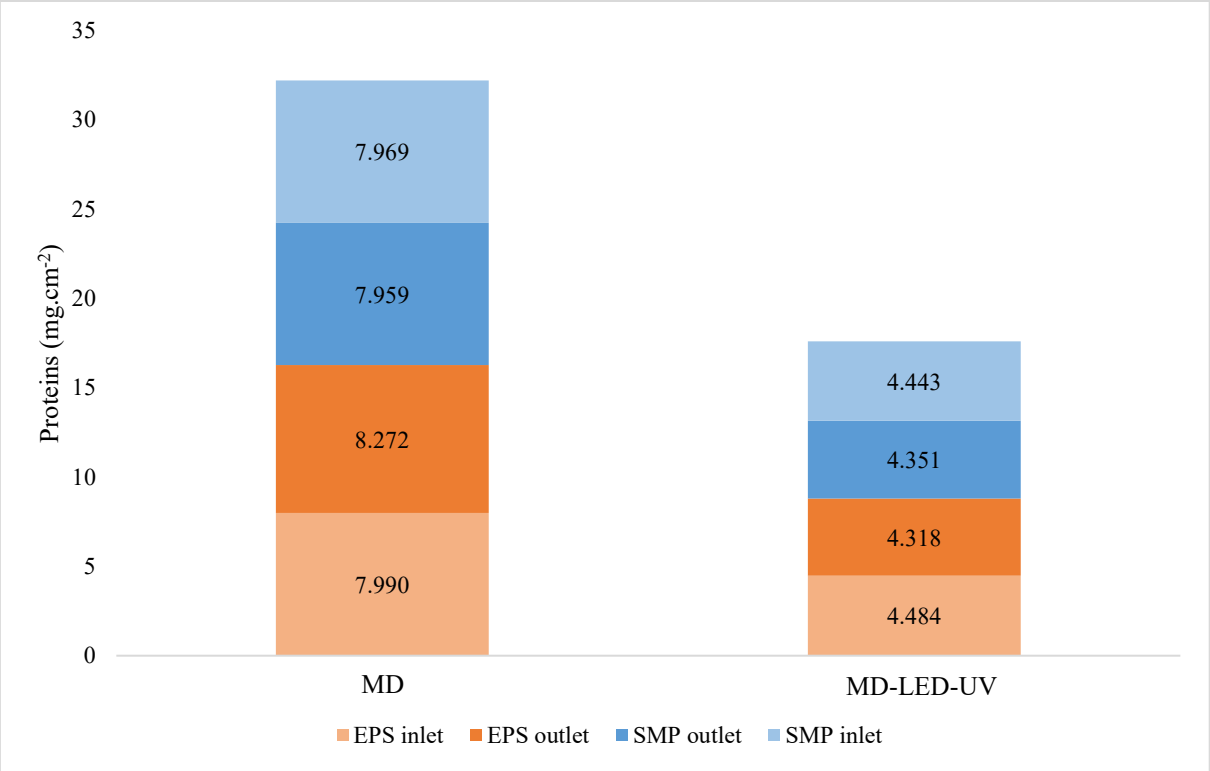

Fig. 2. 13- Composition of SMP and EPS in terms of Proteins

The higher amount of SMP and EPS in the membrane area of the MD test may be explained by the lower fluxes in the MD-LED-UV system (thus fewer organisms were brought into the membrane compartment) and the anti-biofouling activity of the hybrid module developed since these components are actively secreted by active cells. This mitigating action explains the lower adhesion of the MD-LED-UV fouling to the membrane since EPS is responsible for the cohesion of the biofilm and the adhesion to the substrate (SALAMA et al., 2016). Furthermore, proteins are important as they influence the initial attachment process. Proteins may enable the

bacteria-surface contact through biopolymer bridging forces, making biofouling more irreversible and disfavoring detachment (WANG et al., 2020).

Analysis of the contact angle of the new membrane and test membranes (Fig. 2.14) revealed a change in surface hydrophobicity after testing. While the angle in the new membrane was 95.6 ± 0.6 º, the fouling formed over the membranes of the MD and MD-LED-UV tests were, respectively, 81.3 ± 1.2 º and 75.0 ± 0.6 º. The smaller contact angle of the MD-LED-UV fouling layer and, therefore, the more hydrophilic character assumed by the irradiated fouling also explains the lower adhesion to the membrane surface in this test. The interactions between the surface of MD and the fouling layer were more robust, and, therefore, it was more challenging to remove the layer mechanically.

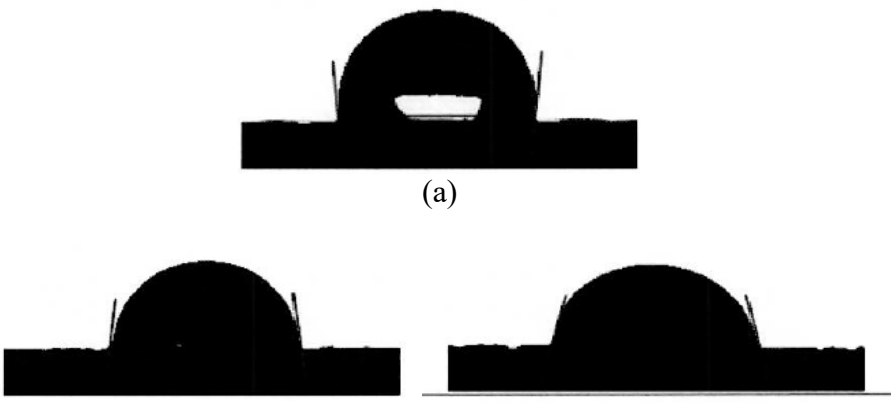

Fig. 2. 14 – Contact angle measurements of (a) new membrane and (b) MD test (c) MD-LEV-UV test

The spectra obtained in the FTRI analysis of the polypropylene support layer of the membranes used in tests are shown in Fig. 2.15. The appearance or disappearance of bands was not detected, suggesting that no chemical changes were arising from the coupling with the LED. However, further studies are needed to assess whether there was any degradation of the selective layer while the membrane was not fouled and exposed to UV radiation.

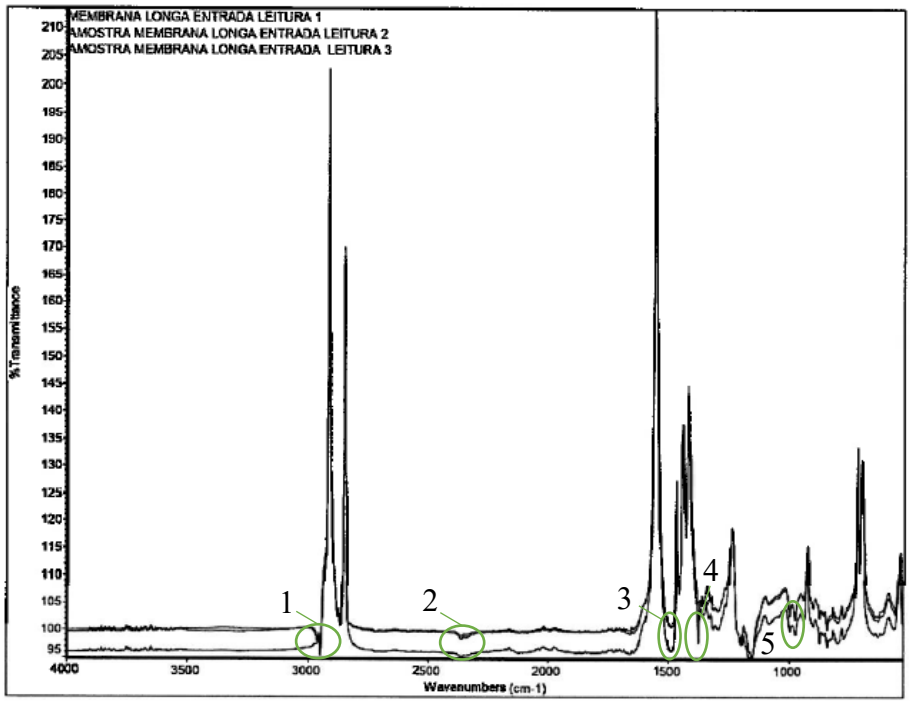

(a)

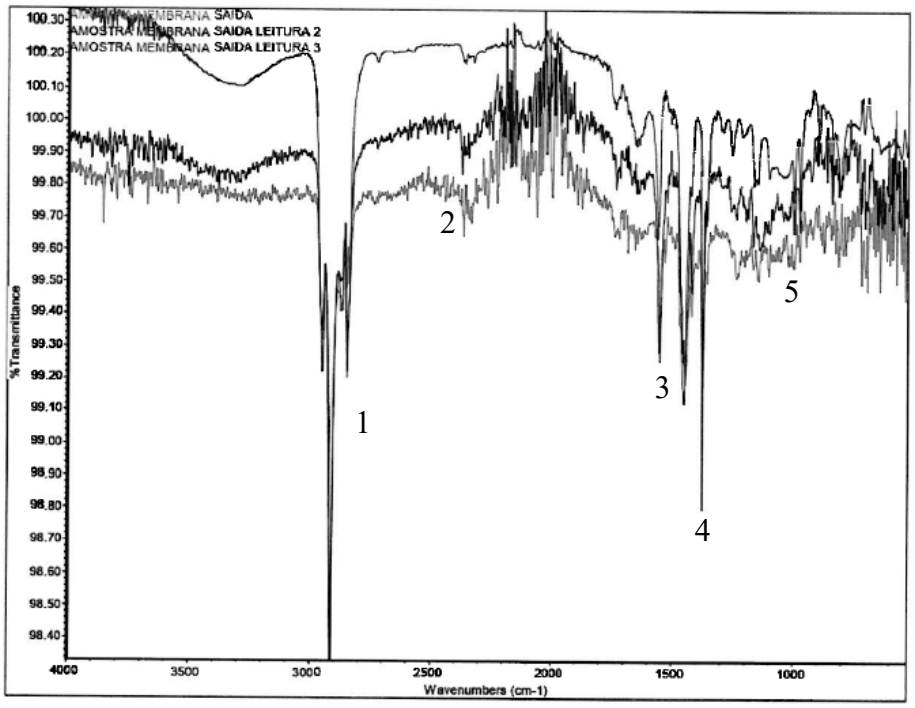

(b)

Fig. 2. 15- FTRI spectra of membranes from (a) MD and (b) MD-LED-UV tests

The vibrations of methyl groups are evidenced by band 1, with a peak between 2840-3000 cm-1. Bands 3 and 4 at 1460 and 1380 cm^{-1} refer to alkyl group bonds. In the fingerprint region, more evident in Fig. 2.15 (a) at peak 5 at 1000 cm^{-1}, there are characteristic bands of the axial

strains of the C-C bonds and the angular strains of the C-C and C-H bonds. (VOLLHARDT; SCHORE, 2013).

4 CONCLUSIONS

In this study, it was observed that the performance of the hybrid system in secondary wastewater treatment was very similar to MD in several aspects, such as conductivity, solids, phosphorus (removals > 95% for MD and > 99% for the MD-LED-UV), and ammonia removal – this was relatively low given the volatile character of the compound. For the control of ammonia permeation, adjusting the feed pH and other strategies for ammonia recovery should be investigated in the future, making the MD relevant to the water-energy-food nexus, promoting sustainable development. The performance of the two systems was different in terms of flux decline and organic matter removal. The flux drop profile in MD-LED-UV system is probably related to changes in organic matter characteristics due to UV radiation. In the beginning, there was a lower COD removal in the hybrid system, which must have led to pore blockage. Over time, COD removal in MD-LED-UV increased until reaching values closer to MD removal, with an instantaneous removal of 94.1% for MD-LED-UV.

Analysis of the membrane surfaces reveals a smaller extension of fouling in the MD-LED-UV system. The fouling layer was much less adhered to the membrane surface, being easily removed mechanically - possibly due to the greater hydrophilic character of the layer formed in the hybrid system and the bacteria inactivation by MD-UV coupling, which led to lower protein content in SMP and EPS. In all tests, membranes in modules' inlet were less fouled than outlets, evidencing the antifouling action of a condition of greater turbulence, avoiding the deposition of organic and inorganic foulants, besides bacterial deposition. In addition, the modules' outlet had a lower temperature than the input, which favors the development of biofilm, which composed the fouling formed in all tests. However, the anti-biofouling action of the developed module needs to be better studied.

REFERENCES

AL-ABRI, M.; AL-GHAFRI, B.; BORA, T.; DOBRETSOV, S.; DUTTA, J.; CASTELLETTO, S.; ROSA, L.; BORETTI, A. Chlorination disadvantages and alternative routes for biofouling control in reverse osmosis desalination. *Npj Clean Water*. v. 2, 2019.

ALKHUDHIRI, A.; DARWISH, N.; HILAL, N. Membrane distillation : A comprehensive review. *Desalination*, v. 287, p. 2–18, 2012.

APHA. Standard Methods for the Examination of Water and Wastewater. 22. ed. Washington: APHA, 2012.

BAKER, R.W. Membrane technology and applications. John Wiley & Sons, 2012.

BATLEY, G. E.; KIRBY, J. K.; MCLAUGHLIN, M. J. Fate and risks of nanomaterials in aquatic and terrestrial environments*, Accounts of Chemical Research*, v. 46, p. 854–862, 2013.

BOGLER, A.; BAR-ZEEV, E. Membrane distillation biofouling : Impact of feed water temperature on biofilm characteristics and membrane performance Membrane distillation biofouling : Impact of feed water temperature on biofilm character. *Environmental science & technology*, v. 52, n. 17, p. 10019-10029, 2018.

BRASIL. Decreto n. 9.470, de 14 de ago. de 2018. Promulgação da Convenção de Minamata sobre Mercúrio, firmada pela República Federativa do Brasil, em Kumamoto, em 10 de outubro de 2013., Brasília,DF, ago 2018.

CHO, M.; KIM, J.; KIM, J.Y.; YOON, J.; KIM, J.H. Mechanisms of Escherichia coli inactivation by several disinfectants. *Water research*, v. 44(11), p. 3410-3418, 2010.

CHOUDHURY, M.R.; ANWAR, N.; JASSBY, D.; RAHAMAN, M.S. Fouling and wetting in the membrane distillation driven wastewater reclamation process – A review, *Advances in Colloid and Interface Science*, v. 269, p. 370–399, 2019.

COSTERTON, J. W.; LEWANDOWSKI, Z.; CALDWELL, D. E.; KORBER, D. R.; LAPPIN-SCOTT, H. M. Microbial biofilms. *Annual review of microbiology*, v. 49(1), p. 711-745, 1995.

EPA. Definition and procedure for the determination of the method detection limit, Revision 2. Environmental Protection Agency EPA, 2016.

FAN, J.; HO, L.; HOBSON, P.; BROOKES, J. Evaluating the effectiveness of copper sulphate, chlorine, potassium permanganate, hydrogen peroxide and ozone on cyanobacterial cell integrity. *Water research*, v. 47(14), p. 5153-5164, 2013.

GOH, S.; ZHANG, Q.; ZHANG, J.; MCDOUGALD, D.; KRANTZ, W. B.; LIU, Y.; FANE, A. G. Impact of a biofouling layer on the vapor pressure driving force and performance of a membrane distillation process. *Journal of Membrane Science*, v. 438, p. 140–152, 2013.

GRYTA, M. The assessment of microorganism growth in the membrane distillation system, *Desalination*, v. 142, p. 79–88, 2002.

GRYTA, M. Calcium sulphate scaling in membrane distillation process, *Chemical Papers*, v. 63, p. 146–151, 2009.

GUO, B.; PASCO, E. V.; XAGORARAKI, I.; TARABARA, V. V. Virus removal and inactivation in a hybrid microfiltration-UV process with a photocatalytic membrane, *Separation and Purification Technology*, v. 149, p. 245–254, 2015.

GUO J.; YAN, D.Y.S.; LAM, F.L.-Y.; DEKA, B.J. An, Self-cleaning BiOBr/Ag photocatalytic membrane for membrane regeneration under visible light in membrane distillation, *Chemical Engineering Journal*. V. 378, 2019.

HE, D. Q.; ZHANG, Y. J.; HE, C. S.; YU, H. Q. Changing profiles of bound water content and distribution in the activated sludge treatment by NaCl addition and pH modification. *Chemosphere*, v. 186, p. 702-708, 2017.

HUANG J.C.; SHANG C. Air Stripping. In: Wang L.K., Hung YT., Shammas N.K. (eds) Advanced Physicochemical Treatment Processes. *Handbook of Environmental Engineering*, vol 4. Humana Press, 2006.

JACOB, P.; PHUNGSAI, P.; FUKUSHI, K.; VISVANATHAN, C. Direct contact membrane distillation for anaerobic effluent treatment. *Journal of Membrane Science*, v. 475, p. 330-339, 2015.

JIANG, L.; CHEN, L.; ZHU, L. Electrically conductive membranes for anti-biofouling in membrane distillation with two novel operation modes : Capacitor mode and resistor mode. *Water Research*, v. 161, p. 297–307, 2019.

JO, W. K.; TAYADE, R. J. New generation energy-efficient light source for photocatalysis: LEDs for environmental applications. *Industrial and Engineering Chemistry Research*, v. 53, p. 2073–2084, 2014.

KIM, J.; SHIN, M.; SONG, W.; PARK, S.; RYU, J.; JUNG, J.; CHOI, S., YU, Y., KWEON, J.; LEE, J.-H. Application of quorum sensing inhibitors for improving anti-biofouling of polyamide reverse osmosis membranes: Direct injection versus surface modification. *Separation and Purification Technology,* v. 255, p. 117736, 2021.

KRIVOROT, M.; KUSHMARO, A.; OREN, Y.; GILRON, J. Factors affecting biofilm formation and biofouling in membrane distillation of seawater, *Journal of Membrane Science*, v. 376, 2011.

LAWSON, K.W.; LLOYD, D.R. Membrane distillation. *Journal of Membrane Science*, v. 124, p. 1–25, 1997.

LIANG, R.; LEUWEN, J. C. Van; BRAGG, L. M.; ARLOS, M. J.; LI, L. C. M.; FONG, C.; SCHNEIDER, O. M.; JACIW-ZURAKOWSKY, I.; FATTAHI, A.; RATHOD, S.; PENG, P.; SERVOS, M. R.; ZHOU, Y. N. Utilizing UV-LED pulse width modulation on TiO 2 advanced oxidation processes to enhance the decomposition efficiency of pharmaceutical micropollutants. *Chemical Engineering Journal*, v. 361, p. 439–449, 2019.

LIU, C.; CHEN, L.; ZHU, L.; WU, Z.; HU, Q.; PAN, M. The effect of feed temperature on biofouling development on the MD membrane and its relationship with membrane performance : An especial attention to the microbial community succession. *Journal of Membrane Science*, v. 573, p. 377–392, 2019.

LIU, C.; ZHU, L.; CHEN, L. Effect of salt and metal accumulation on performance of membrane distillation system and microbial community succession in membrane biofilms. *Water Research*, v. 177, p.115805, 2020.

LOWRY, O. H.; ROSEBROUGH, N. J.; FARR, A. L.; RANDALL, R. J. Protein measurement with the Folin phenol reagent. *Journal of biological chemistry*, v. 193, p. 265-275, 1951.

MANNA, A.; PAL, P. Solar-driven flash vaporization membrane distillation for arsenic removal from groundwater: Experimental investigation and analysis of performance parameters. *Chemical Engineering and Processing: Process Intensification*, v. 99, p. 51-57, 2016.

MANSOURI, J.; CHEN, V. Strategies for controlling biofouling in membrane filtration systems : challenges and opportunities. *Journal of Materials Chemistry*, p. 4567–4586, 2010.

MARCONNET, C.; HOUARI, A.; SEYER, D.; DJAFER, M.; CORITON, G.; HEIM, V.; MARTINO, P. Di. Membrane biofouling control by UV irradiation. *Desalination*, v. 276, p. 75–81, 2011.

MATAFONOVA, G.; BATOEV, V. Recent advances in application of UV light-emitting diodes for degrading organic pollutants in water through advanced oxidation processes : A review. *Water Research*, v. 132, p. 177–189, 2018.

MATIN A.; KHAN Z.; ZAIDI, S.M.J.; BOYCE, M.C. Biofouling in reverse osmosis membranes for seawater desalination: Phenomena and prevention, *Desalination*, v.. 281, p. 1–16, 2011.

MOFIDI, A. A.; GABELICH, C. J.; YUN, T. I.; COFFEY, B. M.; GREEN, J. F. T. Task 2.8 A: Investigation of Scale-Up Issues Associated with Ultraviolet Light Disinfection and Reverse Osmosis Desalination. 2002.

NAIDU, G.; JEONG, S.; VIGNESWARAN, S.; HWANG, T.-M.; CHOI, Y.-J.; KIM, S.-H. A review on fouling of membrane distillation. *Desalination and Water Treatment*, v. 57, p. 10052–10076 2015.

NAGARAJ, V.; SKILLMAN, L.; LI, D.; HO, G. Review – Bacteria and their extracellular polymeric substances causing biofouling on seawater reverse osmosis desalination membranes, *Journal of Environmental Management*, v. 223, p. 586–599, 2018.

NTHUNYA, L.N.; GUTIERREZ, L.; NXUMALO, E.N.; VERLIEFDE, A.R.; MHLANGA, S.D.; ONYANGO, M.S. f-MWCNTs/AgNPs-coated superhydrophobic PVDF nanofibre membrane for organic, colloidal, and biofouling mitigation in direct contact membrane distillation. *Journal of Environmental Chemical Engineering*, v. 8, p. 103654, 2020.

ORTA DE VELASQUEZ, M.T.; NOGUEZ, I.Y.; RODRIGUEZ, B.C.; ROMAN, P.I.R. Effects of ozone and chlorine disinfection on VBNC Helicobacter pylori by molecular techniques and FESEM images. *Environmental technology*, v. 38(6), p. 744-753, 2017.

PEREIRA, E.B.; MARTINS, F.R.; GONÇALVES, A.R.; COSTA, R.S.; LIMA, F.L.; RÜTHER, R.; ABREU, S.L.; TIEPOLO, G.M.; PEREIRA, S.V.; SOUZA, J.G. *Atlas brasileiro de energia solar*. 2.ed. São José dos Campos: INPE, 2017.

QADIR, M.; DRECHSEL P.; CISNEROS B.J.; KIM, Y. A.Pramanik, P.Mehta, O.Olaniyan, Global and regional potential of wastewater as a water, nutrient and energy source, in *Natural Resources Forum*, Blackwell Publishing Ltd, Oxford, 40-51, 2020.

RASTOGI, N. K.; CASSANO, A.; BASILE, A. Water treatment by reverse and forward osmosis. In: *Advances in Membrane Technologies for Water Treatment*. p. 129-154, 2015.

RICCI, B. C.; SKIBINSKI, B.; KOCH, K.; MANCEL, C.; CELESTINO, C. Q.; CUNHA, I. L. C.; SILVA, M. R.; ALVIM, C. B.; FARIA, C. V; ANDRADE, L. H.; LANGE, L. C.; AMARAL, M. C. S. Critical performance assessment of a submerged hybrid forward osmosis - membrane distillation system. *Desalination*, v. 468, p. 114082, 2019.

SALAMA, Y.; CHENNAOUI, M.; SYLLA, A.; MOUNTADAR, M.; RIHANI, M.; ASSOBHEI, O. Characterization, structure, and function of extracellular polymeric substances (EPS) of microbial biofilm in biological wastewater treatment systems: a review. *Desalination and Water Treatment*, v. 57(35), p. 16220-16237, 2016.

SHANNON, M.A.; BOHN, P.W.; ELIMELECH, M.; GEORGIADIS, J.G.; MARIN, B.J.; MAYES, A.M. Science and technology for water purification in the coming decades. *Nature*, v. 452, p. 301–310, 2008.

SHI, M.; HE, Q.; FENG, L.; WU, L.; YAN, S. Techno-economic evaluation of ammonia recovery from biogas slurry by vacuum membrane distillation without pH adjustment. *Journal of Cleaner Production*, v. 265, p. 121806, 2020.

SONG, K.; TAGHIPOUR, F.; MOHSENI, M. Microorganisms inactivation by wavelength combinations of ultraviolet light-emitting diodes (UV-LEDs). *Science of the Total Environment*, v. 665, p. 1103-1110, 2019.

SPERLE, P.; WURZBACHER, C.; DREWES, J. E.; SKIBINSKI, B. Reducing the Impacts of Biofouling in RO Membrane Systems through In Situ Low Fluence Irradiation Employing UVC-LEDs. *Membranes*, v. 10(12), p. 415, 2020.

SRISURICHAN, S.; JIRARATANANON, R.; FANE, A. G. Mass transfer mechanisms and transport resistances in direct contact membrane distillation process. *Journal of membrane science*, v. 277, p. 186-194, 2006.

SWARAJ, S.; KUMAR, R.; HARINATH, Y.V.; RAO, T.S. Biocidal efficacy of Ozone and Chlorine on Planktonic and Biofilm cells of two marine bacteria species. *Ozone: science & engineering*, v. 35(2), p. 90-100, 2013.

TIJING, L.D.; WOO, Y.C.; CHOI, J.-S.; LEE, S.; KIM, S.-H.; SHON, H. K. Fouling and its control in membrane distillation - A review. *Journal of Membrane Science*, v. 475, p. 215-244, 2015.

VOLLHARDT, Peter; SCHORE, Neil E. Química Orgânica-: Estrutura e Função. Bookman Editora, 2013.

WANG, J.; LIU, Q.; DONG, D.; HU, H.; WU, B.; REN, H. In-situ monitoring of the unstable bacterial adhesion process during wastewater biofilm formation: A comprehensive study. *Environment International*, v. 140, p. 105722, 2020.

WANG, W.; DU, X.; VAHABI, H.; ZHAO, S.; YIN, Y.; KOTA, A. K.; TONG, T. Trade-off in membrane distillation with monolithic omniphobic membranes. *Nature Communications*, v. 10, p. 3220, 2019.

WARSINGER, D. M.; SWAMINATHAN, J.; GUILLEN-BURRIEZA, E.; ARAFAT, H. A.; LIENHARD V, J. H. Scaling and fouling in membrane distillation for desalination applications: A review. *Desalination*, v. 356, p. 294–313, 2014.

WARSINGER, D. M.; GONZALEZ, J. V.; VAN BELLEGHEM, S. M.; SERVI, A.; SWAMINATHAN, J.; CHUNG, H. W.; LIENHARD, J. H. The combined effect of air layers and membrane superhydrophobicity on biofouling in membrane distillation. *Proceedings of the American Water Works Association Annual Conference and Exposition*, Anaheim, CA, USA, 2015.

WETZEL, R. G.; HATCHER, P. G.; BIANCHI, T. S. Natural photolysis by ultraviolet irradiance of recalcitrant dissolved organic matter to simple substrates for rapidbacterial metabolism. *Limnology and Oceanography*, v. 40(8), p. 1369-1380, 1995.

YAN, Z.; YANG, H.; QU, F.; ZHANG, H.; RONG, H.; YU, H.; VAN DER BRUGGEN, B. Application of membrane distillation to anaerobic digestion effluent treatment: identifying culprits of membrane fouling and scaling. *Science of The Total Environment*, v. 688, p. 880-889, 2019.

ZHANG, P; KNÖTIG, P.; GRAY, S.; DUKE, M. Scale reduction and cleaning techniques during direct contact membrane distillation of seawater reverse osmosis brine. *Desalination*, v. 374, p. 20–30, 2015.

ZODROW, K. R.; BAR-ZEEV, E.; GIANNETTO, M. J.; ELIMELECH, M. Biofouling and Microbial Communities in Membrane Distillation and Reverse Osmosis. *Environmental Science & Technology,* v. 48, p. 13113164, 2014.

CHAPTER 3

Removal of 17α-ethinylestradiol and Estrogenicic Activity by a novel Hybrid Membrane Distillation-LED-UV system

1 INTRODUCTION

Micropollutants (MPs) are substances present in aquatic environments in low concentrations, typically in the range of ng – μg.L^{-1} (GRANDCLÉMENT et al., 2017). Among MPs, pharmaceutically active compounds (PhACs) are of great concern. In 2017, the total spending on prescription drugs was around $ 1135 billion (OECD, 2017). This number indicates the extent of PhACs consumption, which tends to increase with the advancement of the pharmaceutical field and the aging population. Thus, the non-metabolized fraction of PhACs and their metabolic products reach wastewater, mainly through human excreta and the inappropriate disposal of expired drugs (ARRIAGA et al., 2016; LUO et al., 2014). In their review, Grandclément et al. (2017) verified the existence of 78 peer-reviewed studies in which the presence of drugs in the affluent of wastewater treatment plants (WWTP) was found in concentrations ranging from 1.60 ng.L^{-1} to 373 μg.L^{-1}. The researchers observed that MP removal is commonly conditioned on compound properties and process characteristics in conventional WWTP, with an efficiency that varies from >70% for some MP, like naproxen, caffeine, and bisphenol, to a low rate (<40%) for diclofenac, carbamazepine, and metoprolol.

Among the consequences of the permanence of these compounds in aquatic environments, it can be mentioned: changes in the metabolism; impairment of the immune, reproductive and endocrine systems; and some types of cancer (REUNGOAT et al., 2009; FERNANDES et al., 2011; PARK, 2013). As example, Lydche et al. (2011) found that the increased incidence of obesity and type 2 diabetes may be related to the presence of MPs in the waters. The compounds capable of changing the functioning of the endocrine system are called endocrine-disrupting compounds (EDCs). Among EDCs, estrogenic compounds - which act like the female hormone 17β-estradiol - are drawing attention. Estrogenicity is the ability of a substance to bind to the estrogen receptor and elucidate a biologically similar response to those produced by endogenous hormones. The synthetic hormone 17α-ethinylestradiol, used in birth control pills, is an exogenous hormone and has an estrogenic potency similar to 17β-estradiol (DASTON et al., 1997).

Most conventional treatment plants do not have an adequate monitoring system for these contaminants and are not designed to remove them. The compounds are partially biodegraded or are not removed during treatment, being detected, consequently, in surface water and drinking water sources (EGGEN et al., 2014; COUTO et al., 2019). Miralles-Cuevas et al. (2017) evaluated the effluent from a municipal sewage treatment plant, and more than 30 MPs

were detected. In Brazil, basic wastewater treatment is still a concern since this service does not serve the entire population, leading to MPs pollution being treated as a secondary problem (COLAÇO, 2014). Thus, drugs are detected in raw and treated wastewater, water bodies, and water supplies throughout Brazil (AQUINO et al., 2013; REIS et al., 2019). Santos et al. (2020) verified the presence of MP in drinking water, indicating that conventional drinking water treatment plants cannot completely remove these compounds, which can put human health at risk.

This scenario highlights the need for improvements in the WWTPs treatment processes. Advanced technologies must be applied since they can retain these MPs or transform them into less harmful compounds to living beings. Several technologies capable of producing high-quality water have been researched, among which can be mentioned: membrane separation processes (MSP); adsorption with activated carbon and advanced oxidative processes, which can use UV irradiation, hydrogen peroxide, catalysts, metal complexes, ozonation, or a combination of these (CARLSON et al., 2015).

Membrane distillation (MD) is an MSP considered a promising alternative for the water-energy nexus (DESHMUKH et al., 2018). MD is a thermally-driven separation process capable of generating high-quality water. In MD, a hydrophobic microporous membrane separates a hot phase (feed) from a cold phase (permeate), creating a temperature gradient across the membrane and inducing a vapor pressure gradient between the two phases (BAKER, 2004; ALKHUDHIRI et al., 2012). Typically, a temperature difference of 10 to 20ºC can promote steam permeation, allowing the coupling with renewable energy sources. MD presents a 100% theoretical rejection of non-volatile contaminants. When compared to other MSPs, such as reverse osmosis (RO) and nanofiltration (NF), MD has some additional advantages, such as being conducted without hydraulic pressure, which increases the safety of the system and reduces equipment expenses (MANA; PAL, 2016).

Several studies have applied MD to remove MPs and generate high-quality water. Woldemariam et al. (2016) conducted a pilot-scale study to evaluate the removal of PhACs from a WWTP effluent using MD in the air-gap configuration. The heat source was the return line of a district heating network, a low-temperature source. Most PhACs were removed to a concentration below the detection limit of the method used. Silva et al. (2018) found rejections of ions and drugs greater than, respectively, 99% and 99.6% in seawater matrix in MD in the direct contact configuration.

MD has demonstrated to be more efficient than competitive technologies, such as membrane bioreactors and NF concerning PhACs removal. Regarding RO, similar removals were observed for many MPs. It is important to highlight that MD is a robust alternative since it has greater independence from MPs characteristics, and it is more resistant to variations in the matrix, such as variations in the concentration of compounds in the feed, for example (WOLDEMARIAM et al., 2016; SILVA et al., 2018). Couto et al. (2020) observed a high removal of PhACs by MD than by NF and RO.

However, MD has its performance deteriorated by fouling - the deposition of unwanted material on the membrane surface (WARSINGER et al., 2014). MD is susceptible to all fouling types: inorganic, organic, and biological (TIJING et al., 2015). Recently, many researchers have studied biofouling in MD (BOGLER et al., 2017; LIU et al., 2019; LIU et al., 2020). Biofouling decreases vapor pressure, increases temperature polarization, improves resistance to heat and mass transfer (GOH et al., 2013), and promotes pore wetting. Therefore, flux and quality of the permeate decrease (MANSOURI et al., 2010), increasing energy demand.

UV lamps are promising alternatives to mitigate MD fouling. They are effective as bactericides; are simple to install and maintain; and do not involve chemicals (MATIN et al., 2011). Mofidi et al. (2000) carried out a pilot-scale study of the effect of introducing an irradiation step with a mercury lamp in the control of RO membrane fouling. It was observed that the adherence to the membrane of the irradiated bacteria decreased by 50%, reducing fouling and increasing permeate flux. The disadvantage of UV pretreatment is that it has no residual effect (KIM et al., 2009). Besides, its efficiency is related to feed quality since higher turbidity limits light penetration (AL-ABRI et al., 2019). The hybrid system can overcome this risk of microorganisms regrowth through direct irradiation of the membrane. Another advantage of the hybrid system is the greater robustness to reach the fouling when the treated matrix has high turbidity (GUO et al., 2015). Although there are studies on UV-MD modules, they have been used for other applications, such as photocatalytic membrane regeneration (GUO et al., 2019).

Although the UV-MD coupling is promising, it is still necessary to investigate whether the typical efficiency of MD in removing pollutants of great concern, such as EDCs, is affected. Many organic molecules absorb radiation in the UVC range (wavelengths less than 300nm) (BOREEN et al., 2005), being susceptible to degradation by photolysis. UV radiation has been widely investigated to degrade several MPs in water and wastewater, of which 17β-estradiol (E2), 17α-ethinylestradiol (EE2), diclofenac, ibuprofen, and ketoprofen can be mentioned. In

most studies, direct photolysis is used as a control group of different advanced oxidative processes (POAs), which, in general, have greater efficiencies in removing pollutants than just direct photolysis (YANG et al., 2013).

Photolysis efficiency of degrade EDCs is related to many factors. It can be cited: the compound properties, pollutants initial concentrations, the light source, pH, and temperature. Concerning EE2, photolysis follows pseudo-first-order kinetics (ZHANG et al., 2010). The EE2 removal by photolysis is faster than other EDCs removal, as estrone, E2, and estriol. It is attributed to EE2 instability because of the ethynyl group, which can quickly absorb UV radiation. There is no unique reaction pathway for EDCs photodegradation (SORNALINGAM et al., 2016). Despite the opportunity for MP, such as EDCs, degradation in a UV-MD system concentrate, irradiation in the hybrid module can damage the membrane, impairing the removal of micropollutants.

Most studies concerning irradiated processes use mercury as the radiation source (MATAFONOVA; BATOEV, 2018). However, it is a toxic substance and leads to several problems when disposed of in the environment. It also has a high energy demand and a relatively short lifetime (BOTON; COTTON, 2011; JO; TAYADE, 2014). In addition, there is a global movement to stop using mercury (MATAFONOVA; BATOEV, 2018). In this context, the light-emitting diode (LED) can be used as a UV radiation source (MATAFONOVA; BATOEV, 2018). LED is an n-p type junction semiconductor that releases the excess of energy in light and heat when an electric current is applied. (JO; TAYADE, 2014; CHEN et al., 2017). LEDs have been used in various environmental applications since they are more environmentally friendly, more robust, active immediately, have less toxic components, and a longer lifetime (JO; TAYADE, 2014). As well as the photolysis processes investigated with the mercury lamp, most studies with UV-LEDs investigate direct photolysis as the control group of the coupling with photocatalytic processes, and photolysis is often less efficient than the processes studied (AUTIN et al., 2013; ARLOS et al., 2016; JALLOULI et al., 2017; CASADO et al., 2017; LIANG et al., 2019).

A limitation of UV-LEDs is the more significant loss of energy due to heat, increasing operating costs (MATAFONOVA; BATOEV, 2018). However, it may not be a complete disadvantage in coupling LEDs and MD since the feed must be kept heated to maintain the driving force. Concerning the photolysis lower efficiency, Real et al. (2009) studied the effect of temperature on the degradation by photolysis of three MPs. It was noticed that the increase in temperature

promoted an increase in the reaction constants in the studied conditions. It indicates the possibility of degradation of compounds present in the MD concentrate in MD-LED-UV coupling. Therefore, the present study investigates, for the first time, the removal of EE2 and estrogenicity in a new hybrid MD-LED-UV module.

2 MATERIALS AND METHODS

2.1 Experimental apparatus

The system scheme used in the study is shown in Fig 3.1. The experimental apparatus consists of: a feed tank; a heat exchanger automatically activated by a thermostat controller (MT520E fast, Full Gauge Controls, Canoas, Brazil); a distillate tank; a chiller (Chiller Gelaqua 1/8 hp., Santos, Brazil); a digital scale (L10001, BEL Engineering, Monza, Italy); the hybrid module; four thermometers inserted at the module inlets and outlets (TD08, Tecmak, Belo Horizonte, Brazil); and four diaphragm pumps (SFDP1-012-035-21, Seaflo, Fujian Liancheng County, China) coupled with circulation speed controllers to recirculate, feed, distillate, and both heating and cooling water. The scale was connected to a computer for automatic monitoring of the distillate mass variation.

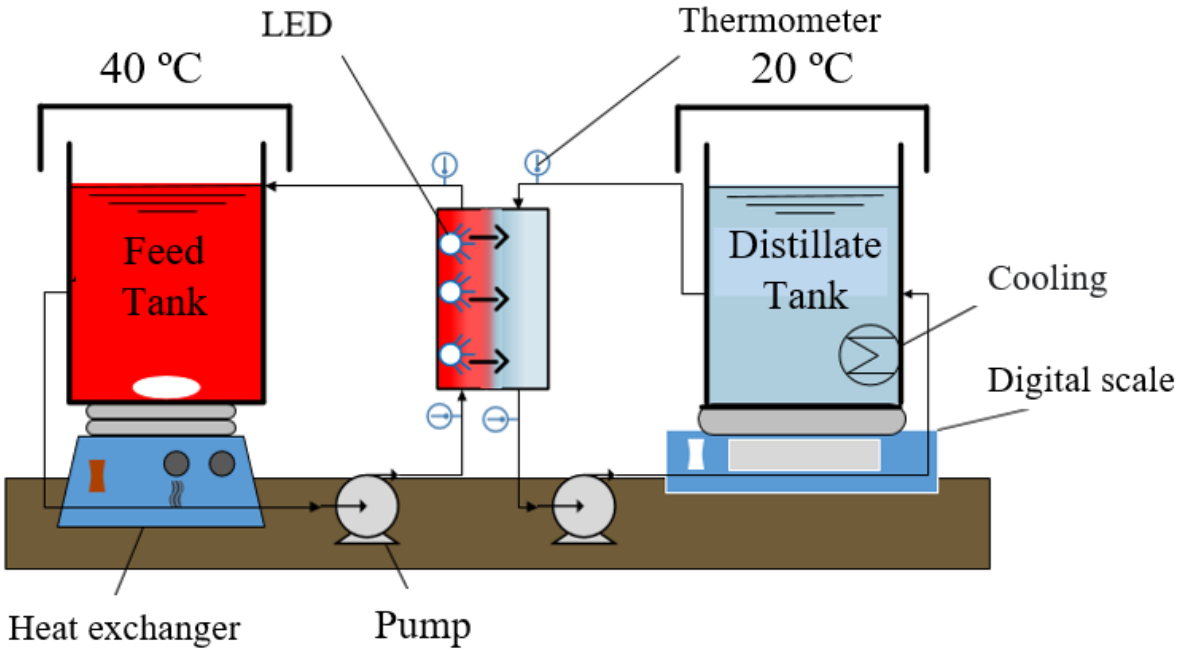

Fig. 3. 1 – Scheme of the experimental apparatus used in all tests

2.1.1 Hybrid MD-LED-UV module

The hybrid MD-LED-UV module is the same used in the tests of the previous chapter. It was manufactured in acrylic in the DCMD configuration. It has a window in the feed compartment in which a quartz plate was fitted, as shown in Fig. 3.2. Quartz is necessary for emitted radiation is not absorbed and can reach EE2, allowing the absorption of energy by the molecules. Thus,

the EE2 solution, previously heated, is recirculated in the feed compartment, where the LED can be coupled so that UV irradiation occurs. Water vapor will permeate the hydrophobic membrane's pores in this same compartment due to the temperature gradient.

The flat-sheet MD membrane was obtained from Sterlitech Corporation (Kent, USA) and was made of polytetrafluoroethylene (PTFE) in a non-woven polypropylene. It has an average pore size of 0.2 μm. The effective membrane area was 89.25 cm^2. The quartz plate area and, therefore, the effective irradiation area was 24.4 cm^2. The UVC-LED wavelength range is 260-280 nm, and it is the 59S brand, model X1.

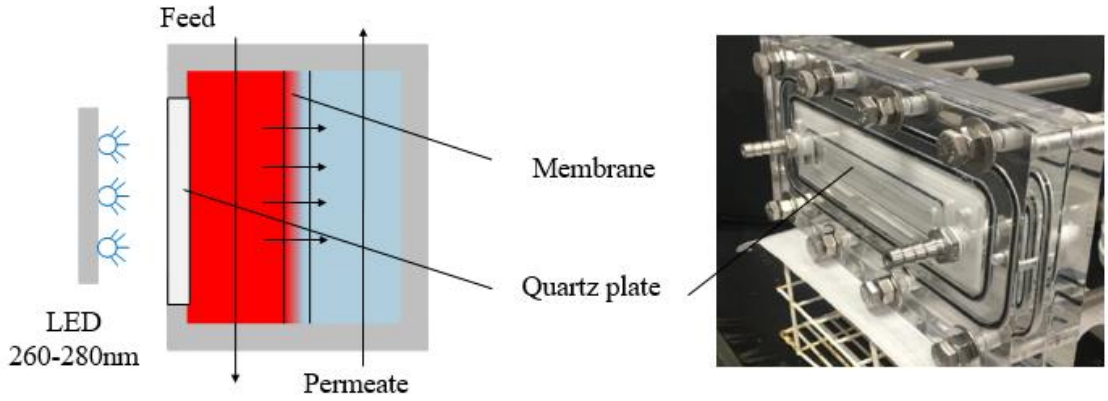

Fig. 3. 2 - On the left, the MD-LED-UV hybrid module (Top view). On the right, a photo of the built module.

2.2 Experimental procedure

17α-ethinylestradiol (Table 3.1) was purchased from Sigma Aldrich (Cotia, São Paulo, Brazil), and a stock solution (251.1 $mg.L^{-1}$) was prepared in pure methanol (Sigma Aldrich). EE2 was chosen to assess the impact of LED on removing EDCs because its potential for endocrine-disrupting is much higher than other synthetic EDC substances (NGHIEM; SCHÄFER, 2002). In addition, EE2 has less biodegradability and, therefore, greater persistence in natural environments when compared to other estrogens (CLOUZOT et al., 2008).

To feed the system, 4 L of a NaCl solution (10 $mmol.L^{-1}$) in distilled water was prepared to obtain a conductivity close to that of the wastewater. Moreover, EE2 (100 $\mu g.L^{-1}$) was added. This concentration level was chosen due to the existence of effluents from contraceptive factories and other industrial effluents, in which the hormone concentration is higher than that

found in natural bodies of water (ZHANG et al., 2010). The initial distillate was 3 L of distilled water.

Table 3. 1- Physicochemical properties of EE2

Molecular Weight	Log K_{ow}	pK_a	pK_H	Vapor pressure
296.41 $g.mol^{-1}$	3.9	−1.66 and 10.33	11.09	3×10^{-7} Pa

Two experiments were carried out, one without LED and one with LED. The recirculating flow rates for feed and distillate were 1.25 $L.min^{-1}$ (a cross-flow velocity of 4.6 $cm.s^{-1}$), indicating a laminar flow regime (Re ≅ 1300). All tests were conducted under atmospheric pressure. The heating and cooling systems were adjusted to maintain approximately 40 and 20ºC in the feed and permeate, respectively. Each 10 min, the conductivity and temperature of the feed and distillate tanks were monitored. The feed and distillate temperature in the module outlet and the distillate weight variations to calculate MD flux were also registered.

To evaluate the effect of the hybrid module, 490 minutes of radiation was provided by the LED, resulting in a residence time in the feed compartment of 1 second and an average radiation time per particle of 3 minutes over the test. The relatively short time of radiation per particle was chosen to not result in higher energy costs. Thus, the total time for each test was 550 minutes.

A test under conditions similar to the tests previously described was performed. It was a 550-minutes test with 490 minutes of radiation and aimed at quantifying the heat that the LED transfers to the system. In this test, the automatic heating and cooling systems remained off.

2.3 Analytical methods

The initial feed, concentrate, and distillate samples were characterized by the electrical conductivity (2510, HI763100 Hanna Instruments conductivity meter) in accordance with the Standard Methods for the Examination of Water and Wastewater.

For the quantification of EE2 by UV spectrophotometry and mass spectrometry, first, the solid-phase extraction was performed, it was performed in C18-E cartridges (Strata C18-E, 55 μm, 70 A, Ref. 8B-S001-HCH). The cartridges were first conditioned with 5 ml of methanol and 5 ml of water. Then, 200 mL of the feed solution and 2.2 L of distillate were percolated through the cartridge for analytes concentration, using a flow rate of 5 $mL.min^{-1}$. After the sample had

passed through the cartridge, the vacuum pump remained in operation for approximately 20 minutes. Elution was performed by percolating 4 ml methanol twice through the cartridge.

For the UV spectrophotometry, first, the solid-phase extraction was performed as described previously. The analyte was eluted in 4 mL of methanol, and the scan was performed on the UV Visible spectrophotometer, PerkinElmer Lambda XLS. The calibration curve was constructed from EE2 solutions in concentrations of 1.6 to 4 $mg.L^{-1}$. The absorbance measurements of the samples were read at values corresponding to the maximum absorbance wavelength (λmax) of the hormone in methanol, equal to 207 nm (Fig 3.3), which represents the conjugated double bonds. The lowest intensity peak at 280 nm is related to the phenolic ring (BILA, 2005). The samples were scanned from 200 to 300 nm.

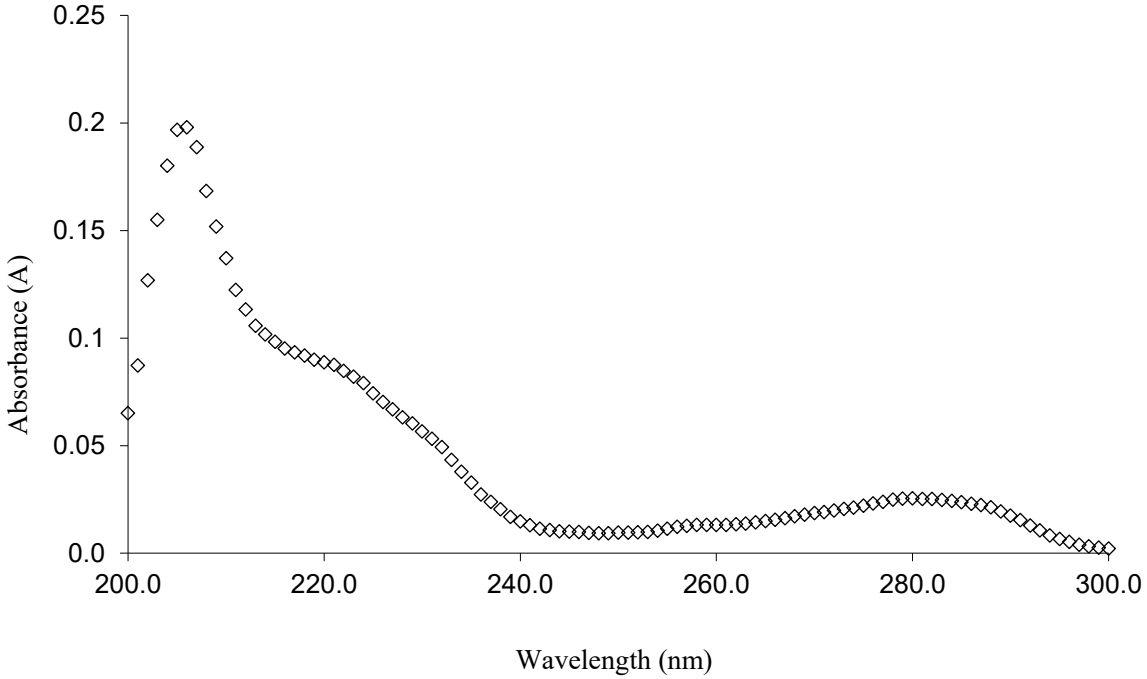

Fig. 3. 3– Absorption spectrum of a solution of 17α-ethinylestradiol in methanol 2.5 $mg.L^{-1}$

Before HPLC injection, the extracts were filtered using a 0.45 µm PTFE syringe filter. The final extracts were refrigerated at -18 ° C until identification and quantification. EE2 in permeate samples was quantified by liquid-chromatography (Shimadzu Prominence UFLC, Shimadzu, Kyoto, Japan) coupled with mass spectrometry (MicrOTOF-QII, Bruket Daltonics, Bremen, Germany) (LC-MS). The method applied is described in detail in Ricci et al. (2019) and Faria et al. (2020), with some modifications. Compounds present in the matrix were separated using

a 50 mm × 2.1 mm Titan^{TM} C18 column with a 1.9 μm particle size (Supelco, Bellefonte, PA, USA). The mobile phase was composed of solvent A (water with 0.1 % formic acid) and solvent B (acetonitrile with 0.1 % formic acid). First, 5 % of B was introduced, which, after 5 min, increased to 50 %. This percentage of B was constant for 6 min. Next, % B was raised to 70 % and kept constant for 12 min. EE2 was identified in 7.3 min.

2.4 YES assay

2.4.1 Sample extraction

For the YES assay, the solid-phase extraction of the samples was carried out according to the methodology of Nascimento et al. (2018). First, the pH of the samples was adjusted to 3 with an HCl solution. The C 18/18% cartridges (500 mg / 6mL - Applied Separations) were conditioned as follows: 3 x 2 ml of hexane, 1 x 2 ml of acetone, 3 x 2 ml of methanol, and 5 x 2 ml of ultrapure water at pH 3. After percolating the samples, elution was carried out with 4 x 1 mL of acetone. The extracts were left at room temperature until the solvent evaporated and were stored at - 20 ºC until the time of the YES test, which was carried out at the Laboratory of Aquatic Ecotoxicology of the Federal University of Viçosa.

2.4.2 Assay procedure

The YES assay was conducted according to the protocols developed by Routledge and Sumpter (1996) and Bila et al. (2007). All the glass containers used to store and prepare the solutions were left in an acid bath (20% HNO_3) for at least 24 h, rinsed with running water, distilled water, ultrapure water, acetone, and, finally, ethanol. The tips were autoclaved at 120°C for 15 min. Not sterile materials that cannot be autoclaved have been placed under UV radiation for 5 min.

Tests were conducted in 96-well microtiter plates (Fig. 3.4). The standard curves contained 12 concentrations, varying from 2.724 ng.L^{-1} to 1.33 ng.L^{-1}. Ethanol was used as blank solvent control. 10 μL of each sample extract was serially diluted in ethanol and tested in duplicate. When ethanol evaporated from the sample and blank wells, 200 μL of analysis medium were added to each well. Then, the plates were sealed, shaken for 2 min on a plate shaker, and maintained at 32 °C. After 72 h incubation, plates were shaken again for 2 min and left to settle for one hour. Absorbances were measured at 540 nm for color and 630 nm for turbidity in a Polaris® microplate reader (Celer Biotechnology, Belo Horizonte, Minas Gerais, Brazil).

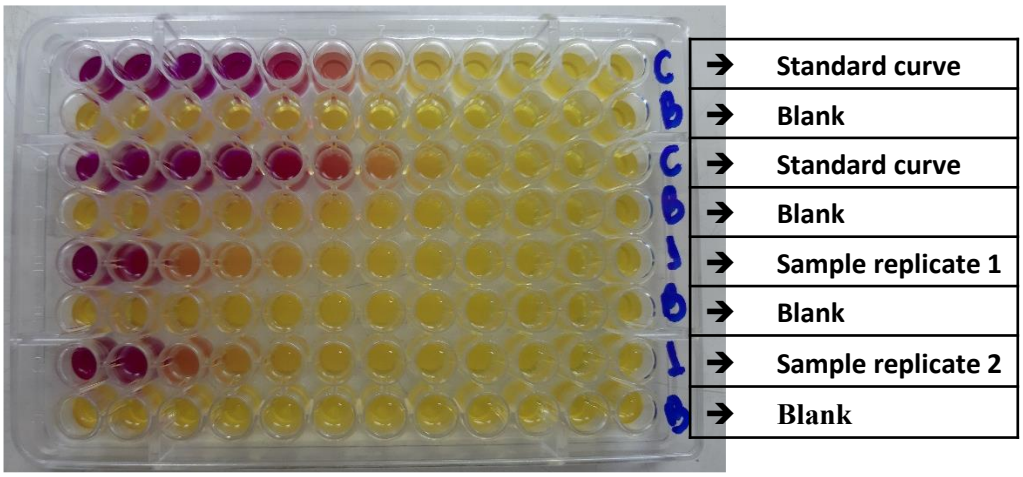

Fig. 3. 4 – Yes assay microplate obtained after 72 h incubation

Source: Arcanjo et al. (2021)

The estrogenic activity of the samples was reported as 17β-estradiol (E2) equivalents (E2-eq.).

Concerning YES assay, the absorbance (C_{abs}) of each well was corrected with Eq. 3.1:

$$C\ abs = S_{540} - (S_{630} - Control_{630}) \quad (3.1)$$

S_{540} and S_{630} are the sample absorbances measured at 540 nm for color and 630 nm for turbidity, respectively.

For the E2 standard curve and EE2, corrected absorbance was plotted versus the concentration and fitted to a four-parameter logistic regression dose-response curve (Eq. 3.2).

$$C\ abs = \frac{A_1 - A_2}{1 + \left(\frac{x}{EC_{50}}\right)^p} + A_2 \quad (3.2)$$

A_1 is the basal induction of estrogenic activity, A_2 is the maximum induction of estrogenic activity, p is the hillslope, EC_{50} is the 50% effective concentration, and x is the concentration of the compound.

To calculate the estrogenic activity of the samples as E2 equivalents (E2-eq.), an interpolation was made from the E2 standard curve. Estrogenic activity is calculated by the average of three wells in which the absorbance has a higher correlation with the dilution. The limit of detection (LOD) was established as the concentration of E2 that produces an effect equal to the blank's average absorbance plus three times its standard deviation. The limit of quantification

(LOQyes) was considered the concentration of E2 that induces an effect equal to the blank's average absorbance plus ten times its standard deviation (EPA, 2016).

2.5 Membrane evaluation

Since the ultraviolet radiation can degrade organic molecules, it is necessary to assess whether the direct membrane irradiation - provided by the hybrid module and the fact that the matrix does not present high turbidity, so there is not a layer of fouling covering the membranes – can damage the PTFE membrane. Thus, the effect of LED-UV on the integrity of the membrane's surface used in the tests was analyzed with Scanning Electron Microscopy (SEM) and Energy Dispersive Spectroscopy (EDS).

To assess the effect of LED-UV membrane hydrophobicity, contact angle measurements were taken from a fresh membrane sample and a membrane irradiated for 32,200 minutes. The measurements were made using the Tensiometer Tilt Controller Phoenix – Phoenix Multi/Tilting. Approximately 10 μL of water was used, and the angle calculation was performed by the Surfaceware 9 software using the tangent method. 5 readings were performed at 3 different points on the membranes. To evaluate the effect of LED exposure on the chemical composition of membranes, attenuated total reflectance infrared spectroscopy (ATR-FTIR) was performed. The evaluation was performed using a NicoletTM IS 50 FT-IR spectrometer – Thermo Fisher Scientific. Three readings were performed in different regions of the sample.

2.6 Calculus

The MD permeate flux (J) was calculated by Eq. 3.3:

$$J = \frac{M_t - M_{t,i}}{A \times t} \tag{3.3}$$

Where J is given in $Kg.h^{-1}m^{-2}$, M_t is the mass of the permeate tank (Kg) at time t (h), $M_{t,i}$ is the initial mass of the permeate tank, and A is the effective area of the membrane (m^2).

The rejection of the evaluated parameters (R) was calculated using equation 3.4.

$$R\ (\%) = \frac{C_f - C_d}{C_f} \times 100\% \tag{3.4}$$

Cf is the concentration of the compound present in the feed, and Cd concentration of the compound permeated the membrane, considering de volume that permeated MD during the tests.

2.6.1 Temperature polarization

The effect of the LED in MD concerning temperature polarization was assessed in accordance with Srisurichan et al. (2006). Heat transfer is divided: (i) in convective heat transfer, which occurs from the bulk heated feed to the membrane surface boundary layer at the feed side (Eq. 3.5), (ii) conduction and latent heat transfer across membrane pores (Eq. 3.6) and convective heat transfer from the membrane surface boundary layer at the permeate side to the bulk permeate (Eq. 3.7).

$$Q = h_f\ (T_f - T_1) \tag{3.5}$$

Where Q is the heat flux; h_f is the heat transfer coefficient in the boundary layer at the feed side; T_f is the mean of the temperatures at the feed inlet and outlet of the module, considered as the MD feed bulk temperature; and T_1 is the temperature at the feed membrane surface.

$$Q = J\Delta H_v + \frac{k_T}{\delta}\ (T_1 - T_2) \tag{3.6}$$

Where ΔHv is the vaporization heat of water (2456 kJ.Kg^{-1} at 20 °C (RICCI et al., 2019)); k_T is the membrane thermal conductivity, calculated according to Ricci et al. (2019) and equals to 90.4 kW.m^{-1}.K^{-1}; δ is the membrane thickness (170 μm (MANAWI et al., 2014)); and T_2 is the temperature in the membrane surface at the permeate side.

$$Q = h_p\ (T_2 - T_p) \tag{3.7}$$

Where h_P is the heat transfer coefficient in the permeate boundary, and TP is the mean of the temperatures measured at the cold entrance and the cold exit of the module, considered as the MD permeate bulk temperature.

h_f and h_p were calculated with Eq. 3.8.

$$h = \frac{Nu\ k_f}{L} \tag{3.8}$$

Where k_f is the fluid thermal conductivity, L is the characteristic length, and Nu is the dimensionless Nusselt number, calculated with the Graetz-Lévêque Equation (Eq. 3.9) for laminar flux.

$$Nu = 1.86\ (Re\ \mathrm{Pr}\ \frac{d_h}{L_c})^{0.33} \tag{3.9}$$

Where d_h is the hydraulic diameter; L_c is the channel length; Re is the Reynolds number (Eq 3.10), and Pr is the Prandtl number (Eq 3.11).

$$Re = \frac{d_h \nu \rho}{\mu} \tag{3.10}$$

$$Pr = \frac{C_p \mu}{k_f} \tag{3.11}$$

Where ν, ρ, μ, and C_p are, respectively, the average fluid velocity, density, dynamic viscosity, and heat capacity.

From equations 3.3, 3.4, and 3.5, and heat balance, temperatures at the membranes' surface can be determined with Eq. (3.12) and (3.13).

$$T_1 = \frac{\frac{k_T}{\delta}\left[T_P + \left(\frac{h_f}{h_P}\right)T_F\right] + h_f T_f - \mathrm{J}\Delta H_v}{\frac{k_T}{\delta} + h_f\left[1 + \left(\frac{k_T}{\delta h_f}\right)\right]} \tag{3.12}$$

$$T_2 = \frac{\frac{k_T}{\delta}\left[T_f + \left(\frac{h_P}{h_f}\right)T_P\right] + h_P T_P + \mathrm{J}\Delta H_v}{\frac{k_T}{\delta} + h_P\left[1 + \left(\frac{k_T}{\delta h_{Af}}\right)\right]} \tag{3.13}$$

Finally, the temperature polarization coefficient (τ) was calculated by Eq. 3.14

$$\tau = \frac{T_1 - T_2}{T_f - T_p} \tag{3.14}$$

2.6.2 Concentration polarization

The effect of LED in the concentration polarization, which is the phenomenon that concentration at the membrane surface at the feed side ($C_{m,f}$) is higher than the concentration in

bulk ($C_{b,f}$). Both concentrations are related by the Nernst film model (RASTOGI et al., 2015) (Eq. 3.15).

$$C_{m,f} = C_{b,f}\, exp\left(\frac{J}{K_m}\right) \tag{3.15}$$

Where Km is the solute coefficient of mass transfer, estimated through Eq. 3.16, with Sherwood (Sh) (Eq. 3.14) and Schmidt (Sc) numbers (Eq. 3.15).

$$Sh = 1.86\left(Re\, Sc \frac{d_h}{L_c}\right)^{0.33} \tag{3.16}$$

$$Sc = \frac{\mu}{\rho D_T} \tag{3.17}$$

$$k_m = \frac{Sh\, D_T}{d_h} \tag{3.18}$$

The coefficient of concentration polarization (ζ) was obtained through Eq. 3.19.

$$\zeta = \frac{C_{m,f}}{C_{b,f}} \tag{3.19}$$

2.6.3 Vapor pressure polarization

The polarization of vapor pressure may occur due to both temperature and concentration polarization. The temperature polarization coefficient (ψ) is given by equation 3.20 and represents the fraction of the applied vapor pressure that effectively promotes permeation.

$$\psi = \frac{\Delta P_m}{\Delta P_b} \tag{3.20}$$

Where ΔP_m e ΔP_b are, respectively, the difference in vapor pressure on both sides of the membrane surface and the difference in vapor pressure between the bulk solutions. Vapor pressure without salinity (P), but dependent on temperature, was calculated using the Antoine relation. To obtain the vapor pressures in the feed compartment considering salinity ($P_{s,f}$), the activity coefficient (a) was calculated, which, due to the low concentration of NaCl, were very close to 1.

(3.21)

$$P_{s,f} = P \times a$$

2.6 Statistic Evaluation

Mann-Whitney test was applied to verify significant differences in the performance of both tests. It aimed at investigating how the coupling with the LED affects the system. The non-parametric test was applied at a 5% significance level. STATISTICA 8.0 software was used for the statistical analyses.

3 RESULTS AND DISCUSSION

3.1 MD and MD-LED-UV performance

3.1.1 Flux and polarization

At the beginning of the tests, the permeate flux (J) decreased in the MD test and increased in MD-LED-UV (Fig 3.5 (a)). The variations in flux profile are related to temperature variations in feed. In the last three hours of the experiment, the flux in the MD-LED-UV system was stable for more than two hours, tended to stabilize at an average value of 3.5 LMH. Without coupling with LED, the flux tended to stability in the last hour of the experiment, at an average value of 3.1 LMH.

Flux in this order of magnitude was expected. Liu et al. (2019), when operating the MD with PTFE membrane at 40ºC, obtained a flux of 4.0 LMH and 9.7 LMH when the temperature was 60ºC. A preliminary test of 500 minutes was carried out in conditions similar to the test without LED with a feed temperature of 60 ºC. Although a higher average flux (8.5 LMH) was obtained, there was much loss through evaporation. Allied to this, the lower energy expenditure of the operation at 40ºC was decisive in choosing to conduct this study at this temperature.

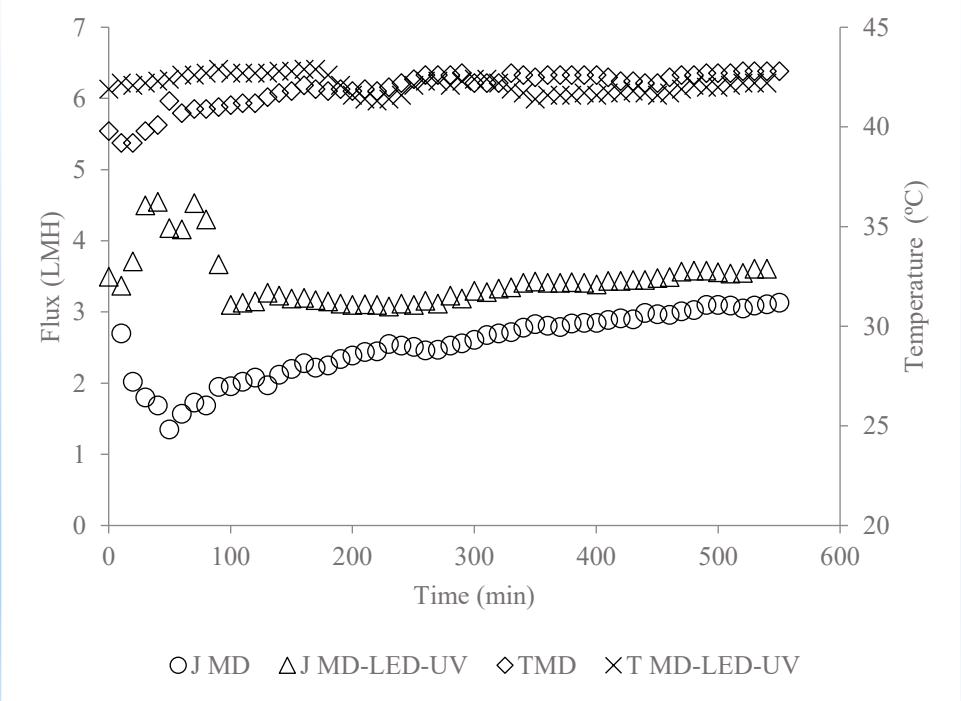

(a)

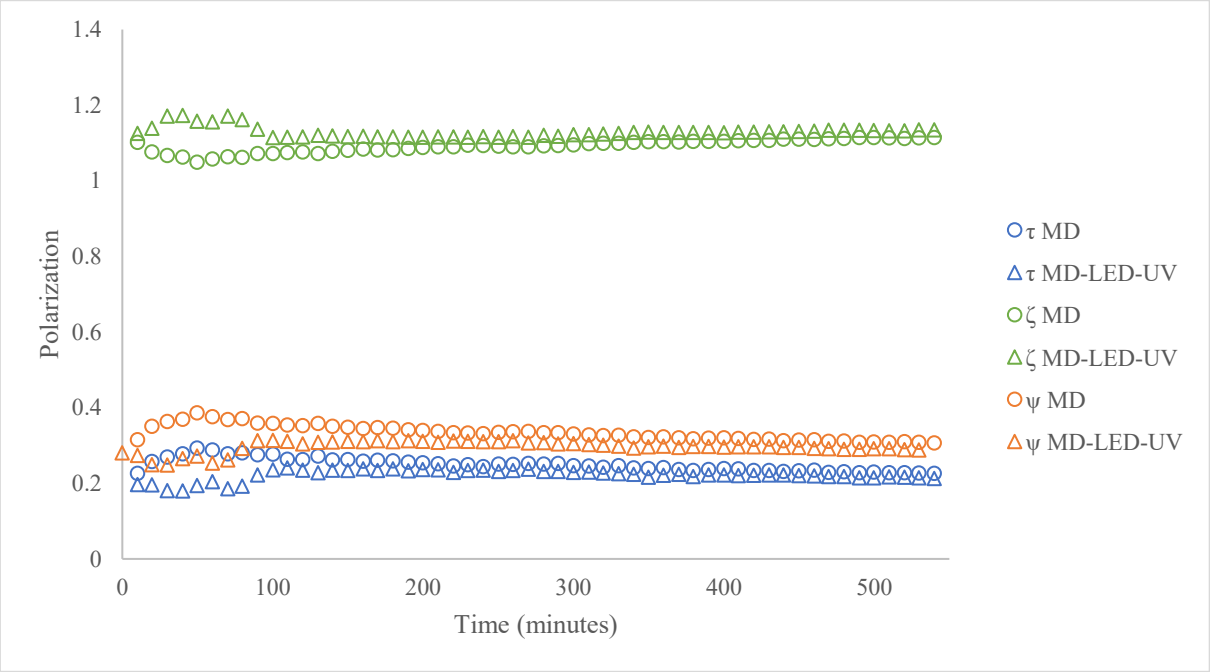

(b)

Fig. 3. 5 – Variations of the (a) flux and vapor pressure polarization

The flux in the MD-LED-UV system was significantly higher than in the system without LED ($p = 0.0007$). When comparing the effect of the LED on the increase in flux by applying the statistical test to the normalized flux data, the hybrid module also promotes a significantly higher flux increment ($p = 0.02$). However, the coupling with the LED did not significantly change the temperature difference between the membrane feed and bulk permeate (Table 3.2). The mean ΔT in the membrane in the systems without and with LED were, respectively, 5.0 ± 0.36 and 4.9 ± 0.4.

In addition, the temperature polarization coefficient for the hybrid system was lower than for the hybrid module (Fig. 3.5 (b)). As τ decreases, the effect of temperature polarization on the MD process increases (ABU-ZEID et al., 2015). The vapor pressure in the bulk feed of the MD-LED-UV system was higher than in the system without LED. However, the vapor pressure on the membrane surface in the MD-LED-UV system was lower, resulting in greater pressure polarization. The slightly lower presence of compounds on the irradiated membrane (C_m) surface was insufficient to increase the vapor pressure, collaborating for a higher flux. Ricci et al. (2019) observed that lower concentrations on boundary layers do not lead to a great increase in vapor pressure, which is even more evident in this study. The low salt concentration led to water activity coefficients close to one. The greater independence of MD concerning feed

concentration is an advantage compared to pressure-driven processes, which have their flux drastically reduced by the polarization of concentration (DRIOLI; MACEDONIO, 2015).

Table 3. 2 – MD polarization without and with the LED-UV

Test	$T_{f,b}$[a] (ºC)	$T_{p,b}$[b] (ºC)	T_1[c] (ºC)	T_2[d] (ºC)	τ[e]	C_m[f] (g.L^{-1})	ζ[g]	$P_{b,f}$[h] (Pa)	$P_{m,f}$[i] (Pa)	ψ[j]
MD	40.9 ± 0.9	20.8 ± 0.6	33.4 ± 0.6	28.4 ± 0.8	0.249 ± 0.018	0.64 ± 0.01	1.09 ± 0.02	7780 ± 370	5170 ± 171	0.333 ± 0.020
MD-LED-UV	41.1 ± 0.5	20.1 ± 0.6	32.7 ± 0.0.4	27.8 ± 0.6	0.222 ± 0.015	0.60 ± 0.01	1.13 ± 0.01	7830 ± 189	4946 ± 121	0.296 ± 0.017

[a] Bulk feed temperature; [b] Bulk permeate temperature; [c] Temperature at membrane feed surface; [d] Temperature at membrane permeate surface; [e] Coefficient of temperature polarization; [f] NaCl concentration at feed surface; [g] Coefficient of concentration polarization; [h] Bulk feed vapor pressure; [i] Membrane surface vapor pressure; [j] Coefficient of vapor pressure polarization.

Thus, the higher MD-LED-UV fluxes are not due to the heat transferred by the LED to the system. During operation, the LED provided 60 kJ of heat to the system (33 and 27 kJ for feed and permeate, respectively). It is worth mentioning that the effect of the LED on the feed temperature could not be observed since the temperatures were controlled automatically. As the LED provides heat, there is a saving on the heating system of the feed tank, which is activated fewer times with the additional heat source.

3.2 Membrane evaluation

The most likely explanation for the higher flux of the hybrid system is the surface modification by direct UV radiation, as suggested by the SEM images (Fig 3.6). However, it is noteworthy that the difference observed, although significant, does not have great relevance from the practical point of view of the operation.

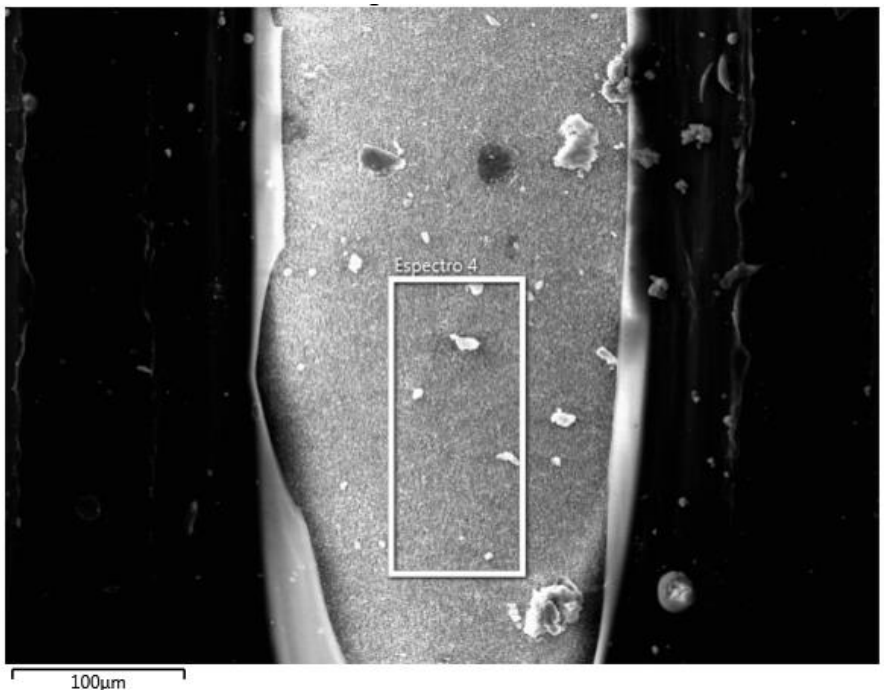

(a)

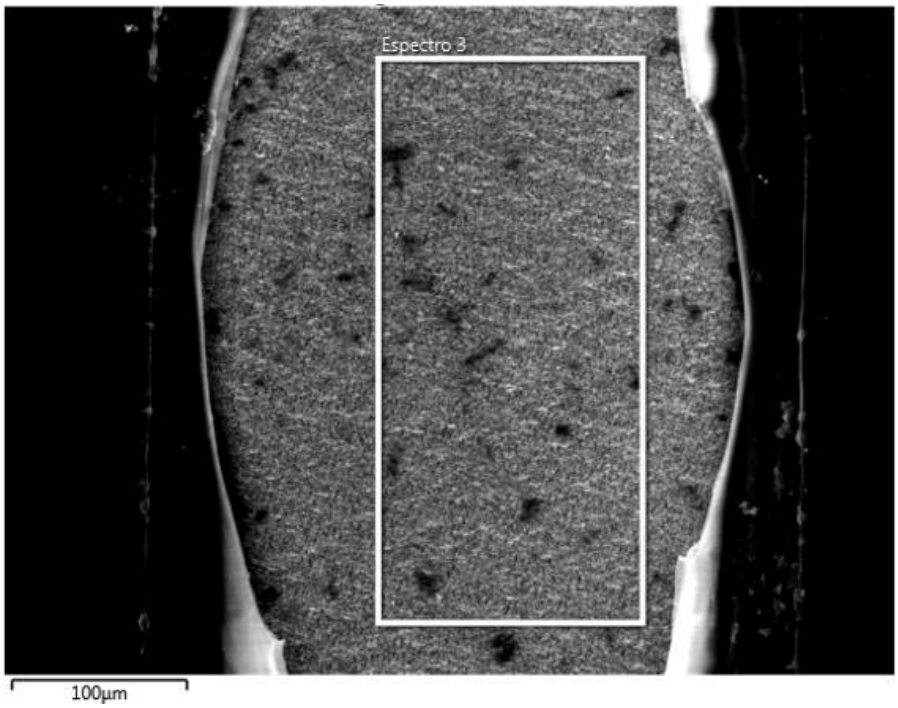

(b)

Fig. 3. 6 – SEM membrane surface analysis from (a) MD and (b) MD-LED-UV tests

The presence of crystals on the membrane surface is evidenced in Fig. 3.6 (a). It was caused by the deposition of NaCl present in the matrix. Fig. 3.6 (b) shows the damage to the membrane surface. The degradation of PTFE under UV irradiation has been observed previously. Ferry et al. (1998) observed some characteristics of PTFE degradation by UV radiation: heterogeneous

degradation takes place (which, in this work, is evidenced by the black dots in Fig. 3.6 (b); both surface and bulk material are degraded since the first moments of irradiation; and photothermal degradation results in the PTFE carbonization. SEM images from this study were similar to Fig. 3.6 (b).

The membrane used in the test with the hybrid module to calculate the heat transferred by the LED to the system was also analyzed (Fig. 3.7). The SEM image reveals several black dots that indicate the degradation of the surface, similar to the MD-LED-UV test. The localized degradation of the membrane explains the greater flux since there is more free space for steam passage.

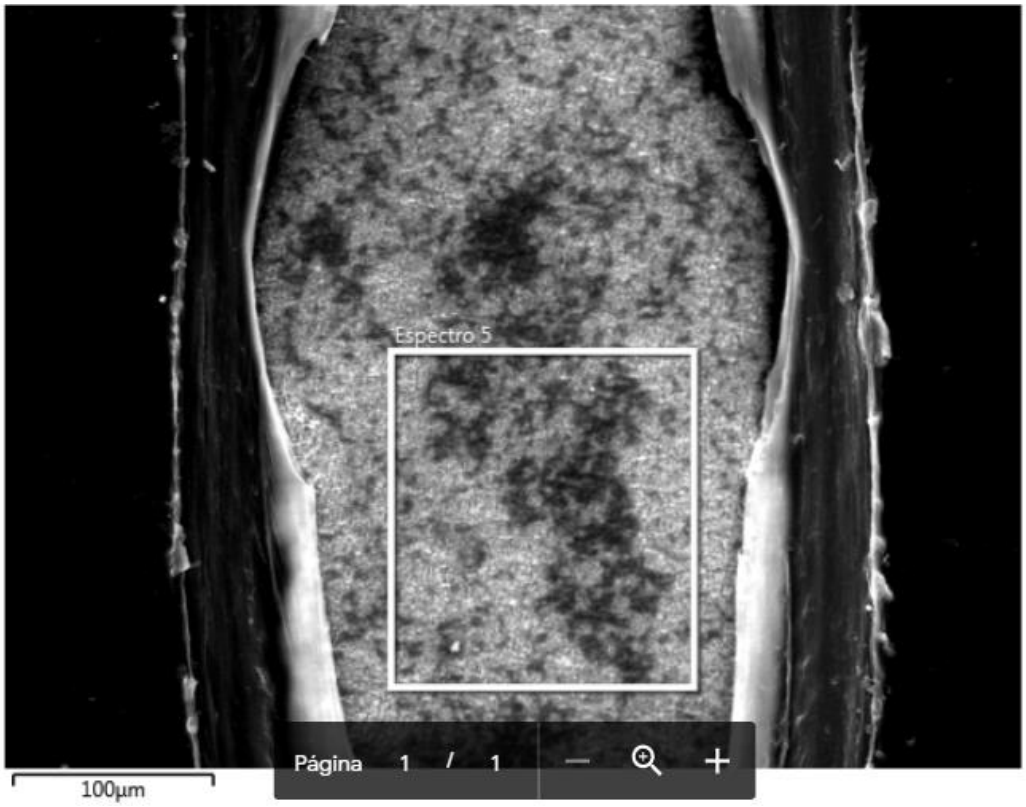

Fig. 3. 7 – SEM membrane surface analysis from MD-LED-UV test without heat

Regarding the contact angle, while the new membrane has 95.6 ± 0.6 °, the irradiated membrane has an angle of 86.5 ± 0.9 ° (Fig. 3.8), which suggests that direct irradiation from the membrane surface gives it a more hydrophilic character, which, in long-term operations, can compromise the permeate flux and its quality due to the greater propensity to pore wetting (DUMÉE et al., 2013).

(a) (b)

Fig. 3. 8 – Contact angle measurements of (a) new membrane and (b) 32,200 minutes irradiated membrane

An alternative to avoid degradation and hydrophilicity of the membrane surface is to design a module in which, at the entrance, the irradiation of the feed is made, without reaching the membrane, as proposed by Sperle et al. (2021) in an RO-LED-UV module. However, the membrane remains the most favorable place for biofilm development, which can develop over time if an insufficient UV dose is provided. Another alternative is to perform the MD-LED-UV coupling after forming the fouling layer and carry out optimization studies to provide a dose capable of mitigating the problems with fouling without damaging the membrane. This option is especially attractive because, when dealing with real matrices, the membrane is coated with the fouling layer, which is formed quickly and protects the surface.

The spectra obtained in the FTRI analysis of the polypropylene support layer of the membranes are shown in Fig. 3.9. Despite the degradation observed in the selective layer after irradiation (Figs. 3.6 and 3.7), the appearance or disappearance of bands was not detected, which suggests that there were no chemical changes.

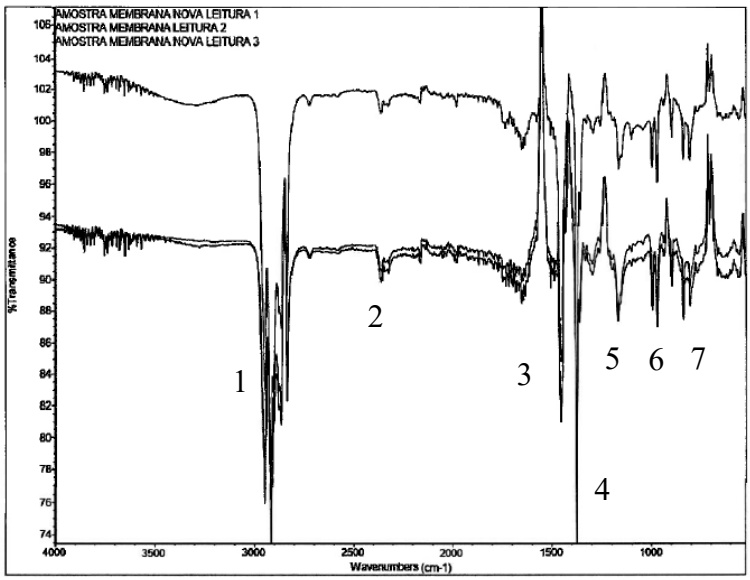

(a)

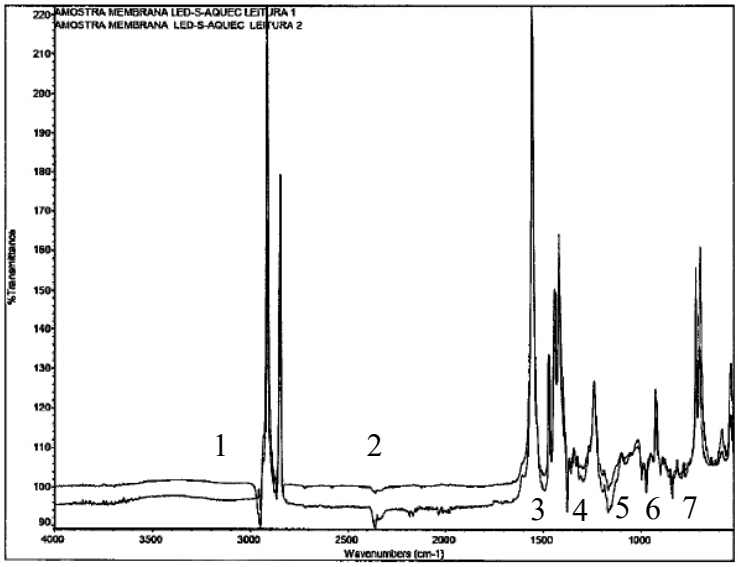

(b)

Fig. 3. 9 – Espectros de infravermelho da amostra de (a) new membrane and (b) 32,200 minutes irradiated membrane

Band 1 is related to the vibrations of methyl groups, which range from 2840-3000 cm^{-1}. Bands 3 and 4, respectively 1460 and 1380 cm^{-1}, are also common to the alkyl group bonds. In the fingerprint region, there are the characteristic bands of the axial deformations of the C-C bonds and the angular deformations of the C-C and C-H bonds (VOLLHARDT; SCHORE, 2013).

3.3 Conductivity

The conductivity of both feed and permeate tanks from MD and MD-LED-UV are shown in Fig 3.10. Permeate conductivity in MD remained significantly lower than in the system with LED. Notably, the observed differences in conductivity are minimal in terms of system performance.

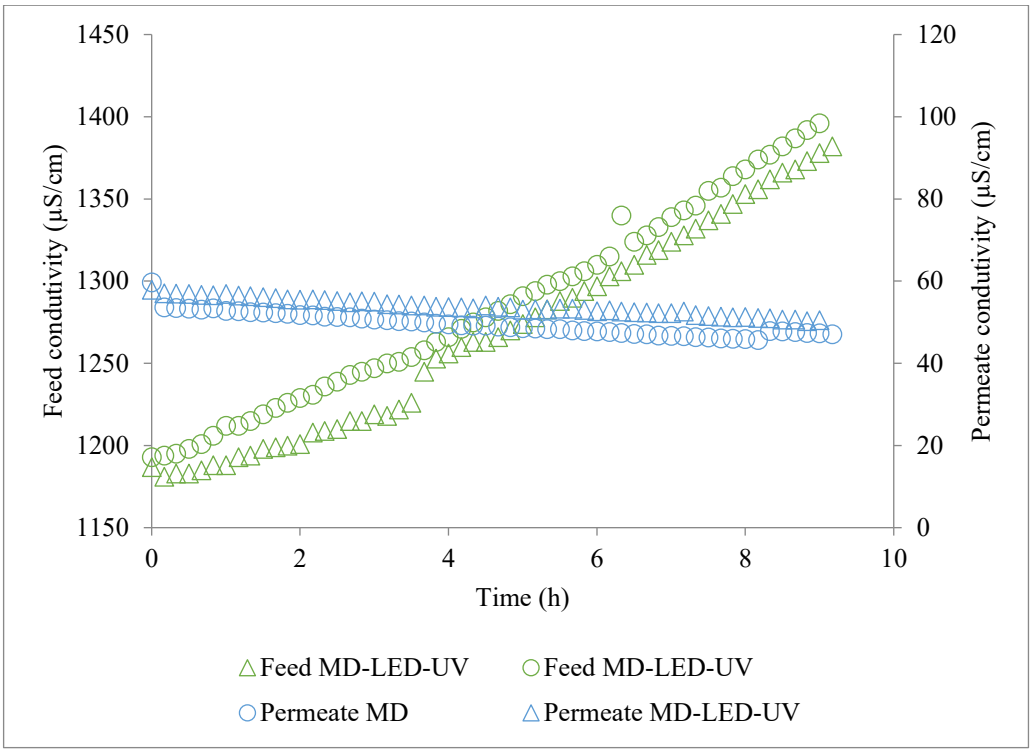

Fig. 3. 10 – Currents' conductivity over the test

However, the permeate conductivity reduced during the two tests, causing the conductivity in the last period of the operations to be around 50 $\mu S.cm^{-1}$. Besides, the statistical analysis of the normalized data - which assesses the effect of the LED on the decay conductivity profile throughout the operation - reveals no significant difference between the conductivities. It is interesting, as it may indicate that the LED's action on damaging the membrane has been limited. This hypothesis agrees with the profile of increased conductivity in the feed. Until the fourth hour of operation, the increase in conductivity in the hybrid system was less than in the MD.

3.4 Estrogenic activity removal

The YES test of the initial feed showed an estrogenic activity of 6217.29 $ng.L^{-1}$ (EQ.E2) (Fig. 3.11). The concentrate from MD had an estrogenic activity of 2675.34. The lower estrogenicity of the concentrates is due to EE2 losses in MD, which has been observed previously. Wijekoon et al. (2014) found the loss of more than 50% of the EE2 when assessing the fate of MPs in MD. The most significant losses of the evaluated micropollutants were attributed to evaporation for moderately volatile compounds; and adsorption for hydrophobic compounds. Given the

non-volatile and hydrophobic character of EE2, it may tend to adsorb to the membrane, contributing to less estrogenicity in the concentrate.

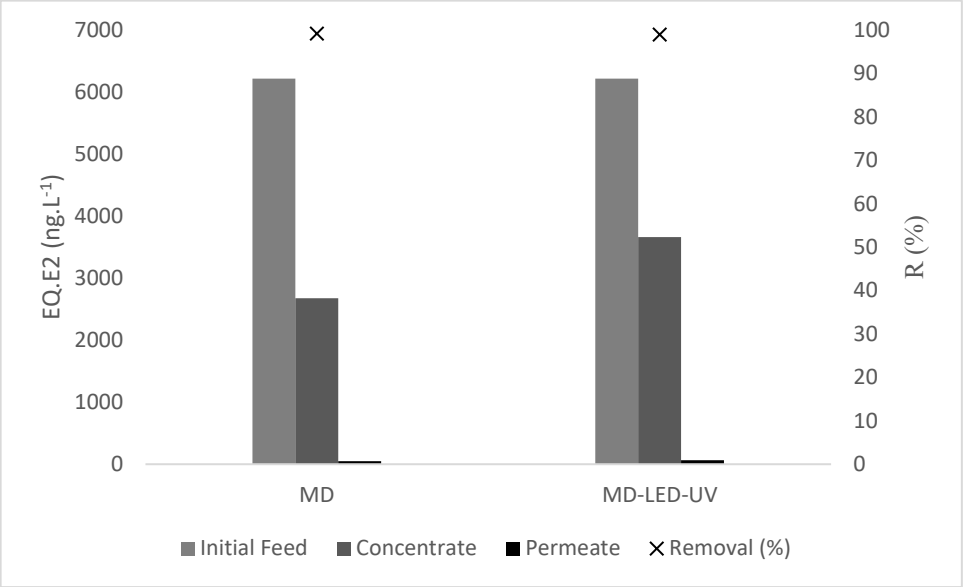

Fig. 3. 11 – Estrogenic activity and removal

However, the estrogenic activity of the MD-LED-UV system concentrate was 3660.03 ng.L^{-1} (EQ.E2). A reasonable explanation for the MD-LED-UV concentrate having greater estrogenicity is that the hybrid system has promoted the breakdown of the compound in by-products that have estrogenic activity, as estrone, one of the main by-products of EE2 degradation (ZHANG et al., 2010).

According to Bila et al. (2007), it is necessary to break the phenolic ring to remove estrogenicity, so degradation until this by-product does not provide effective estrogenicity removal. Comparing LED-UV performance to the photolysis promoted by traditional mercury lamps, it was previously observed that low-pressure lamps could not reduce the estrogenicity associated with EE2. Only medium pressure lamps at higher fluences can disintegrate EE2 through photolysis (ROSENFELDT et al., 2007). For effective removal of estrogenicity from the concentrate stream, advanced oxidative processes can be used, such as the association of UV with peroxide, which has already proved to be efficient to remove estrogenicity associated with EE2 (CHAVES et al., 2020)

The estrogenicity removal was 99.2% and 99.0% for MD and MD-LED-UV, which permeated with, respectively, 49.8 and 62.1 ng.L^{-1} (EQ.E2). Even with a higher estrogenicity in the concentrate of the MD-LED-UV system, both systems showed high removal efficiencies. The

removal of EE2 is due to the low volatility of the compound, which has a vapor pressure of 3.74×10^{-9} mmHg. The higher concentration in the permeate of the hybrid system may be associated with higher estrogenic activity in the MD-LED-UV feed. By comparing instant removals (the removal considering the feed concentration at the end of the experiment), the removal efficiencies were 98.3 and 98.1% for MD-LED-UV and MD. Therefore, the MD-LED-UV module was efficient even with the modification on the membrane surface - which was not operationally relevant, as it did not cause pore wetting.

3.5 EE2 identification

The analysis of concentrate samples by UV spectrophotometry revealed that concentrate from MD and MD-LED-UV tests had, respectively, an EE2 concentration of 87.1 $\mu g.L^{-1}$ and 95.7 $\mu g.L^{-1}$ (Table 3.3). However, as discussed in item 3.2, it is known that the non-identification of micropollutants, such as EE2, is closely related to losses in the system associated with evaporation and adsorption (WIJEKOON et al., 2014).

The MD-LED-UV test concentrate seems to have had a higher concentration of the hormone. The higher apparent concentration in MD-LED-UV may be due to the formation of byproducts with an estrogenic effect and absorption peaks similar to EE2, as observed by ZHANG et al. (2010). The authors noted that, although the chemical analysis indicated that there was almost no EE2 in the system after 100 min of irradiation, an apparent absorption peak at $\lambda = 207$ still appeared, which was attributed to the estrone byproduct.

Table 3.3 – EE2 concentration and removal

Test	**Concentrate** ($\mu g.L^{-1}$)	**Permeate** ($\mu g.L^{-1}$)	**Removal efficiencies** (%)
MD	87.1	< 2.3	97.7
MD-LED-UV	95.7	< 2.1	97.9

The EE2 in the permeate samples was not identified by liquid-chromatography coupled with mass spectrometry (LC-MS). Thus, considering the method's detection limit, the EE2 concentrations for the permeates of the MD and MD-LED-UV tests were, respectively, 2.3 and 2.1 $\mu g.L^{-1}$, resulting in efficiencies greater than 97.7 and 97.9%. Assessing the removal of EE2 in domestic wastewater treatment by an anaerobic osmotic bioreactor coupled to MD, Ricci et

al. (2021) found overall removals similar to the present study, greater than 97.8%. The authors attributed the high removal of the system to the MD.

Given the values obtained in the YES assay, whose detection limit is lower than the limit of the LC-MS method, it can be concluded that the removal of the MD and the hybrid system were both higher than 97.7 and 97.9%. As stated by Arcanjo et al. (2021), this demonstrates the importance of performing estrogenic activity tests, in addition to detection and quantification tests, because in a future analysis of risks to human health, the effects can be better estimated, even at lower concentrations.

Cartinella et al. (2006) observed that the rejection of estrone and 17-β-estradiol in doubly deionized water and wastewater by MD was higher than 99.5%. Rejection was not affected by feed retrieval and composition. Thus, given the structural similarity of EE2, it can be concluded that the hybrid system will also not result in losses in the removal of endocrine disruptors as a result of the matrix when treating real feed as seawater or wastewater. Moreover, with the retention of the hormone in the concentrate, it undergoes photolysis and is degraded to its byproducts, which would be even more evident in longer operations. Studies on the optimization of UV radiation intensity can be carried out in the future since the greater the intensity, the greater the EE2 degradation rate (ZHANG et al., 2010). Thus, the treatment of the produced concentrate is facilitated since byproducts, as estrone, is significantly more biodegradable than EE2, which is more stable against microbial degradation due to the presence of the ethynyl group introduced into the molecule (STUMPE et al., 2009).

4 CONCLUSION

Coupling membrane distillation - an effective process for removing micropollutants from aqueous matrices - and UV radiation by manufacturing a hybrid module of MD-LED-UV to mitigate fouling in real matrices is a promising alternative. The hybrid module had a very similar performance to MD. The permeate flux in MD-LED-UV was significantly higher than in MD (at the end of the experiments, respectively 3.5 and 3.1 LMH), despite MD-LED-UV undergone a higher vapor pressure polarization effect. There was no significant difference between the two tests in the increment in the feed and the permeate conductivity. Furthermore, the temperature differences between the membrane surfaces were also not significantly different after stabilizing.

Although it was observed that the surface of the irradiated membrane was damaged - which promoted an increase in the permeate flux - the hormone removal efficiencies (97.7 and 97.9% for MD and MD-LED-UV, respectively) and the estrogenic effect (99.2 and 99.0% for MD and MD-LED-UV, respectively) were not decreased. Thus, when applying the MD-LED-UV module to mitigate fouling in treating real wastewater and seawater, radiation is unlikely to lead to a performance decline regarding a complex matrix. As the fouling layer forms quickly, the membrane surface will be protected from being degraded continuously. Besides, LED can act as a treatment step for the concentrate. Thus, the MD-LED-UV hybrid system is a promising alternative to mitigate fouling and is capable of reducing environmental and human health risks.

REFERENCES

ABU-ZEID, M. A.; E. R., ZHANG, Y.; DONG, H.; ZHANG, L.; CHEN, H. L.; HOU, L. A comprehensive review of vacuum membrane distillation technique. *Desalination*, v. 356, p. 1-14, 2015.

AL-ABRI, M.; AL-GHAFRI, B.; BORA, T.; DOBRETSOV, S.; DUTTA, J.; CASTELLETTO, S.; ROSA, L.; BORETTI, A. Chlorination disadvantages and alternative routes for biofouling control in reverse osmosis desalination. *Npj Clean Water*. v. 2, 2019.

ALKHUDHIRI, A.; DARWISH, N.; HILAL, N. Membrane distillation : A comprehensive review. *Desalination*, v. 287, p. 2–18, 2012.

APHA. Standard Methods for the Examination of Water and Wastewater. 22. ed. Washington: APHA, 2012.

AQUINO, F. S.; BRANDT, E. M. F.; CHERNICHARO, C. A. L. Remoção de fármacos e desreguladores endócrinos em estações de tratamento de esgoto : revisão da literatura. *Engenharia Sanitaria e Ambiental*, v. 18, p. 187–204, 2013.

ARCANJO, G. S.; RICCI, B. C.; DOS SANTOS, C. R.; COSTA, F. C.; SILVA, U. C., MOUNTEER, A. H.; KOCK K.; SILVA, P.R.; SANTOS, V.L.; AMARAL, M.C.S (2021). Effective removal of pharmaceutical compounds and estrogenic activity by a hybrid anaerobic osmotic membrane bioreactor–Membrane distillation system treating municipal sewage. *Chemical Engineering Journal*, v. 416, p. 129151, 2021.

ARLOS, M. J.; HATAT-FRAILE, M. M.; LIANG, R.; BRAGG, L. M.; ZHOU, N. Y.; ANDREWS, S. A.; SERVOS, M. R. Photocatalytic decomposition of organic micropollutants using immobilized TiO 2 having different isoelectric points. *Water Research*, v. 101, p. 351–361, 2016.

ARRIAGA, S.; DE JONGE, N.; NIELSEN, M. L.; ANDERSEN, H. R.; BORREGAARD, V.; JEWEL, K.; TERNES, T. A.; NIELSEN, J. L. Evaluation of a membrane bioreactor system as post-treatment in waste water treatment for better removal of micropollutants. *Water Research*, v. 107, p. 37–46, 2016.

AUTIN, O.; ROMELOT, C.; RUST, L.; HART, J.; JARVIS, P.; MACADAM, J.; PARSONS, S. A.; JEFFERSON, B. Evaluation of a UV-light emitting diodes unit for the removal of micropollutants in water for low energy advanced oxidation processes. *Chemosphere*, v. 92, n. 6, p. 745–751, 2013.

BAKER, R.W. Membrane technology and applications. John Wiley & Sons, 2012.

BILA, D.; MONTALVAO, A. F.; AZEVEDO, D. D. A.; DEZOTTI, M. Estrogenic activity removal of 17β-estradiol by ozonation and identification of by-products. *Chemosphere*, v. 69(5), p. 736-746, 2007.

BOTON J.; COTTON, C. The ultraviolet disinfection handbook. American Water Works Association, New York, U.S.A., 2011.

BOREEN, A. L.; ARNOLD, W. A.; MCNEILL, K. Triplet-sensitized photodegradation of sulfa drugs containing six-membered heterocyclic groups: identification of an SO2 extrusion photoproduct. *Environmental science & technology*, v. 39, n. 10, p. 3630-3638, 2005.

CARLSON, J. C.; STEFAN, M. I.; PARNIS, J. M.; METCALFE, C. D. UV photolysis of selected pharmaceuticals , personal care products and endocrine disruptors in aqueous solution. *Water Research*, v. 84, p. 350–361, 2015.

CARTINELLA, J. L.; CATH, T. Y.; FLYNN, M. T.; MILLER, G. C.; HUNTER, K. W.; CHILDRESS, A. E. Removal of natural steroid hormones from wastewater using membrane contactor processes. *Environmental science & technology*, v. 40(23), p. 7381-7386, 2006.

CASADO, C.; TIMMERS, R.; SERGEJEVS, A.; CLARKE, C. T.; ALLSOPP, D. W. E.; BOWEN, C. R.; VAN GRIEKEN, R.; MARUGÁN, J. Design and validation of a LED-based high intensity photocatalytic reactor for quantifying activity measurements. *Chemical Engineering Journal,* v. 327, p. 1043–1055, 2017.

CHAVES, F. P.; GOMES, G.; DELLA-FLORA, A.; DALLEGRAVE, A.; SIRTORI, C.; SAGGIORO, E. M.; BILA, D. M. Comparative endocrine disrupting compound removal from real wastewater by UV/Cl and UV/H2O2: Effect of pH, estrogenic activity, transformation products and toxicity. *Science of The Total Environment*, v. 746, p. 141041, 2020.

CHEN, J.; LOEB, S.; KIM, J. H. LED revolution: fundamentals and prospects for UV disinfection applications. *Environmental Science: Water Research & Technology*, v. 3, n. 2, p. 188-202, 2017.

CLOUZOT, L.; DOUMENQ, P.; VANLOOT, P.; ROCHE, N.; MARROT, B. Membrane bioreactors for 17α-ethinylestradiol removal. *Journal of Membrane Science*, v. 362(1-2), p. 81-85, 2010.

COLAÇO, R.; PERALTA-ZAMORA, P. G.; GOMES, E. C. Poluição por resíduos contendo compostos farmaceuticamente ativos: aspectos ambientais, geração a partir dos esgotos domésticos e a situação do Brasil. *Revista de Ciências Farmacêuticas Básica e Aplicada*, v. 35, n. 4, p. 539–548, 2014.

COUTO, C. F.; LANGE, L. C.; AMARAL, M. C. S. Occurrence , fate and removal of pharmaceutically active compounds (PhACs) in water and wastewater treatment plants — A review. *Journal of Water Process Engineering*, v. 32, n. August, p. 100927, 2019

DESHMUKH, A.; BOO, C.; KARANIKOLA, V.; LIN, S.; STRAUB, A. P.; TONG, T.; WARSINGER, M.; ELIMELECH, M. Membrane distillation at the water-energy nexus: limits, opportunities, and challenges. *Energy & Environmental Science*, v. 11, p. 1177–1196, 2018.

DRIOLI, E.; ALI, A.; MACEDONIO, F. Membrane distillation: Recent developments and perspectives. *Desalination*, v. 356, p.56-84, 2015

DUMEE, L. F.; GRAY, S.; DUKE, M.; SEARS, K.; SCHÜTZ, J.; FINN, N. The role of membrane surface energy on direct contact membrane distillation performance. *Desalination*, v. 323, p. 22-30, 2013.

EGGEN, R. I. L.; HOLLENDER, J.; JOSS, A.; SCHÄRER, M.; STAMM, C. Reducing the discharge of micropollutants in the aquatic environment: The benefits of upgrading wastewater treatment plants. *Environmental Science and Technology,* v. 48, n. 14, p. 7683–7689, 2014.

EPA. Definition and procedure for the determination of the method detection limit, Revision 2. Environmental Protection Agency EPA, 2016.

ESSALHI, M.; KHAYET, M. Fundamentals of membrane distillation. In: *Pervaporation, Vapour Permeation and Membrane Distillation*. Woodhead Publishing, 2015. p. 277-316.

FERNANDES, A. N; GIOVANELA, M.; ALMEIDA, C. A. P; ESTEVES, V. I.; SIERRA, M. M. D.; GRASSI, M. T.. Remoção dos hormônios 17β-estradiol e 17α-etinilestradiol de soluções aquosas empregando turfa decomposta como material adsorvente. *Química Nova*, v. 34, n. 9, p.1526-1533, 2011.

FERRY, L.; VIGIER, G.; ALEXANDER-KATZ, R.; GARAPON, C. Interaction between UV radiation and filled polytetrafluoroethylene (PTFE). I. Degradation processes. *Journal of Polymer Science Part B: Polymer Physics*, v. 36(12), p. 2057-2067, 1998.

GOH, S.; ZHANG, Q.; ZHANG, J.; MCDOUGALD, D.; KRANTZ, W. B.; LIU, Y.; FANE, A. G. Impact of a biofouling layer on the vapor pressure driving force and performance of a membrane distillation process. *Journal of Membrane Science*, v. 438, p. 140–152, 2013.

GRANDCLÉMENT, C.; SEYSSIECQ, I.; PIRAM, A.; WONG-WAH-CHUNG, P.; VANOT, G.; TILIACOS, N.; ROCHE, N.; DOUMENQ, P. From the conventional biological wastewater treatment to hybrid processes, the evaluation of organic micropollutant removal: A review. *Water Research*, v. 111, p. 297–317, 2017.

GUO, B.; PASCO, E. V.; XAGORARAKI, I.; TARABARA, V. V. Virus removal and inactivation in a hybrid microfiltration-UV process with a photocatalytic membrane, *Separation and Purification Technology*, v. 149, p. 245–254, 2015.

GUO J.; YAN, D.Y.S.; LAM, F.L.-Y.; DEKA, B.J. An, Self-cleaning BiOBr/Ag photocatalytic membrane for membrane regeneration under visible light in membrane distillation, *Chemical Engineering Journal*. V. 378, 2019.

JALLOULI, N.; PASTRANA-MARTÍNEZ, L. M.; RIBEIRO, A. R.; MOREIRA, N. F. F.; FARIA, J. L.; HENTATI, O.; SILVA, A. M. T.; KSIBI, M. Heterogeneous photocatalytic degradation of ibuprofen in ultrapure water, municipal and pharmaceutical industry wastewaters using a TiO2/UV-LED system. *Chemical Engineering Journal*, v. 334, p. 976-984 2017.

JO, W. K.; TAYADE, R. J. New generation energy-efficient light source for photocatalysis: LEDs for environmental applications. *Industrial and Engineering Chemistry Research*, v. 53, p. 2073–2084, 2014.

KIM, J.; SHIN, M.; SONG, W.; PARK, S.; RYU, J.; JUNG, J.; CHOI, S., YU, Y., KWEON, J.; LEE, J.-H. Application of quorum sensing inhibitors for improving anti-biofouling of polyamide reverse osmosis membranes: Direct injection versus surface modification. *Separation and Purification Technology,* v. 255, p. 117736, 2021.

LIANG, R.; LEUWEN, J. C. Van; BRAGG, L. M.; ARLOS, M. J.; LI, L. C. M.; FONG, C.; SCHNEIDER, O. M.; JACIW-ZURAKOWSKY, I.; FATTAHI, A.; RATHOD, S.; PENG, P.; SERVOS, M. R.; ZHOU, Y. N. Utilizing UV-LED pulse width modulation on TiO 2 advanced oxidation processes to enhance the decomposition efficiency of pharmaceutical micropollutants. *Chemical Engineering Journal*, v. 361, p. 439–449, 2019.

LIU, C.; CHEN, L.; ZHU, L.; WU, Z.; HU, Q.; PAN, M. The effect of feed temperature on biofouling development on the MD membrane and its relationship with membrane performance : An especial attention to the microbial community succession. *Journal of Membrane Science*, v. 573, p. 377–392, 2019.

LIU, C.; ZHU, L.; CHEN, L. Effect of salt and metal accumulation on performance of membrane distillation system and microbial community succession in membrane biofilms. *Water Research*, v. 177, p.115805, 2020.

LUO, Y.; GUO, W.; NGO, H. H.; NGHIEM, L. D.; HAI, F. I.; ZHANG, J.; LIANG, S.; WANG, X. C. A review on the occurrence of micropollutants in the aquatic environment and their fate and removal during wastewater treatment. *Science of the Total Environment*, v. 473–474, p. 619–641, 2014

LYCHE, J. L.; NOURIZADEH-LILLABADI, R.; KARLSSON, C.; STAVIK, B.; BERG, V.; UTNE, J.; ALESTRØM, P.; ROPSTAD, E. Natural mixtures of POPs affected body weight gain and induced transcription of genes involved in weight regulation and insulin signaling. *Aquatic Toxicology*, v. 102, n. 3–4, p. 197–204, 2011.

MANAWI, Y. M.; KHRAISHEH, M.; FARD, A. K.; BENYAHIA, F.; ADHAM, S. Effect of operational parameters on distillate flux in direct contact membrane distillation (DCMD): Comparison between experimental and model predicted performance. *Desalination*, v. 336, p. 110-120, 2014.

MANNA, A.; PAL, P. Solar-driven flash vaporization membrane distillation for arsenic removal from groundwater: Experimental investigation and analysis of performance parameters. *Chemical Engineering and Processing: Process Intensification*, v. 99, p. 51-57, 2016.

MANSOURI, J.; CHEN, V. Strategies for controlling biofouling in membrane filtration systems : challenges and opportunities. *Journal of Materials Chemistry*, p. 4567–4586, 2010.

MATIN A.; KHAN Z.; ZAIDI, S.M.J.; BOYCE, M.C. Biofouling in reverse osmosis membranes for seawater desalination: Phenomena and prevention, *Desalination*, v.. 281, p. 1–16, 2011.

MARCONNET, C.; HOUARI, A.; SEYER, D.; DJAFER, M.; CORITON, G.; HEIM, V.; MARTINO, P. Di. Membrane biofouling control by UV irradiation. *Desalination*, v. 276, p. 75–81, 2011.

MATAFONOVA, G.; BATOEV, V. Recent advances in application of UV light-emitting diodes for degrading organic pollutants in water through advanced oxidation processes : A review. *Water Research*, v. 132, p. 177–189, 2018.

MIRALLES-CUEVAS, S.; OLLER, I.; AGÜERA, A.; LLORCA, M.; PÉREZ, J. A. S.; MALATO, S. Combination of nanofiltration and ozonation for the remediation of real municipal wastewater effluents : Acute and chronic toxicity assessment Munic ipal Mun icipal treatment plant. *Journal of Hazardous Materials*, v. 323, p. 442–451, 2017.

MOFIDI, A. A.; GABELICH, C. J.; YUN, T. I.; COFFEY, B. M.; GREEN, J. F. T. Task 2.8 A: Investigation of Scale-Up Issues Associated with Ultraviolet Light Disinfection and Reverse Osmosis Desalination. 2002.

NASCIMENTO, M. T. L.; DE OLIVEIRA SANTOS, A. D.; FELIX, L. C.; GOMES, G.; E SÁ, M. D. O.; DA CUNHA, D. L.; VIEIRA, N.; HAUSER-DAVIS, R. A.; NETO, J. A. B.; BILA, D. M. Determination of water quality, toxicity and estrogenic activity in a nearshore marine environment in Rio de Janeiro, Southeastern Brazil. *Ecotoxicology and environmental safet*y, v. 149, p. 197-202, 2018.

NGHIEM, L. D.; SCHÄFER, A. I. Adsorption and transport of trace contaminant estrone in NF/RO membranes. *Environmental engineering science*, v. 19, n. 6, p. 441-451, 2002.

PARK, J. Effects of 17-α ethynyl estradiol on proliferation, differentiation & mineralization of osteoprecursor cells. Indian Journal Of Medical Research, v. 136, n. 3, p. 466, 2012.

RASTOGI, N. K.; CASSANO, A.; BASILE, A. Water treatment by reverse and forward osmosis. In: *Advances in Membrane Technologies for Water Treatment*. p. 129-154, 2015.

REAL, F. J.; BENITEZ, F. J.; ACERO, J. L.; SAGASTI, J. J. P.; CASAS, F. Kinetics of the chemical oxidation of the pharmaceuticals primidone, ketoprofen, and diatrizoate in ultrapure and natural waters. *Industrial & Engineering Chemistry Research*, v. 48, n. 7, p. 3380-3388, 2009.

REIS, E. O.; FOUREAUX, A. F. S.; RODRIGUES, J. S.; MOREIRA, V. R.; LEBRON, Y. A. R.; SANTOS, L. V. S.; AMARAL, M. C. S.; LANGE, L. C. Occurrence, removal and seasonal variation of pharmaceuticals in Brasilian drinking water treatment plants. *Environmental Pollution*, p. 773–781, 2019.

REUNGOAT, J.; MACOVÁ, M.; ESCHER, B. I.; CARSWELL, S.; MUELLER, J.; KELLER, J. Removal of micropollutants and reduction of biological activity in a full scale reclamation plant using ozonation and activated carbon filtration. *Water Research*, v. 44, n. 2, p.625-637, 2009.

RICCI, B. C.; SKIBINSKI, B.; KOCH, K.; MANCEL, C.; CELESTINO, C. Q.; CUNHA, I. L. C.; SILVA, M. R.; ALVIM, C. B.; FARIA, C. V; ANDRADE, L. H.; LANGE, L. C.; AMARAL, M. C. S. Critical performance assessment of a submerged hybrid forward osmosis - membrane distillation system. *Desalination*, v. 468, p. 114082, 2019.

ROSENFELDT, E. J.; CHEN, P. J.; KULLMAN, S.; LINDEN, K. G. Destruction of estrogenic activity in water using UV advanced oxidation. *Science of the Total Environment*, v. 377(1), p. 105-113, 2007.

ROUTLEDGE, E. J.; SUMPTER, J. P. Estrogenic activity of surfactants and some of their degradation products assessed using a recombinant yeast screen. *Environmental toxicology and chemistry*, v. 15, p. 241–248, 1996.

SANTOS, A. V.; COUTO, C. F.; LEBRON, Y. A. R.; MOREIRA, V. R.; FOUREAUX, A. F. S., REIS, E. O., V.S.S., SANTOS; ANDRADE, L.H.; AMARAL, M.C.S; LANGE, L. C. Occurrence and risk assessment of pharmaceutically active compounds in water supply systems in Brazil. *Science of The Total Environment*, v. 746, p. 141011, 2020.

SILVA, L. L. S.; MOREIRA, C. G.; CURZIO, B. A.; FONSECA, F. V. Micropollutant Removal from Water by Membrane and Advanced Oxidation Processes — A Review. *Journal of Water Resource and Protection*, v. 9, p. 411–431, 2017.

SORNALINGAM, K.; MCDONAGH, A.; ZHOU, J. L. Photodegradation of estrogenic endocrine disrupting steroidal hormones in aqueous systems: progress and future challenges. *Science of the Total Environment*, v. 550, p. 209-224, 2016.

SPERLE, P.; WURZBACHER, C.; DREWES, J. E.; SKIBINSKI, B. Reducing the Impacts of Biofouling in RO Membrane Systems through In Situ Low Fluence Irradiation Employing UVC-LEDs. *Membranes*, v. 10(12), p. 415, 2020.

SRISURICHAN, S.; JIRARATANANON, R.; FANE, A. G. Mass transfer mechanisms and transport resistances in direct contact membrane distillation process. *Journal of membrane science*, v. 277, p. 186-194, 2006.

STUMPE, B.; MARSCHNER, B. Factors controlling the biodegradation of 17β-estradiol, estrone and 17α-ethinylestradiol in different natural soils. *Chemosphere*, v. 74(4), p. 556-562, 2009.

TIJING, L.D.; WOO, Y.C.; CHOI, J.-S.; LEE, S.; KIM, S.-H.; SHON, H. K. Fouling and its control in membrane distillation - A review. *Journal of Membrane Science*, v. 475, p. 215-244, 2015.

VOLLHARDT, Peter; SCHORE, Neil E. Química Orgânica-: Estrutura e Função. Bookman Editora, 2013.

WARSINGER, D. M.; SWAMINATHAN, J.; GUILLEN-BURRIEZA, E.; ARAFAT, H. A.; LIENHARD V, J. H. Scaling and fouling in membrane distillation for desalination applications: A review. *Desalination*, v. 356, p. 294–313, 2014.

WIJEKOON, K. C.; HAI, F. I.; KANG, J.; PRICE, W. E.; CATH, T. Y.; NGHIEM, L. D. Rejection and fate of trace organic compounds (TrOCs) during membrane distillation. *Journal of Membrane Science*, v. 453, p. 636-642, 2014.

WOLDEMARIAM, D.; KULLAB, A.; FORTKAMP, U.; MAGNER, J.; ROYEN, H.; MARTIN, A. Membrane distillation pilot plant trials with pharmaceutical residues and energy demand analysis. *Chemical Engineering Journal*, v. 306, p. 471–483, 2016.

YANG, W.; ZHOU, H.; CICEK, N. Treatment of organic micropollutants in water and wastewater by UV-based processes: a literature review. *Critical reviews in environmental science and technology*, v. 44, p. 1443-1476, 2013.

ZHANG, Z.; FENG, Y.; LIU, Y.; SUN, Q.; GAO, P.; REN, N. Kinetic degradation model and estrogenicity changes of EE2 (17α-ethinylestradiol) in aqueous solution by UV and UV/H2O2 technology. *Journal of hazardous materials*, v. 181(1-3), p. 1127-1133, 2010.

CHAPTER 4

Biofouling in Membrane Distillation - A Review

1 INTRODUCTION

Water is an essential resource for life that has been degraded by human activities such as agricultural, industrial, domestic, and leisure activities and energy production. In addition, population growth is a concern since it increases water demand. According to the World Health Organization (WHO), 50% of the population worldwide will be in countries characterized by conditions of water instability by 2025. In this context of increasing necessity and loss of water sources, it is important to consider alternatives to secure high-quality water.

Desalination processes are very attractive since more than 95% of the water in the world is available in seas or oceans. However, although desalination technologies are already well established, the energy efficiency of these processes, such as multi-stage flash and multi-effect distillation and even reverse osmosis (RO), is still a challenge (GUILLÉN-BURRIEZA et al., 2012). The energetic requirement is an issue, especially when the water demand is small, a common situation in remote locations with poor infrastructure or during emergencies. Under those circumstances, there is a relatively high capital expenditure (CAPEX) for low productivity (GUILLÉN-BURRIEZA et al., 2012).

Another alternative is water reuse, which also avoids more contamination to aquatic environments (SHANNON et al., 2008). Nevertheless, conventional biological technologies are not projected to eliminate trace organic contaminants (ARCHER et al., 2017) - like hormones, pharmaceuticals, pesticides (BARBOSA et al., 2016), illegal drugs, and personal care products (GRANDCLÉMENT et al., 2017) – that must be removed by advanced water treatment processes prior to water reuse. Several of these substances can cause adverse health effects, and not all of these effects have been fully understood (ANDERSON et al., 2006). Even for disposal, wastewater effluents may present adverse effects to aquatic organisms due to the presence of these contaminants (TERNES; JOSS; OEHLMANN, 2015). Consequently, specifications for drinking water quality, water reuse, and discharge to receiving streams are becoming stricter, calling for advanced technologies capable of providing a suitable water quality (BARBOSA et al., 2016).

In this context, great attention has been paid to advanced technologies such as membrane separation processes (SUDHAKARAN; KYU; AMY, 2013). Membranes have been becoming competitive in costs with traditional treatment processes, provide high separation efficiency, are suitable to many applications, and are in a constant process of further advancement

(ESSALHI; KHAYET, 2015). Among membrane processes, membrane distillation (MD) has been highlighted as a promising technology at the water-energy nexus (DESHMUKH et al., 2018).

MD is a technique capable of generating high-quality water (ALKHUDHIRI; DARWISH; HILAL, 2012) that combines the advantages of conventional distillation and membrane separation. MD has a lower heat demand than conventional distillation-based processes, as it is not necessary to heat the feed solution to the boiling point. In this way, it is possible to promote a sustainable distillation process by coupling MD to renewable energy sources (such as geothermal or solar heat) or residual heat available in the industry, which can make MD competitive with RO (GONZÁLEZ; SUÁREZ, 2017) or urban heating systems (MANNA; PAL, 2016). These sources can provide an appropriate amount of heat to provide a sufficient temperature gradient between membrane surfaces, inducing a vapor pressure difference resulting in vapor passing through the pores of a hydrophobic membrane (ALKHUDHIRI; DARWISH; HILAL, 2012). This hydrophobic character impedes water passage since only vapor can permeate the non-wetted pores. At the permeate side, the vapor condenses, and freshwater can be recovered (LAWSON; LLOYD, 1997).

MD presents several other advantages. A 100% theoretical rejection of non-volatile substances can be achieved. It is more resistant to concentration polarization (CP) than other membrane separation processes to treat high-salinity feeds. Because MD is not a pressure-oriented process, the mechanical properties of membranes are less exigent, and the operation is safer and does not require typical expensive equipment (MANNA; PAL, 2016). Therefore, besides low energy demand, MD is expected to be a cost-effective process in terms of low-cost materials too (ALKHUDHIRI; DARWISH; HILAL, 2012).

However, MD development faces limitations for full-scale applications (LAWSON; LLOYD, 1997). The deposition of undesirable material on the membrane surface can lead to performance deterioration, known as fouling. Pore wetting is also a key challenge to be overcome or at least to mitigate by satisfactory operation. Pore wetting happens when liquid penetrates and floods pores, creating a hydrophilic channel. When the membrane loses hydrophobicity as one of its most important characteristics, contaminants can pass through pores to the distillate side (WARSINGER et al., 2014).

MD is susceptible to all fouling types, including inorganic, organic, and biological fouling (TIJING et al., 2014). Inorganic fouling is caused mainly by crystallization and precipitation of

salts, such as carbonates, phosphates, sulfates, sodium chloride (CHOUDHURY et al., 2019), and metallic deposits which comprise scaling (ALKLAIBI; LIOR, 2004). Adsorption or deposition of colloidal organic compounds like proteins, polysaccharides, humic acids, polymers, or extracellular polymeric substances (EPS) leads to organic fouling. This kind of fouling is harder to handle and often requires a chemical cleaning, which might compromise the life expectancy of membranes. Chemical cleaning interrupts the operation and causes additional costs. In several studies scaling and organic fouling in MD has been reported (GRYTA, 2009), and their mechanisms and control techniques are receiving more attention recently.

Microorganism deposition, growth, and metabolic activity execution on the membrane surface leads to biological fouling, also called biofouling. Microorganisms secrete EPS and form complex matrix covering the membrane (MANSOURI et al., 2010). Previously, MD biofouling did not receive much attention since MD usually operates at temperatures higher than most microorganisms can sustain (GRYTA, 2002). In 2006, Meindersma et al. attributed MD flux decline to biofouling. Nevertheless, the authors did not observe microorganisms' breakthroughs. Hence, many researchers focused on scaling and organic fouling effects on MD performance mainly and on mitigation techniques against these two types of fouling.

However, it was later perceived that biofouling results in flux and separation decay of membrane processes, aside from reducing the membrane lifetime (MANSOURI et al., 2010; GOH et al., 2013). Microorganisms from MD biofilm can survive at higher temperatures, and membrane surfaces often present milder temperatures than the bulk solution due to the temperature polarization (TP) effect. Recently, many research studies have paid attention to MD biofouling since understanding biofouling and providing efficient mitigation approaches are essential for expanding MD operations (BOGLER; LIN; BAR-ZEEV, 2017; LIU; ZHU; CHEN, 2020).

MD fouling is often considered less severe and compact since the MD membrane presents larger pores and pressure is not applied (MACEDONIO; DRIOLI, 2019). However, the extent of biofilm consequences on MD performance is much less studied compared to other membrane processes. When evaluating MD and RO in similar initial conditions of flux and crossflow velocity, MD seemed to be more susceptible to fouling upon some changes in feed conditions. The underlying fouling mechanisms are significantly different. In RO, EPS enhance resistance to permeation of the dense membrane, while in MD, pores are blocked, leading to resistance to vapor passage through then (ZODROW et al., 2014). In another study, although MD presented

the faster flux decline when scaling occurred, MD exhibited more resistance than forward osmosis and RO in terms of alginate fouling, a good model for algal fouling (TOW, et al., 2018), which often composes MD biofouling when treating seawater (WARSINGER et al., 2015). Therefore, further studies are still required to elucidate the magnitude of the effects of biofouling on MD.

This review presents the current knowledge about biofilm in membrane distillation, its mechanisms of development, consequences for MD performance, and mitigation techniques specifically evaluated to alleviate biofouling in MD. Challenges and opportunities in MD biofouling studies are also discussed. For this purpose, a systematic and careful review of the literature was carried out.

To the best of our knowledge, this is the first review to focus exclusively on MD biofouling. It is expected that this review may represent another step to revisit the idea that MD is not subject to biofouling and its consequences, inciting further studies and developments of appropriate mitigation techniques.

2 MEMBRANE DISTILLATION FEATURES

Although the first reports on the membrane distillation process were made in 1963 by Bodell (1968) and 1967 by Findley, for economic reasons, the membrane distillation process took a long time to develop. Only during the 1980s, a better understanding of the principles of mass and heat transfer in the process was obtained, and new membranes and modules were developed (ANDERSON; KJELLANDER; RODESJO, 1985).

Temperature differences between 10 and 20ºC are usually sufficient to promote separation in MD. This difference is enough to create a liquid-steam interface at both membrane sides, causing evaporation and diffusion of vapor molecules through the pores (LAWSON; LLOYD, 1987). This feature made the MD process very attractive due to the possibility of using alternative low-value energy sources. This possibility and the availability of new membranes accelerated research on MD in several areas (DRIOLI; ALI; MACEDONIO, 2015), including applications such as desalination (DUONG et al., 2016), wastewater treatment (LEAPER et al., 2019), brackish water desalination (SUWAILEH et al., 2019), and juice concentration process (AN et al., 2019).

Despite more than 50 years of MD development, the MD process is still not widespread at a commercial scale, the main obstacles being energy consumption and cost (ZARAGOZA; ANDRÉS-MAÑAS; RUIZ-AGUIRRE, 2018). However, many pilot-scale studies have been carried out to overcome these obstacles with specific techniques, such as coupling solar energy for desalination (CHA et al., 2014), improving modules and configurations (ANDRÉS-MAÑAS et al., 2020).

Characteristics, such as the membrane surface, morphology, pore size, charge, and porosity, are key factors to MD performance. A particularity of MD is the hydrophobicity of the membrane surface. Due to the hydrophobic nature, penetration of the feed solution into the pores does not occur, allowing only the passage of steam. MD membranes are often made of polytetrafluoroethylene (PTFE), polyvinylidene fluoride (PVDF), and polypropylene (PP). These polymers present good service life and hydrophobic characteristics. MD membranes must also be porous (porosity between 80 and 90%) with pore sizes between 0.1-1 μm (EYKENS et al., 2016).

MD module configurations can be classified into four configurations according to differences at the permeate side: Direct Contact Membrane Distillation (DCMD), Air Gap Membrane

Distillation (AGMD), Sweeping Gas Membrane Distillation (SGMD), and Vacuum Membrane Distillation (VMD). In all configurations, the heated feed solution is in direct contact with the membrane surface.

3 BIOFILM

To better understand MD biofouling, it is essential to know basic concepts related to biofilm and its characteristics. Biofilm is typically defined as a microbial aggregation formed at an interface between liquid-solid, solid-air and liquid-air interfaces (IVLEVA et al., 2017). Almost all surfaces immersed in natural water environments are prone to be coated by bacteria (CHARCKLIS; COOKSEY, 1993). Alive and dead microorganisms are involved in a hydrated extracellular matrix made of extracellular polymeric substance (EPS) produced by organisms that compose the biofilm. Between cells and molecules, water channels transport oxygen in aerobic biofilms, nutrients, and other substances. In terms of mass, bacteria represent less than 10% of the biofilm's total dry mass (FLEMMING; WINGENDER, 2010).

3.1 Biofilm non-living components

More than 90% of the biofilm's dry mass consists of extracellular components. EPS is composed mainly of polysaccharides, proteins, lipoproteins, glycoproteins, and DNA (MATIN et al., 2011). These biopolymers form the biofilm skeleton and enable the building of structures with a high density of cells, providing a protective barrier (against inhibitors, for example), which makes bacteria more resistant in biofilm than in planktonic lifestyle. EPS also permits water retention; it is a nutrient source, confer cohesion, provides mechanical stability, and allows communication between cells. EPS enable adhesion to surfaces, which is the first step of the transition from the planktonic to biofilm way of life. The type of EPS varies according to the species of microorganism. Its composition is important for the characteristics of the biofilm. For example, the presence of charged groups retains cations better, which can make scaling worse (ANSARI et al., 2020). EPS proved to be especially relevant in MD biofilms since bacteria release more EPS under thermal stress. This protective mechanism intensifies biofouling and worsens the system performance (BOGLER; BAR-ZEEV, 2018). Given its importance, investigations on biofouling may consider not only microbial analyses but should also investigate EPS formation.

Another class of aquatic particles relevant to comprehending biofilm formation is transparent exopolymer particles (TEP) (BAR-ZEEV et al., 2014). TEP are organic microgels (NAGARAJ et al., 2018) produced and released by organisms like planktonic bacteria and microalgae and can be considered a kind of EPS (PASSOW, 2002). According to Passow (2002), on average, 5-10% of all marine bacteria are attached to TEP. They are mainly composed of acid polysaccharides and were first proposed by Alldredge et al. (1993) in the marine environment.

However, it is nowadays known that these particles are present in all-natural water matrices (BAR-ZEEV et al., 2014).

TEP polysaccharides, formed by sugars such as fucose and rhamnose, confer gel characteristics as high flexibility (PASSOW, 2002; MOPPER et al., 1995). This composition results in a high capacity to coagulate or attach to a surface in case of collision, which is essential to biofilm establishment. Furthermore, these particles provide favorable conditions for microorganism colonization. Therefore, the initial development of protobiofilm may take place. The term protobiofilm was first introduced by Bar-Zeev et al. (2014) to designate TEP with intense microbial activity, which consists of particles with initial biofilm characteristics, except for their free movement in bulk solution. Hence, TEP protobiofilm may deposit on the membrane surface and condition it for subsequent biofilm formation. Recently, researchers have investigated the TEP's role in membrane fouling, supporting the relevance of TEP in feed to the system performance (MENG; LIU, 2017).

When studying biofilm formation, it is essential to address autoinducer molecules. Although they are not essentially biofilm components, these molecules must be considered due to their importance to biofilm development. Bacteria can sense the presence of other bacteria. This sense of the number of other organisms is decisive for the social activities of the bacterial community (XIONG; LIU, 2010). The production, release, and detection of these molecules allow communication between cells in a process known as quorum sensing (QS) (GONZA; KESHAVAN, 2006).

The QS mechanism is related to microbial population density: as the bacterial population density increases, the concentration of autoinducer molecules proportionally increases. In this way, the molecules inform the neighboring bacteria about the number of organisms. When a critical mass is reached, all bacteria react through regulator proteins being activated. It results in the expression of genes that may generate community behaviors (WEI et al., 2020). Therefore, QS coordinates biofilm formation, motility, and EPS production (MADDELA et al., 2019). Studies have already correlated worse biofouling conditions under temperature changes with higher autoinducers production, which led to higher EPS production (NAHM et al., 2019). Besides, QS also plays a role in biofilm detachment and return to planktonic life, coordinating the production of surfactants and flagella (KIM. LEE, 2015).

The most common QS molecules are autoinducing peptides (AIP), N-acyl-homoserine lactones (AHL), and autoinducer-2 (AI-2), related to Gram-positive, Gram-negative, and interspecies

communication for both kinds of bacteria, respectively. Among these molecules, AHL and AI-2 consist of QS signals capable of leading to biofilm formation (MADDELA et al., 2019).

3.2 MD biofouling development

Membrane biofouling results from a succession of events during the operation (NAGARAJ et al., 2018). Recent studies suggest that MD biofilm development follows a five-phase model, similar to other membrane processes, namely i) the establishment of the conditioning film, ii) reversible and iii) irreversible attachment, iv) mature biofilm, and v) dispersion (Fig. 4.1). Understanding the phases of MD biofouling is essential to predict system performance and to improve mitigation strategies (JIANG et al., 2019).

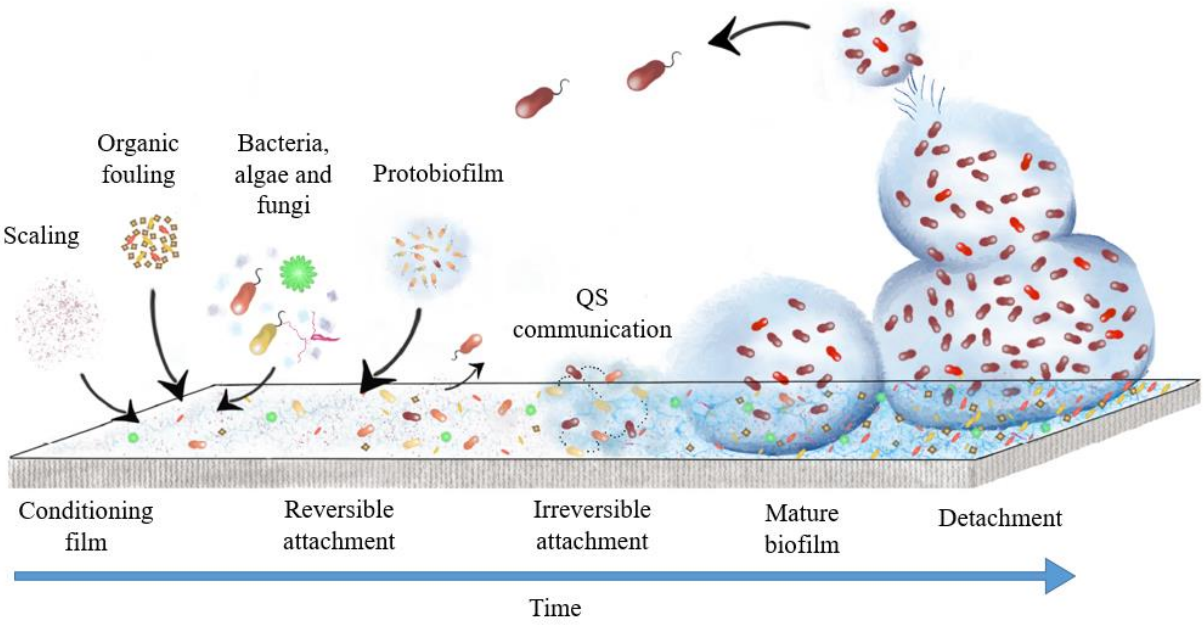

Fig. 4. 1 – Stages of biofouling development

3.2.1 Attachment stage

The bacterial attachment stage can be divided into two moments related to adhesion reversibility. Within a few seconds, inorganic and organic compounds, such as proteins and polysaccharides, compose the feed solution attached to the membrane surface, forming the conditioning film (BAKER; DUDLEY, 1998). The membrane is also conditioned by EPS, TEP, and protobiofilm deposition (BAR-ZEEV et al., 2015). Due to MD thermal stress, substances released due to cell lysis also may constitute the conditioning film (LIU et al., 2019). This film enables the deposition of individual cells, transported with colloids and suspended solids from the bulk solution to the membrane surface (JIANG; CHEN, 2020), leading bacteria to interact

mildly with the macromolecular film. The conditioning film allows microorganisms to move to the substratum, where they can aggregate (MANSOURI et al., 2010). Migration to the membrane surface is advantageous for microorganisms since the membrane is the most favorable place for microorganisms in the feed compartment due to milder temperatures, resulting from the temperature polarization (TP) effect (LIU et al*.,* 2019). This effect leads to a lower temperature at the membrane interface than in the bulk solution, generally recognized as reduced energy efficiency (SRISURICHAN et al., 2006).

This first interaction consists of bacteria attachment to the conditioning film by reversible interactions as van der Waals forces and electrostatic interactions. Electrical interactions between bacteria and the conditioning film are more favorable than bacteria and the hydrophobic MD membrane (GARRET et al., 2008). Many researchers investigated bacteria adhesion to surfaces in terms of the Derjaguin–Landau–Verwey–Overbeek (DLVO) theory to provide qualitative models and estimate free energy changes due to microbial adhesion (HERMANSSON, 1999). Meanwhile, real attachment in membranes is more complex since there are changes in interactions, and the cell surface is different from colloidal particles, among other reasons. Subsequently, irreversible attachment occurs with covalent and hydrogen bonding (HORI; MATSUMOTO, 2010).

At the membrane, bacteria secret EPS, get linked to each other, and are stuck to the surface (LIU et al*.,* 2019). Irreversible adhesion is also related to physical bacteria components, like flagellum and pili, which overcome repulsive forces between microorganisms and the surface (DE WEGER et al*.*, 1987). When these bacteria parts and the conditioning film interact, chemical reactions are stimulated, enhancing attachment (GARRET et al., 2008). Once the irreversible attachment is reached, a significant effort is required to remove it. The attachment stage happens in seconds or minutes in other membrane processes (MANSOURI et al., 2010). Nevertheless, bacteria deposition over the MD surface can take much longer and can be noticed after more than one day of operation.

Krivorot et al. (2011) evaluated the rate of MD biofilm formation. Samples were taken after 0, 20, 28, 48 hrs and 4, 9, 13, and 19 days, and the presence of bacteria was assessed through scanning electron microscopy (SEM). Although the conditioning film was formed after 20 hrs, bacteria were not present yet. Microorganisms attachment was observed after 28h, a biofilm layer was detected after 48h, and subsequent samples had larger areas covered by biofilm. The deposition of microorganisms on the MD membrane may take longer than in other membrane separation processes due to the time required for adaptation to high temperatures (JIANG et al.,

2020). This explanation is consistent with Zodrow et al. (2014), who observed a decrease of bacterial concentration in MD feed, attributed to MD temperature, compared to a RO system operated at similar conditions (same initial feed solution, crossflow velocity, and initial distillate flux) except for high temperature in MD and hydraulic pressure in RO.

3.2.2 Biofilm growth and community succession

Attached cells pass through binary division, and bacteria multiplication goes from adhered-cell to outward, leading to clusters formation in half-sphere shape containing living and dead bacteria involved in an EPS matrix. The shape of this structure promotes nutrients to cross the biofilm, reaching even bacteria in the half-sphere center. The first lag phase is followed by exponential growth. Now, bacteria growth is more significant to biofilm development than physicochemical mechanisms that lead to microorganisms adhesion (GARRET; BHAKOO; ZHANG, 2008). Moreover, interactions between cells are enhanced due to divalent cations' presence in media (DUNNE, 2002), as they favor cohesion between structural species (EPS) (EDGAR, 1979), and increasing recalcitrance (NAGARAJ et al., 2018). Now, the first significant performance decrease is observed (JIANG et al., 2020). From hours to days, microcolonies form a mature biofilm; from days to months, these colonies' dissolution takes place (MANSOURI et al., 2010).

The biofilm development rate, diversity, and biological composition are strongly related to environmental conditions like temperature, hydrodynamic conditions, pH, carbon and nutrients ratio, as well as redox potential (BESEMER, 2015). The progressive modification in the ecosystem diversity at the beginning of species establishment in a specific environment is called "succession" (LYAUTEY et al., 2005), a field of study that was enabled in microecology by DNA sequencing tests development (MARGULIES et al., 2005). Succession typically follows this sequence: after a significant reduction caused by the death of some species due to location characteristics, diversity increases quickly. Later, the variety of species enhances again, although the total mass cannot grow limitless (WOODCOCK; SLOAN, 2017). In MD, many bacteria die due to the sudden change in temperature at first. It has been observed that heat and the progressive concentration of the feed lead to the change of the microbial community, selecting species more adapted to the temperature and the concentration of the feed (JIANG et al., 2020). Therefore, the biological succession phenomenon contributes to biofouling in MD (Fig. 4.2) (LIU et al., 2019).

Assessing the biological community succession appears to be relevant for understanding membrane fouling. The correlation between some organisms of the microbial community and the increasing quantity of metabolic products on membrane fouling was previously observed (CHEN et al., 2015). At the same time, succession may lead to more deposition of EPS and soluble microbial products (SMP), and increased metabolic products in the environment promote succession. Recently, microbiological succession in MD biofouling has received increasing attention, and researchers have perceived significant changes in the bacterial population during biofilm development (Table 4.1).

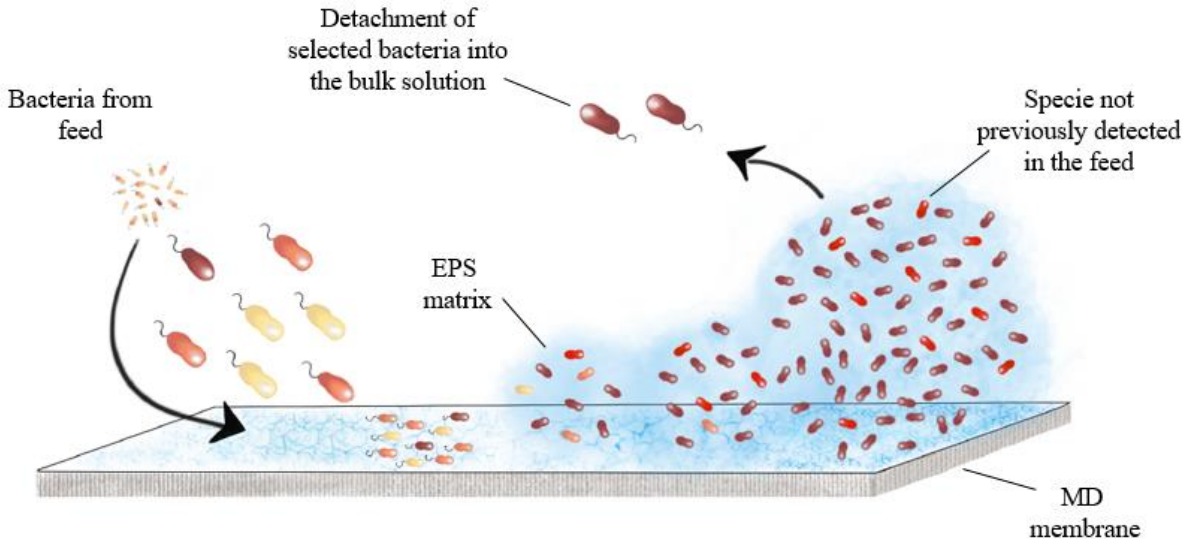

Fig. 4. 2 – Biological succession over time

The typical dynamic of the bacteria community's succession during biofilm development was evident in a study presented by Liu et al. (2019). In terms of bacteria, the feed treated by the MD system was mainly composed of *Actinobacteria, Cyanobacteria, Bacteroidetes,* and *Proteobacteria,* which was the phylum that prevailed in the biofilm formed over the MD membrane at 60 ºC. Other researchers have also observed that *Proteobacteria* phylum was a dominant species in the MD biofilm (JIANG et al., 2020). *Acidobacteria* appeared in the MD biofilm during the microbiological succession due to temperature stress and feed features (LIU et al., 2019). However, the microbial community is also susceptible to selection by increasing pH and the high concentration of salt crystals, which led to the subsequent death of bacteria from this phylum. Progressively, *Proteobacteria* became

the dominant phylum of the matured biofilm. At 40ºC*, Proteobacteria* and *Bacteroidetes* predominated (LIU et al., 2019).

At the end of the experiments conducted by Zodrow et al. (2014), thermotolerant organisms capable of forming spores were the predominant microorganisms in bulk solution. However, succession did not reach the stage when specific species can prevail in the environment since only the initial stages of biofilm formation were investigated. Thus, the biofilm on MD was relatively enriched in diversity, and its colonies were heterogeneous, as documented in Table 1. Besides, it is worth mentioning that less thermophilic bacteria composed the biofilm, which is likely an effect of temperature polarization.

Jiang et al. (2020) reported a similar dynamic. The organisms capable of surviving at high temperature and concentration environments were selected, and the diversity in MD biofilm increased again. *Bacillus* genus, for example, was favored, explained by the fact that this genus includes bacteria being able to form spores, providing thermal and hypertonic resistance. At the family level, *Rhodobacteraceae* was considered an essential constituent for the primary development of biofilms. *Planctomycetes* also played a relevant role during the initial stages since these organisms carry genes associated with pili and flagella.

Liu et al. (2020b) reported that at the genus level, *Tepidimonas* and *Meiothermus* genus significantly composed MD biofilm because they are thermophilic organisms. However, these genera's presence reduced with increased concentration of metal ions, and the establishment of bacteria tolerant to Zn and Fe ions was observed. Also, the increased concentration of $FeCl_3$ (36 g/L Fe^{3+} after 15 days) in the feed solution seemed to favor selecting pathogenic organisms in MD.

Evaluating the treatment of three different surface water sources by PTFE membrane in MD process, Chen et al. (2021) observed that the bacterial community on each membrane surface after 8 days of operation was similar for the three tests, despite the different microbial composition of the feeds. It was attributed to the fact that the membrane surface microenvironment of each test was similar. However, after 16 days, the microbiological succession caused the community composition to change, likely due to the different compositions of each feed.

When biofouling reaches the plateau stage, bacteria multiplication, attachment, detachment, and sloughing happen in the same extension. This stage depends on feed characteristics, shear

stress, and biofilm mechanical features. At this degree of maturity, some biofouling characteristics may prevail to the detriment of some membrane properties (MATIN et al., 2011), leading to severe operation problems.

Table 4. 1 – State-of-the-art abundance (%) of main microorganisms found in the MD biofilm and in MD bulk solution

Feed source	Temperature* and taxonomic level	Feed**	Biofilm**	Ref.***
Seawater	T_f = 50.4 ºC T_p = 18.1 ºC Taxonomic level	Initial feed Family level *Rhodobacteraceae* Genus level *Sediminicola*, *Pseudomonas* Final feed Order level *Bacillales* Genus level *Ralstonia, Methylobacteriaceae, Methylobacterium, Pseudomonas, Erythrobacter, Sediminicola*	Family level *Pelagibacteraceae, Rhodobacteraceae* Genus level *Octadecabacter, Sediminicola*, *Ralstonia*	(i)
Lake water with NaCl, $ZnCl_2$ and $FeCl_3$	T_f = 60 ºC T_p = 10 ºC Genus level	*Cyanobium PCC-6307, hgcI clade*	*Tepidimonas*,*Meiothermus, Sphingobium, Sphingomonas, Novosphingobium*,*Pelomonas, Microbacteriaceae_Unclassified Escherichia- Shigella*	(ii)
Lake water under two temperatures	$T_{f,1}$ = 40 °C $T_{f,2}$ = 60 ºC T_p = 10 ºC Taxonomic level	Phylum level *Actinobacteria, Cyanobacteria*, *Bacteroidetes*, *Proteobacteria*	$T_{f,1}$ = 40 Phylum level *Proteobacteria*, *Bacteroidetes* Genus level *Caulobacter*, *Novosphingobium*, *Sediminibacterium* $T_{f,2}$ = 60 ºC Phylum level *Proteobacteria* Genus level *norank_f__Blastocatellaceae__ Subgroup_4_ , Cal- dimonas*	(iii)
Seawater ,	T_f = 50 ºC T_p = 10 ºC Phylum level	*Proteobacteria*, *Bacteroidetes Parcubacteria, Actinobacteria, Verrucomicrobia*, *Cyanobacteria*	*Proteobacteria*, *Firmicutes*, *Bacteroidetes*, *Planctomycetes*, *Chlamydiae*	(iv)
River water	T_f = 60 ºC T_p = 10 ºC Taxonomic level	Phylum level *Proteobacteria*, *Bacteroidetes*, *Actinobacteria*	Phylum level *Proteobacteria* Genus level *Vulcaniibacterium*, *Schlegelella*, *Tepidimonas, Methyloversatilis, Novosphingobium*, *Paucimonas*	(v)

Lake water	T_f = 60 ºC T_p = 10 ºC Taxonomic level	Phylum level *Cyanobacteria, Proteobacteria, Bacteroidetes*	Phylum level *Deinococcus-Thermus, Proteobacteria* Genus level *Anoxybacillus*, *Meiothermus*, *Schlegelella, Tepidimonas, Vulcaniibacterium*	(vi)
Lake and river water	T_f = 60 ºC T_p = 15 ºC Taxonomic level	Phylum level *Cyanobacteria, Proteobacteria,* Genus level Chloroplast_norank, Cyanobium *PCC-6307, Rheinheimera, Pseudomonas, Limnohabitans*	Early phase Genus level *Tepidimonas, Meiothermus, OLB14_norank, Env.OPS 17_norank, Schlegelella* Later phase Genus level *Armatimonadetes_norank, Hydrogenophilaceae_uncultured, Methyloversatilis*	(vii)

* T_f = temperature from feed and T_p = temperature from permeate. ** The results shown are from RNA based tests. ***References: (i) ZODROW et al., 2014; (ii) LIU et al., 2020b; (iii)LIU et al., 2019; (iv) JIANG et al., 2020; (v) LIU et al., 2020c; (vi) LIU et al., 2020a; (vii) CHEN et al., 2021

4 MD OPERATIONAL FACTORS AFFECTING BIOFILM FORMATION

4.1 Temperature effects

Operational conditions, such as the hydrodynamic regime, feed characteristics, and membrane features, may affect biofilm formation (GHAYENI et al., 1998). Nevertheless, due to high-temperature particularity, some effort to understand its effects on MD biological fouling has been made (KRIVOROT et al., 2011). Membrane biofouling on MD was previously reported to be less severe due to special temperature conditions (ALKHUDHIRI; DARWISH; HILAL, 2012). Indeed, microorganisms have no temperature regulatory mechanisms, and temperatures higher than optimal lead to enzyme denaturation and ultimately cell death. The optimal temperature range for mesophilic bacteria is between 30-39 ºC. However, mainly thermophilic organisms greatly concern MD biofilm (BOGLER; LIN; BAR-ZEEV, 2017).

The operational temperature may affect MD biofouling direct and indirectly. Direct effects involve the primary consequences of heat over microorganisms, like selecting organisms more resistant to heat stress and bacteria more adapted to lower oxygen concentrations in the typical MD temperature range (GRYTA, 2002). Indirect outcomes include operational characteristics or conditions affected by elevated temperature, and these changes influence biofilm formation and features. For instance, higher feed temperatures (thus, a higher driving force and a more

intense flux) result in higher concentration rates and more severe deposition over the membrane surface, leading to salt stress and more severe scaling (LIU et al., 2019).

Bogler and Bar-zeev (2018) reported dead cells predominated over both membrane and spacer due to temperature. They also perceived that operating MD in the optimal growth temperature of a microorganism present in feed leads to a denser biofilm and more severe consequences on MD performance, such as flux decline and pore wetting. In temperatures lower than optimal, microorganism metabolism is slower, and consequences of biofouling to MD performance may be due to deposition, impairing performance to a lesser degree. At temperatures higher than optimal, although a thinner biofilm covers the membrane, bacteria are stressed, produce a large EPS, and form endospores. Therefore, biofouling decreases the membrane performance by leading to complete pore wetting.

Liu et al. (2019) elucidated different fouling development profiles in their research operating MD at 40 and 60 ºC. During the attachment phase, when physical factors had a major impact on the conditioning film development, the impact in MD flux was similar in both temperature operations. Afterward, a considerable diversity of microbial biota covered the MD membrane. Bacteria also produced more EPS as a protective mechanism against heat stress, worsening fouling consequences. At this stage, temperature effects were evident. There was a higher abundance of microorganisms on biofouling at 40ºC, which presented a relatively stable community over time. At higher temperatures, more bacteria died. Thus, intracellular material was released due to cell lysis, leading to more fouling.

Consequently, biofilm passes through more biological community changes at higher temperatures and is mainly composed of salts and organic compounds. The decrease in flux was prominent. Finally, the authors did not perceive that temperature had caused differences in biofouling reaching a stable stage. Flux decline was observed to a similar extent for both conditions during this phase.

Among thermal effects on biofouling, temperature cycling has proved to be an effective alternative to reduce MD biofilm in heat exchangers (KNIGHT et al., 2004). This technique consists of heating feed solution to higher temperatures before feeding the module. Krivorot et al. (2011) assessed heating the feed to 70 ºC for less than one minute and cooling it to the operational temperature of 40 ºC before feeding the MD system. It was observed that the biofilm decreased. Indeed, bacteria were exposed to such impacting thermal stress that a kind of

pasteurization effect occurred, eliminating vegetative forms sensitive to this temperature, so less performance decay happened.

According to these recent findings, unlike previously stated knowledge, MD high temperature can make biofouling condition a severe issue instead of inhibiting biofilm growth. For this reason, understanding how operational conditions influence biofouling is essential to anti-biofouling techniques and technology development, as well as for long-term operation. Even though the temperature is the exclusive MD feature, other effects or conditions common to other membrane processes also need to be understood to prevent biofouling adequately.

4.2 Feed characteristics

In general, fouling is strongly dependent on feed source characteristics, such as pH, organic and inorganic compounds concentration, and typical microbiota (CHOUDHURY et al., 2019). Among water sources, studies highlighted MD potential for treating water from natural environments, like the sea (LI; LU, 2020), lake (LIU et al., 2019), river (FONSECA et al., 2020), and groundwater (TOMASZEWSKA et al., 2020), as well as industrial (KHAING et al., 2010) and domestic wastewater (KWON; BAE; KIM, 2021). Given the wide application in desalination, most of the research evaluated the consequences of feed components focusing on MD scaling and fouling (NAIDU et al., 2015). However, feed biofouling potential is receiving more attention even in brine water sources (KRIVOROT et al., 2011).

Knowing the feed composition allows for predicting the dominant fouling type and extension, and its control is facilitated. In terms of biofouling control, it is important to consider seasonal variability in feed water quality, for example, algae reproduction, when treating seawater (WARSINGER et al., 2014). Changes in feed composition cause changes to the conditioning film and the biofilm formation can be inhibited or fostered (VROUWENVELDER; KOOIJ, 2001).

Nutrient availability is an essential factor related to the selection of microorganisms, affecting biological growth and biofilm development. Usually, in the initial stage, the membrane surface is still poor in nutrients, and only pioneer microorganisms able to survive in this environment can start to establish a biofilm (JIANG et al., 2020). Furthermore, a more severe biological layer is formed on the MD surface if the feed presents a higher content of total organic carbon, macro and micronutrients, and microbial population. This condition results in faster flux decay (KRIVOROT et al., 2011). It may be a problem in wastewater-fed MD systems since it was

perceived that MD performance in synthetic wastewater treatment is strongly related to biofilm development, regardless of feed temperature (BOGLER; BAR-ZEEV, 2018).

Gryta et al. (2002) assessed microorganism growths in an MD bioreactor (MDBR) treating different feed solutions: acid industrial wastewater, tap water to produce demineralized water, salt wastewater from animal intestines processing (containing a large number of bacteria and fungi), and fermenting broth consisting of sugar with *Saccharomyces cerevisiae* yeast. In concentrating acid, few bacteria signals were observed, although it was not expected due to nutrients' absence in feed, besides the expectation that an acidic environment prevents microorganisms' development. Hence, the observed biological growth was attributed to tap water used to flush the module. The membrane used to treat the tap water presented biofouling potential since bacterial deposits were detected. The MDBR membrane presented only a few yeast organisms. Finally, when treating wastewater rich in microorganisms, MD biofouling development was more dependent on temperature, salt concentration, and operation time than on the presence of bacteria and fungi.

A high salinity feed is expected in the treatment of seawater, brackish water, wastewater, and brine solutions from other membrane processes. The hypertonic saline medium selects halotolerant and halophilic bacteria in the long-term operation (LUO et al., 2017), causing changes in the fouling microbial community (JIANG et al., 2020) . Liu et al. (2020b) evaluated the effects of high salinity and metals concentration on MD feed on biofilm growth. Feeds consisted of lake water supplemented with NaCl, $ZnCl_2$, and $FeCl_3$. Higher concentrations of $ZnCl_2$ and NaCl in the feed mitigated microbiological growth and a larger volume of dead bacteria was found in the biofilm. In the experiment with water supplemented with NaCl only, the membrane presented less biomass being attached to its surface. $ZnCl_2$ was successively hydrolyzed and decomposed into ZnO, which is a sterilant compound. In contrast, $FeCl_3$ accumulation proved to promote biofilm development since iron ions are an essential factor in microbial metabolism. This biofilm presented a great proportion of living bacteria, although it was lower compared to the control test membrane. It can be explained by feed acidification caused by $FeCl_3$ hydrolysis, which caused some bacteria to die. Finally, comparing high temperature and salt stress, metallic compounds had an outstanding role in affecting biofilm formation and composition.

Jang et al. (2020) assessed the feed concentration effect on MD biofouling when treating seawater. Concentrating and non-concentrating modes tests were performed and compared. The authors detected lower bacteria amount over the concentrating mode due to salt-stress

inhibition. Interestingly, more EPS was released, and a thicker $CaCO_3$ layer was formed, worsening MD performance. Fouling was mainly affected by temperature in non-concentration mode and by both temperature and salinity in concentration mode. Thus, hypertonic media consequences can be summarized as scaling enhancement, thermophilic and halotolerant bacteria selection, and concentration polarization.

Liu et al. (2020c) also assessed feed quality impacts on biofilm development and characteristics in a DCMD system. Two feed sources, namely river water with higher organic and bacteria content and lake water presenting higher salinity, were compared. Attachment on membrane surface occurred to a larger extent when treating river water. The formed biofilm presented a higher quantity of bacteria and organic components. Thus, a more severe flux drop took place. The biological variety was mildly reduced by heat stress during operation. In contrast, the biofilm formed during the lake water feed treatment exhibited less bacteria and organic content, so biofouling presented a moderate development. However, because of salinity and heat stress, microbial succession in biofilm was affected, leading to a more heterogeneous biofilm. Therefore, it can be concluded that feed composition impacts biofilm composition, microbial abundance, and diversity.

4.3 Membrane characteristics and module configurations

Characteristics of the membrane surface, such as charge, hydrophobicity, and roughness, may be relevant mainly in the first stages of biofilm development. Although almost all surfaces are susceptible to biofilm formation, they are less prone to biofouling if there is a lower degree of roughness, it is not charged, and presents higher hydrophilicity (PASMORE et al., 2002). While there is a weak correlation linking initial adhesion and the mature biofouling extension - since its development decreasingly depends on membrane-bacterial interaction over the operation - primary comprehension of bacterial-membrane interactions in the initial stage of biofilm development may be useful for advancements in biofouling control approaches (HABIMANA et al., 2014). EW

Cell wall properties of bacteria present in feed influence the initial biofilm, too. Intuitively, bacteria with hydrophobic cell wall preferentially adhere to hydrophobic surfaces, and the attachment happens to a larger extent compared to hydrophilic bacteria-hydrophilic surfaces interaction (VAN LOOSDRECHT et al., 1987). Considering that hydrophobic groups composing the bacteria cell wall, particularly groups constituted of nonpolar proteins, are usually involved in the attachment stage in aquatic ecosystems (HABIMANA et al., 2014), the

hydrophobic character of MD polymeric materials might influence biofilm development during the attachment stage. Bogler and Bar-zeev (2018) observed that the MD membrane itself accumulated more biofilm than the spacer in tests in a DCMD module. The authors attributed the higher bacteria attachment to both the higher hydrophobic character of the membrane concerning the spacer and the hydrodynamic conditions (see section 4.4).

Saeki et al. (2017) evaluated the biofilm formation process on polymeric materials with different hydrophobicity characters: polyvinyl alcohol (PVA), cellulose acetate (CA), polyvinylidene chloride (PVC), polyethersulfone (PES), polysulfone (PS), and polyvinylidenefluoride (PVDF). Among polymeric materials, PVDF was the polymer with the strongest hydrophobic characteristics. Adhesion tests conducted by material immersion in bacterial solution resulted in higher biofilm coverage on the PVDF surface. The most hydrophilic polymer studied, PVA, did not present bacterial coverage after 1 hour immersion.

Many of the chemical modifications carried out on MD membranes' surfaces aim to synthesize superhydrophobic membranes to provide wetting resistance and increased flux (DONG et al., 2015). Although studies show that the superhydrophobic character decreases fouling and scaling (RAZMJOU et al., 2012), other researchers have revealed that this attempt does not satisfactorily mitigate fouling (NTHUNYA et al., 2019). These membranes are still susceptible to biofouling and other mitigation techniques, as additional structural changes in the membrane are required, as will be further discussed (WARSINGER et al., 2015). Assessing biofilm formation on hydrophobic and superhydrophobic materials, Zhang et al. (2005) observed that the superhydrophobic character had more success in biologic fouling prevention. Nonetheless, surfaces had no more anti-fouling characteristics after two months of immersion in seawater.

Electrostatic interactions may influence the primary deposition of foulants when they are already very near the membrane surface (GUO et al., 2020). In aquatic environments, bacteria in neutral pH, in general, are negatively charged (HABIMANA et al., 2014) and MD membrane materials, such as PVDF (GUO et al., 2018) and PTFE (LIU et al., 2018), as well. Thus, prevention of microbiological attachment by electrostatic repulsion could be expected.

A less dense biofilm was observed over the MD membrane surface in an electrical anti-biofouling approach because of stronger Coulomb repulsion between bacteria and a negatively charged membrane (JIANG et al., 2019). Factors as microorganism species, feed pH, and ionic strength influence the magnitude of the charges. Also, in high ionic strength solutions, the

effects of electrostatic forces between bacteria and the polymeric surface are reduced (GOTTENBOS et al., 2000).

In addition to membrane properties, the module configuration may also affect biofilm development. Qin et al. investigated combinations of scaling and organic fouling in three MD configurations, specifically DCMD, VMD, and SGMD. VMD had the worst performance for most tests since the membrane's deformation under unbalanced pressure generated dead zones, intensifying supporting conditions for fouling. Although DCMD exhibited the highest fluxes among the configurations, it presented the highest fouling rate in the test combining all evaluated foulants. For this combination, concentration polarization was more significant to intensify fouling than turbulence conditions, leading to more critical fouling in DCMD. SGMD was the most resistant-to-fouling configuration due to the lower flux and the hydrodynamic mixing introducing shear forces. However, further investigation of MD biofouling behavior in different MD configurations is required.

4.4 Other operational conditions

Hydrodynamic forces are responsible for carrying foulants to the membrane surface. Since organisms must pass through the hydrodynamic layer to be deposited on the membrane, the factors that affect its thickness, such as feed and permeate crossflow velocity, impact the biofilm growth rate. Regardless of Brownian motion and bacteria motility, which allows bacteria to cross the hydrodynamic layer, the higher the convection from a higher permeate water flux, the more bacteria deposit over the membrane. A higher permeate flux also lowers the detachment rate and increases nutrients and dissolved oxygen concentrations, fostering biofilm maintenance (GHAYENI et al., 1998; ZOU et al., 2013). In addition, higher fluxes may be more important to fouling accumulation in supercritical conditions than other factors, such as microbial succession (CHEN; FU; GAO, 2015).

The quantity of biological film, its thickness, and porosity diminish while Reynolds numbers rise reaching turbulent conditions (VIEIRA et al., 1993). As shear stress also increases the detachment rate (RADU et al., 2012), keeping the flow conditions of turbulence inside the module helps to avoid contact between bacteria and the membrane surface and diminish biofouling extension (ALWATBAN et al., 2019). An appropriated module design and placing a spacer on the feed channel favor turbulence and shear stress, mitigating fouling. However, under higher shear stress, the developed biofilm may present greater cohesive forces, mechanical resistance, and density due to microbiological protective reaction to shear stress,

promoting EPS production and reinforcing biofilm structure. Because of this, the diffusivity in biofilms formed under higher turbulence is lower (VIEIRA et al., 1993). Still, there are not many studies about hydrodynamic effects on mature MD biofouling available to date.

Bogler and Barzeev (2018) recognized that turbulent conditions at the MD feed spacer reduced the prospect of irreversible biofilm developing on it. Additionally, concerning the MD spacer, more biofilm was observed at the intersections between the spacer fibers because of the formation of vortexes with decreased shear stress and slower flow velocity.

Krivorot et al. (2011) evaluated the biofilm in MD under two hydrodynamic conditions: parallel flow (the circulation direction of both streams is parallel to the membrane) and crossflow (the feed is introduced perpendicular to the membrane). The fibers next to the module's exit under crossflow operation were the most fouled, mainly attributed to the lower temperature at the module outlet. The authors also observed that the temperature might be more relevant to MD biofilm than hydrodynamic influences. At the module inlet, where the driving force was higher and, the flux brought more nutrients and bacteria to the membrane surface, the fouling occurred to a lower extent.

Another operational condition that affects biofilms in MD is the mode of operation. Liu et al. (2020a) evaluated the effect of recirculating the concentrate in the feed compartment (closed-loop) and operating with an open-loop, discharging the concentrate flow and maintaining a constant feed composition. Under continuous feed concentration, the concentration polarization effect favored microorganisms to inhabit the membrane surface during initial operation stages due to higher nutrient availability. However, salt and metal enrichment over operation caused the death and the succession of the biofilm species. Bacteria under this stress condition released more EPS, which intensified biofilm formation. On the other hand, under open-loop, a more stable biofilm was formed.

Fig 4.3 shows a scheme that summarizes how biofilm in DM is affected by the factors and characteristics discussed.

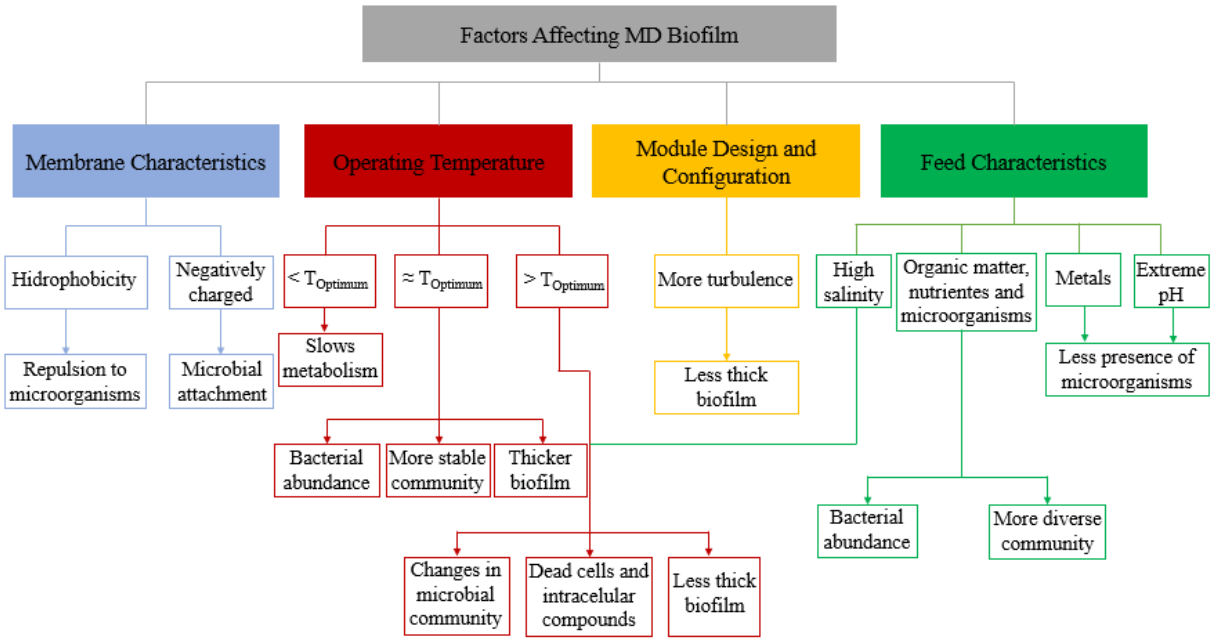

Fig. 4. 3 – MD characteristics and operational factors affecting biofilm formation

5 BIOFOULING CONSEQUENCES IN MD

Biofilms are known to increase costs associated with industrial systems, and MD is no different. Fig 4.4 presents some consequences of biofilm in MD (GOH et al., 2019), which will be discussed in greater depth in this section.

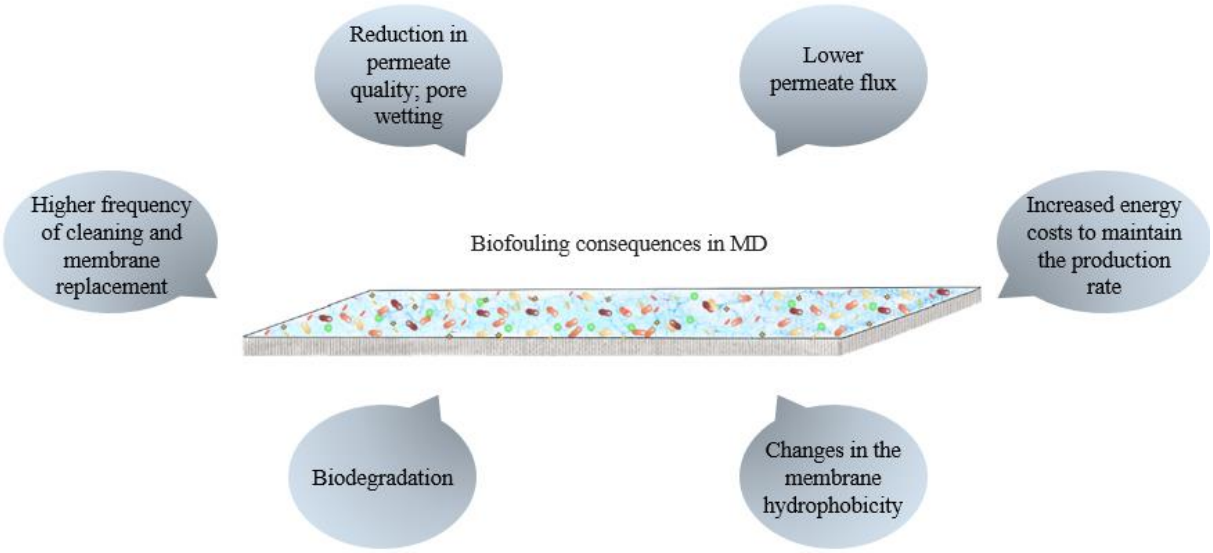

Fig. 4. 4 – General consequences of the development of biofouling in MD over the operation

5.1 Biofouling affecting MD flux

Flux in MD is closely related to heat transfer since the temperature gradient induces a vapor pressure difference between the membrane surfaces, resulting in vapor permeation (ALKHUDHIRI; DARWISH; HILAL, 2012). It has already been shown that biofilm can significantly reduce heat transfer (KIRKPATRICK; MCINTIRE; CHARACKLIS, 1980) by convection, so diffusion and conduction mainly promote heat transfer (GOH et al., 2013). Thus, the biologic layer can enhance thermic resistance over the operation (MELO; BOTT, 1997). Characklis et al. (1981) estimated the thermal conductivity of biofilms between 0.57 and 0.71 W/(m·K). It is a range of values close to the water's thermal conductivity, which is consistent with the fact that the biofilm is mainly composed of water.

Besides heat transfer, which some researchers concluded was not the principal cause of the observed flux decline, there is a resistance to mass transfer (SRISURICHAN et al., 2006). Water diffusion through the EPS matrix is decreased; the reduction of effective membrane area

due to pore blockage provides additional hydraulic resistance (GOH et al., 2013) and leads to flux decay (BOGLER; BAR-ZEEV, 2018). Denser biofilm layers may also provide extra hydraulic resistance, and these structures may increase temperature and concentration polarization.

The different characteristics of the fouling layer will cause different mechanisms to reduce flux. Gryta (2008) observed that homogeneous fouling layers lead to a notable resistance to mass transfer, while porous fouling results in flux reduction principally due to thermic resistance. Biofilms typically have small pores, with diameters less than 50 nm, and are relatively thin. Therefore, the reduction in flux may be explained by the higher resistance to both heat transfer and water permeation (WEI et al., 2014). The less biofilm is porous, the lower the heat transfer by convection happens (GOH et al., 2013).

Goh et al. (2013) evaluated if biofilm hydrophobicity also affects MD flux. There is an increase in vapor pressure, and consequently, a higher flux when a more hydrophobic layer covers the membrane. On the contrary, more hydrophilic fouling results in vapor pressure decrease and flux reduction. Although the difference in flux due to hydrophobicity was not observed to a significant extent, it was demonstrated that biofouling caused a vapor pressure depression of 21 and 31% for the less and more hydrophilic fouling, respectively. Biofouling provided vapor-pressure depression, due to the Kelvin effect, besides resistance to mass and heat transfer, which led to a flux decline of 60%. Corroborating the study conducted by Goh et al. (2013), Chew et al. (2014) developed a model that supports that the biofilm layer can reduce the flux due to the depression in the vapor pressure. This factor's influence becomes more critical as the pore diameter of the layer gets smaller and under reduced temperature differences between feed and distillate.

Simultaneously, the conditions of higher TP foster a more favorable environment for bacteria (ZODROW et al., 2014), and biofilm formation aggravates the TP effect. Since the temperature difference on both membrane surfaces is reduced compared to the bulk solution, the driving force for permeation is reduced (SRISURICHAN et al., 2006), and the effective temperature difference (ΔT_{eff}) is reduced when the membrane is biofouled (Fig. 5). Bogler et al. (2017) proposed a temperature decline in two stages from feed bulk solution. First, there is a reduction across the boundary layer formed right over the biofilm layer and after across the biofilm layer until the membrane interface. Because of the heat flux, the interface between membrane and permeate is at a higher temperature than the bulk permeation. In this way, the effective temperature difference in a biofouled MD is much smaller, reducing the system's energy

efficiency. The authors also described the adaptation of the equation of heat flux to calculate the effects of TP increased by biofilm on water flux (J_W), in which heat flux across the membrane is equal also to heat flux across both boundary ($Q_{f,BL}$) and biofilm layers ($Q_{Bio,BL}$):

$$Q_{Bio,BL} = J_W \cdot H_{L,B} + h_B \left(T_B - T_{m,f}\right) = Q_{f,BL} = J_W.H_{L,f} + h_f \left(T_f - T_B\right)$$

Where $H_{L,B}$ and $H_{L,f}$ are the enthalpies of the solutions in the interface feed-biofilm and in bulk feed; h_B and h_f are the heat transfer coefficient of the biofilm and of the feed, and T_B, $T_{m,f}$ and T_f are temperatures at the feed-biofilm interface, at membrane-feed interfaces and at feed bulk, respectively.

As in other membrane processes, biofilm worsens the CP effect, bringing consequences for the MD's mass transfer since vapor pressure is reduced due to higher concentrations near the membrane (JIANG et al., 2020). CP can promote supersaturation conditions next to the biofilm (KRIVOROT et al., 2011), supporting nucleation and crystal formation, which improves inorganic scaling and induces pore wetting (. In this way, it is relevant to remember that in real samples, all types of fouling coexist, and this situation illustrates the possibility of the formation of one type of film (in this case, biofilm, which enhances TP, lowers the temperature and changes salts solubility) can generate more favorable conditions for the development of another type (here, TP promoting scaling). Nonetheless, MD's high temperatures lessen CP, which enables MD to be operated in a bit more supersaturated conditions than other membrane processes (TOW et al., 2018).

5.2 Biofouling affecting MD permeate quality

A great problem in the MD process is the wetting of the membrane pores (Fig. 4.5), which lowers the quality of the permeate (SHIRAZI et al., 2016) and limits the technology's applications, such as for wastewater reclamation, since organic compounds and nutrients may worse wetting conditions further (GOH et al., 2013). The wetting of the membrane pores can happen because:

i. Hydrostatic pressure supersedes the liquid entry pressure (LEP), described by the Laplace-Young equation (ALKHUDHIRI; DARWISH; HILAL, 2012), and liquid enters the pores (CAMACHO et al., 2013);
ii. The high content of organics or surfactant in the feed reduces the surface tension of the feed solution (FRANKEN et al., 1987);

iii. Fouling takes place (GRYTA, 2005).

The polymer's surface energy and pore size distribution determine LEP (BOGLER; LIN; BAR-ZEEV, 2017). In addition, fouling may lower LEP and block pores, leading to a performance decline (REZAEI et al., 2018).

The secretion of EPS with amphiphilic character by the bacteria favors pore wetting (KRIVOROT et al., 2011). Wetting happens in three stages, namely superficial, partial and complete pore wetting (LI et al., 2018). Although an increase in flux can be observed during the stage of partial pore wetting caused by biofouling, the performance is compromised (BOGLER; BAR-ZEEV, 2018). As wetting advances to a complete pore wetting, separation becomes more dependent on pore size, and the rejection of contaminants reduces. It was previously observed that microorganisms from the biofilm might contaminate the distillate compartment, despite being larger than MD pores, which was explained by the formation of endospores and the passage of differently shaped bacteria.

Larger pores, the lower surface tension of the liquid, lower angle of contact of the membrane surface, and the progressively increased concentration of non-volatile components near the membrane can promote fouling and reduce surface tension and contact angle overall accelerating wetting (GOH et al., 2013). Liu et al. (2020b) verified the presence of *Mycobacteriaceae Unclassified* in the MD biofilm, a genus that has species capable of secreting a lot of EPS. Some of these organisms can also accumulate metabolites that act as biological surfactants around the cells. It led to a decreased surface tension of the membrane and pore wetting. When wetting occurs, the biofilm can develop inside the pores, resulting in pores blockage and, therefore, flux decline (KRIVOROT et al., 2011). Hence, wetting and fouling influence each other (CHOUDHURY et al., 2019).

The extension of the consequences of wetting depends on:

i. Operational conditions, like temperature;
ii. Presence of microorganisms that form the biofilm. If there is a secretion of EPS that may act as surfactants, for example, wetting can be significantly worse (BOGLER; BAR-ZEEV, 2018);
iii. If the hydrophilic biofilm covers pores internally. Biofilm exclusively on the surface leads to reduced flux, not wetting (ZODROW et al., 2014).

The role of biofilm in wetting is not a consensus. Depending on operational factors and feed composition, as in MDBR, the presence of a biofilm can prevent wetting since microorganisms can also biodegrade organic compounds that promote wetting (GOH et al., 2013).

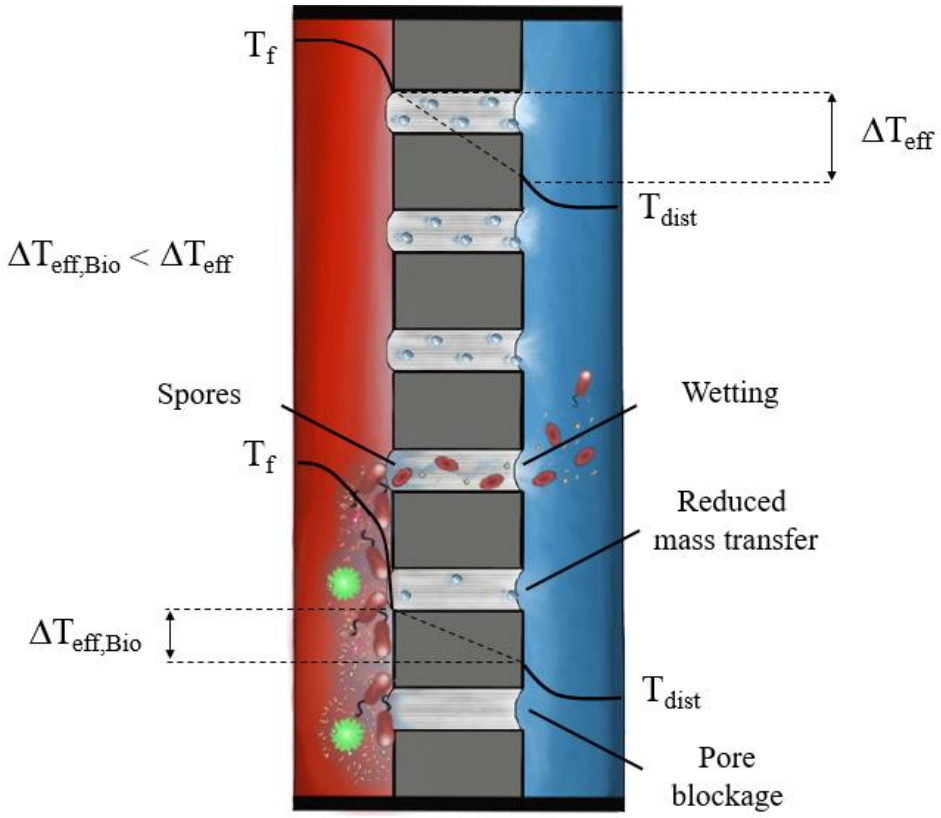

Fig. 4. 5 – Biofouling consequences on MD performance

6 BIOFOULING MITIGATION IN MD

Given the presence of bacteria in real matrices is expected, biofilm formation is just a matter of time. Bacteria in a biofilm are more resistant than isolated organisms (GRYTA, 2002) and fouling brings various negative consequences to MD. Several efforts have been made to develop methods that prevent or mitigate it. These methods vary from traditional methods, such as chemical cleaning, to modifications in the membrane surface. In practice, biofouling mitigation should combine the integration of several techniques (GOH et al., 2019). The principle of mitigation by operational methods was previously discussed in chapter 3, and pre-treatments are closely related to the feed composition, from which compounds that can promote biofouling should be removed (RAY et al., 2021). Therefore, membrane modification, which was the most studied for preventing MD biofouling, is discussed in the following. Besides, biocides, cleaning, and biological methods are overviewed since these methods have not been further studied in MD yet, focusing on their power and limitations and application feasibility in the MD system.

6.1 Membrane modifications

In order to minimize wetting and fouling, chemical modifications have been made to manufacture superhydrophobic, omniphobic, and self-cleaning membranes (WANG; LIN, 2017). Superhydrophobic membranes arise through the addition of nanoparticles, such as silica and titanium dioxide, to generate rougher surfaces with lower membrane surface energy (RAZMJOU et al., 2012; NTHUNYA, et al., 2019). The lower tendency to wetting, when compared to the hydrophobic membrane, can be explained by the greater difficulty for the liquid to enter the pores (lower surface tension and/or smaller size of the pores) and because of the lower energy of the surface membrane, which reduces the chances of nucleation and, therefore, scaling (LU; ZUO; CHUNG, 2016). However, if the feed contains substances that also have low surface tension or surfactants, the membrane's performance will also be compromised (CHOUDHURY et al., 2019). Besides, superhydrophobic membranes seem to be more susceptible specifically to biological fouling (WARSINGER et al., 2015). Therefore, other types of chemical modifications or even integration with other mitigation methods is necessary.

Omniphobic membranes repel liquids with high and low surface tension (JIA; CHEN; CHUNG, 2019), presenting an apparent contact angle greater than 90º in both types of liquids. Thus, resistance to wetting is greater for a broader range of matrices (LU et al., 2018; WANG et al.,

2019), for example, seawater contaminated with oil, wastewater with low surface tension contaminants, and water produced in natural gas fields (DIZGE; SHAULSKY; KARANIKOLA, 2019). These membranes are generally produced by combining reentrant structure and materials with low surface energy (WANG; LIN, 2017). However, resistance to organic fouling caused by contaminants like oil and grease can be achieved with a hydrophilic layer (LI et al., 2019). The necessity of opposing surface properties to mitigate this type of fouling and wetting for treating some complex wastewaters can be solved with Janus membranes. These membranes consist of a hydrophobic substrate coated with a hydrophilic layer (LEE et al., 2020). In contrast to omniphobic membranes, Janus membranes exhibit a superior performance (LI et al., 2019).

Antimicrobial nanoparticles are usually made of heavy metals whose atoms' electronic configuration exhibits a partially filled d orbital. It is a favorable electronic configuration to form nanoparticles due to the more redox-active character. Antibacterial mechanisms involve the generation of reactive oxygen species, organisms' membranes interaction, and other metabolisms aspects, like ATP reduction. Ag, Fe, Zn, and Ti are some of the elements that have been used in antibacterial nanoparticle manufacture (SLAVIN et al., 2017).

A superhydrophobic membrane was coated with a layer containing carboxylated multiwalled carbon nanotubes and silver nanoparticles. Biofouling tests were carried out with effluent from a reactor that contained thermophilic bacteria as the feed of DCMD. Cake formation was reduced by membrane coating, and silver nanoparticles inhibited microorganisms' activity. Despite the enhanced resistance to biofouling, flux and salt rejection were reduced (NTHUNYA et al., 2020). Ray et al. (2021) produced superhydrophobic membranes with anti-wetting, self-cleaning and antibacterial properties. They were produced by plasma treatment, and the membrane was submitted to TiO_2 coating. The manufactured membrane had a better performance due to increased salt rejection and water flux, combined with a decrease of 99% of bacteria activity.

Chew et al. (2019) produced a Janus membrane with multilevel roughness covered with silver nanoparticles (AgNPs). Resistance to surfactant and petroleum droplets adhesion, bacteria attachment, and biofouling development were evaluated. The membranes covered with AgNPs showed an evident biofilm development inhibition, rarely presenting living cells on the membrane surfaces. Nanoparticles interact with proteins and enzymes, disrupting the electron transport chain, leading to DNA dimerization and to cell wall membrane detachment. In contrast, pristine PVDF membranes were covered with a thick biofilm layer after similar

operating times. Janus membranes manufactured with single-level structures exhibited an intermediate anti-biofouling performance. Their surfaces had a more hydrophilic character than the PVDF membrane. However, it is still subjected to the attachment of microorganisms, and biofouling over the operation was still observed.

Although there is promising evidence that chemical modifications can mitigate both wetting and fouling, many of the membrane production techniques are complex, time-consuming, and expensive (WANG et al., 2019). In addition, the consequences for the environment and health of the use of these nanoparticles are not known at all (BATLEY et al., 2013). Chemical modifications were previously made to obtain superhydrophobic and antimicrobial membranes for oil and water separation, taking into account the ease of scale-up and low costs (MA et al., 2020). Wang et al. (2019) took these premises into account when synthesizing an omniphobic membrane. The authors also raised the importance of identifying the trade-off between vapor permeability and wetting resistance. However, antimicrobial activity was not evaluated. Hammami et al. (2017) produced poly (ether imide) composite nanofiber membranes doped with ethylene-pentafluorophenylene-based periodic mesoporous organosilica nanoparticles in an attempt to produce a scalable and more environment-friendly membrane. The membrane showed a higher surface roughness and less surface energy, which reduced the bacterial attachment. The addition of Eugenol as an antibacterial agent to the pores increased the anti-biofouling properties by 70%, with a higher flux than commercial PTFE membranes.

Coupling chemical modification with other techniques to effectively mitigate biofouling can be required. Warsinger et al. (2015) produced a superhydrophobic membrane and observed that introducing air layers reduced biofouling by 96%, as air displaced the gel that gives cohesion to the biofilm. However, inorganic fouling aggravates with air layers introduction (WARSINGER, et al., 2016). The necessity of evaluating feed composition and the question of which foulants are more critical in the overall context is again highlighted.

6.2 Biocides

Inactivation of bacterial metabolism utilizing biocides is the main method to control biofouling. The biocide must be applied regularly to control biological growth (MATIN et al., 2011). Chlorination is a widely used procedure since free residual chlorine effectively reduces biofilms development (LUND; ORMEROD, 1995), whose typical doses for preventing biofouling are 1 and 50 ppm for continuous exposure and shock treatment (HENDREN; BRANT; WIESNER, 2009), respectively. However, chlorine can damage many polymeric membranes, though it is

possible to develop membranes resistant to chlorination (MANALO et al., 2019). Chlorination may also form carcinogenic by-products, like trihalomethanes, and is not effective against some microorganisms (AL-ABRI et al., 2019).

Ozone is a commonly applied biocide due to its high oxidation potential to inactivate protozoa, viruses, bacteria, and endospores (NGUYEN; RODDICK; FAN, 2012). It was observed that alleviation of specifically biofouling by pre-treatment with ozone effectively contributes to mitigating fouling in membranes (LEE et al., 2005) although there is no consensus on the effect of ozone on the mitigation of complex fouling since the ozonation efficiency is related to influencing factors, such as the nature of EPS and membrane pore size, as ozone may lead to microflocculation of the particles (YU; ZHANG; GRAHAM, 2017).

Ozone promotes less toxic by-product formation (NGUYEN; RODDICK; FAN, 2012). The effect of ozone on MD fouling mitigation was studied in a hybrid catalytic ozonation membrane reactor. While in the MD test, the flux decreased by 39.6%, because of organic fouling, in the hybrid system with ozone applied, the reduction was only 9.5% (ZHANG et al., 2016). Organic fouling mitigation also indicates ozone as a promising anti-biofouling agent since organic and biological fouling are closely related. Nevertheless, there is still a vacancy for further research to compare the pre-treatment and hybrid treatment of ozone to reduce MD biofouling. As for disadvantages, ozone generation costs are higher than chlorination, it is necessary to generate ozone in situ due to its instability, and it can damage the membrane surface due to its highly oxidizing character (MATIN et al., 2011). Besides, as higher temperatures decrease ozone solubility (AL-ABRI et al., 2019), the process's efficiency can be compromised if the MD feed's temperature is already relatively high.

UV irradiation (specifically UVC at 200-300 nm) has several advantages: no production of harmful by-products, easy installation and maintenance (KIM et al., 2009), pH-independency, and no involvement of chemicals. UV irradiation penetrates the cell and damages the genetic material, and its efficiency is related to feed quality (high turbidity water limits the penetration of light) (AL-ABRI et al., 2019). UV treatment decreases EPS on the membrane surface (MARCONNET et al., 2011), favors the formation of less thick biofilms, with less cell density and less microbial diversity (HARIF et al., 2011). The coupling of UV irradiation and membrane treatment can be done as pre-treatment with irradiation (MARCONNET et al., 2011) or in a hybrid way (GUO et al., 2015). The disadvantages of UV pre-treatment are that UV has no residual effect, and regrowth can occur if the time between treatment and permeation is long enough and if some bacteria receive a dose of radiation below that required for inactivation

(MARCONNET et al., 2011). The hybrid system can overcome the regrowth risk by direct irradiation of the membrane and photocatalytic membranes. Another advantage of the hybrid system is the greater robustness to reach microorganisms when the treated matrix has high turbidity (GUO et al., 2015).

Although there are studies on hybrid radiation-MD module, it was used for other applications, such as for photocatalytic membrane regeneration (GUO et al., 2019), so it is still necessary to assess specifically biofilm mitigation by UV and investigate whether the MD membrane's integrity is impaired when irradiated directly in the long-term. Besides, it requires mercury lamps, which have been avoided in processes and products worldwide because of toxic mercury gas (MATAFONOVA; BATOEV, 2018). An alternative is the use of LED lamps, which have been studied to inactivate several microorganisms (SONG; MOHSENI; TAGHIPOUR, 2016).

However, once established, it is known that the biofilm becomes resistant to biocides, which start to act only in its outermost layers (BAR-ZEEV et al., 2012).

6.3 Cleaning

Membrane lifetime is closely related to the recovery of the membrane's characteristics after use. It is essential for chemical cleaning to consider feed composition and foulants types that the membrane is subjected to when choosing the cleaning solution. Thus, it is possible to optimize the frequency and chemicals concentration (CHOUDHURY et al., 2019), since chemical cleaning can also lead to membrane structural damage, as assessed in a study conducted on a long-term pilot-scale MD solar system that aimed at removing scaling, given the feed characteristics (GUILLEN-BURRIEZA, 2014). Therefore, employing other mitigation techniques decreases chemical cleaning frequency and increases membrane lifetime, which is imperative to viability.

So far, cleanings on MD membranes have focused more on removing scaling and organic fouling with acidic or basic solutions, respectively. Considering biofouling, it is more difficult to recover the MD membrane back to its original hydrophobicity and flux after irreversible attachment. As organic and biological fouling are intertwined, alkaline cleaning, recommended for organic fouling, will certainly remove many microorganisms present in fouling and generate less favorable conditions. In a pilot-scale study, chemical cleaning to remove organic fouling was assessed, and MD flux was recovered by 79% (DOW et al., 2017).

However, there are still few studies on specific methodology for MD biofouling cleaning. When studying biofilm in MD, Krivorot et al. (2011) cleaned MD membranes following these steps: flushing with NaOH at pH 12 and 40ºC, which was expected to hydrolyze microorganisms, as well as organic compounds; washing with distilled water, 70% ethanol, and distilled water again, before vacuum drying. This cleaning methodology enabled the recovery of the original flux. Bogler et al. (2017) suggested minimizing the use of chemicals to mitigate biofilm, but instead giving preference to grafting active agents onto the membrane surface, paying attention to the controlled release of antimicrobial species to reduce the need for agents to be refilled. Moreover, it is essential to concern with the discharge of chemical compounds and by-products into the environment.

Therefore, it is essential to emphasize the need for further studies to develop MD cleaning strategies against biofouling. The effect of chemicals on the membrane surface, on wettability, and the effect of cleaning on biofilm formation in long-term operations must be assessed further in the future.

6.4 Other mitigation methods

6.4.1 Biological Mitigation

Among biological methods for biofilm prevention, the inhibition or interruption of the QS has been widely researched in the last decades. Disrupting QS is a strategy to avoid bacterial attachment and membrane biofouling development (GU et al., 2018). The inhibition involves autoinducer molecule analogs that can bind to QS receptor proteins. Analogs do not lead to the autoinducer response. Furanones, their synthetic derivatives, and polyphenols are some examples of molecules used to inhibit QS. QS inhibition has several advantages because of its efficiency in biofouling control, low toxicity, and low risk of developing resistance. Quorum sensing inhibitors can be injected in solution or incorporated into the membranes' surface, which is a promising attempt to inhibit biofouling (KIM et al., 2021). Besides, quorum quenching (QQ) has been evaluated to mitigate biofouling and has been considered an economical and efficient technology (YANLING et al., 2018). Combining QQ bacteria and conventional methods, such as chlorination, is efficient in controlling biofouling (WEERASEKARA; CHOO; LEE, 2016). However, evaluations must be made with microorganisms from biofilms formed from real matrices, and the treatment of real wastewater with QQ bacteria will have to be evaluated for competition with other organisms for nutrients (YANLING et al., 2018). Further studies are also needed to investigate the possibility of

microorganisms acquiring resistance to inhibitory molecules, as well as the associated risks to aquatic environments.

Among other biological methods, nitric oxide (NO) control should be mentioned, which is a molecular messenger that antagonizes the proliferation of bacteria. However, NO is poorly soluble in water and unstable, which reduces the efficiency of the direct application of NO, requiring the use of NO owners. In addition, there are methods that involve enzymatic hydrolysis of EPS and the enzymatic hydrolysis of the cell wall (XIONG, 2010). However, it is necessary to evaluate the action of these enzymes at temperatures typical of MD.

6.4.2 Electrical Mitigation

The application of electric fields has been shown to be promising as an anti-fouling technique (AHMED et al., 2016) and anti-biofouling mechanisms include direct or indirect oxidation, Joule effect, and Coulomb repulsion. The anti-biofouling properties of an electrically conductive PTFE membrane covered with a layer of carbon nanotubes were assessed operating in capacitor and resistor modes. In capacitor mode, the repulsion between bacteria and membrane, besides the distortion of the bacteria shape, led microorganisms to death. In resistor mode, the Joule effect elevated surface temperature, and bacteria were under greater stress (JIANG et al., 2019).

7 FUTURE PERSPECTIVES AND FINAL CONSIDERATIONS

MD is a promising technology for obtaining high quality water, which will be increasingly necessary for the coming years. Nevertheless, fouling remains a challenge, as it is for other membrane processes. Contrary to what was initially thought, biofouling is very relevant in MD and leads to several performance problems, so biofilm development must be well-understood to promote the development of technologies that mitigate biofouling. Thus, biofouling has been the subject of study in several recently published papers, after a period when most studies focused only on scaling assessment. Nevertheless, there are still many gaps in MD biofouling knowledge.

Although there is some information about how temperature affects biofilm formation, it is still necessary to assess how other aspects can favor or mitigate biofouling. The module configuration and type of membrane, for example, are some points that deserve more attention in the future. Most studies focused on investigating fouling in the DCMD configuration and only assessed biofilm impacts in the feed compartment. More studies are also needed to understand eukaryotic beings' role in biofilm. In addition, MD biofilm has been evaluated with synthetic effluent and surface waters, but further studies are needed on biofilm formation with MD treating real effluents. Evaluations of cleaning procedures for MD membranes recovery must be done since biofouling leads to loss of hydrophobicity. It is also necessary to conduct feasibility studies on applying mitigation techniques in a full-scale MD system to verify the simultaneous mitigation of scaling and organic fouling, besides biofouling, since all types are present in real membrane fouling and are strongly interlinked. When evaluating mitigation techniques, long-term studies on the lifetime of the MD membrane are also required to assess economic aspects considering a larger scale. These evaluations will be fundamental for MD consolidation considering the current context requires simple, inexpensive, and environmentally friendly technologies.

REFERENCES

A. ALKHUDHIRI, N. DARWISH, N. HILAL, Membrane distillation : A comprehensive review, Desalination. 287 (2012) 2–18. https://doi.org/10.1016/j.desal.2011.08.027.

A. ANSARI, J. PEÑA-BAHAMONDE, S.K. FANOURAKIS, Y. HU, D.F. RODRIGUES. Microbially-induced mineral scaling in desalination conditions: mechanisms and effects of commercial antiscalants. Water research, 179 (2020) 115863. https://doi.org/10.1016/j.watres.2020.115863

A. BOGLER, E. BAR-ZEEV, Membrane distillation biofouling: Impact of feedwater temperature on biofilm characteristics and membrane performance, Environmental Science & Technology. 52 (2018) 10019–10029. https://doi.org/10.1021/acs.est.8b02744.

A. BOGLER, S. LIN, E. BAR-ZEEV, Biofouling of membrane distillation, forward osmosis and pressure retarded osmosis: Principles, impacts and future directions, Journal of Membrane Science. 542 (2017) 378–398. https://doi.org/10.1016/j.memsci.2017.08.001.

A. CHAFIDZ, S. AL-ZAHRANI, M.N. AL-OTAIBI, C.F. HOONG, T.F. LAI, M. PRABU, Portable and integrated solar-driven desalination system using membrane distillation for arid remote areas in Saudi Arabia, Desalination. 345 (2014) 36–49. https://doi.org/10.1016/j.desal.2014.04.017.

A. DESHMUKH, C. BOO, V. KARANIKOLA, S. LIN, A.P. STRAUB, T. TONG, D. M. WARSINGER, M. ELIMELECH, Membrane distillation at the water-energy nexus: limits, opportunities, and challenges, Energy & Environmental Science 11 (2018) 1177–1196. https://doi.org/10.1039/C8EE00291F.

A. MATIN, Z. KHAN, S.M.J ZAIDI, M.C. BOYCE, Biofouling in reverse osmosis membranes for seawater desalination: Phenomena and prevention, Desalination 281(2011) 1–16.

A. RAZMJOU, E. ARIFIN, G. DONG, J. MANSOURI, V. CHEN, Superhydrophobic modification of TiO2 nanocomposite PVDF membranes for applications in membrane distillation, Journal of Membrane Science. 415–416 (2012) 850–863. https://doi.org/10.1016/j.memsci.2012.06.004.

A.C.M. FRANKEN, J.A.M. NOLTEN, M.H.V. MULDER, D. BARGEMAN, C.A. SMOLDERS, Wetting criteria for the applicability of membrane distillation, Journal of Membrane Science. 33 (1987) 315–328. https://doi.org/10.1016/S0376-7388(00)80288-4.

A.I. RADU, J.S. VROUWENVELDER, M.C.M. VAN LOOSDRECHT, C. Picioreanu, Effect of flow velocity, substrate concentration and hydraulic cleaning on biofouling of reverse osmosis feed channels, Chemical Engineering Journal. 188 (2012) 30–39. https://doi.org/10.1016/j.cej.2012.01.133.

A.K. MANNA, P. PAL, Solar-driven flash vaporization membrane distillation for arsenic removal from groundwater: Experimental investigation and analysis of performance parameters, Chemical Engineering and Processing: Process Intensification. 99 (2016) 51–57. https://doi.org/10.1016/j.cep.2015.10.016.

A.L. ALLDREDGE, U. PASSOW, B.E. LOGAN, The abundance and significance of a class of large, transparent organic particles in the ocean, Deep Sea Research Part I: Oceanographic Research Papers. 40 (1993) 1131–1140. https://doi.org/10.1016/0967-0637(93)90129-Q.

A.M. ALKLAIBI, N. LIOR, Membrane-distillation desalination: Status and potential, Desalination. 171 (2005) 111–131. https://doi.org/10.1016/j.desal.2004.03.024.

A.M. ALWATBAN, A.M. ALSHWAIREKH, U.F. ALQSAIR, A.A. ALGHAFIS, A. OZTEKIN, Performance improvements by embedded spacer in direct contact membrane distillation - Computational study, Desalination. 470 (2019) 114103. https://doi.org/10.1016/j.desal.2019.114103.

B. GOTTENBOS, H.C VAN DER MEI, H.J. BUSSCHER, Initial adhesion and surface growth of Staphylococcus epidermidis and Pseudomonas aeruginosa on biomedical polymers, Journal of Biomedical Materials Research. 50 (2000) 208-214. https://doi.org/10.1002/(SICI)1097-4636(200005)50:2%3C208::AID-JBM16%3E3.0.CO;2-D.

B. GUO, E.V. PASCO, I. XAGORARAKI, V.V. TARABARA, Virus removal and inactivation in a hybrid microfiltration-UV process with a photocatalytic membrane, Separation and Purification Technology. 149 (2015) 245–254. https://doi.org/10.1016/j.seppur.2015.05.039.

B. TOMASZEWSKA, J. BUNDSCHUH, L. PAJAK, M. DENDYS, V.D. QUEZADA, M.A. ARMIENTA, M.O. MUÑOZ, A. KASZTELEWICZ, Use of low-enthalpy and waste geothermal energy sources to solve arsenic problems in freshwater production in selected regions of Latin America using a process membrane distillation – Research into model solutions, Science of The Total Environment. 714 (2020) 136853. https://doi.org/10.1016/j.scitotenv.2020.136853.

B.R. BODEL, Distillation of saline water using silicone rubber membrane, United States Patent No. 3,361,645, 1968.

C. GRANDCLÉMENT, I. SEYSSIECQ, A. PIRAM, P. WONG-WAH-CHUNG, G. VANOT, N. TILIACOS, N. ROCHE, P. DOUMENQ, From the conventional biological wastewater treatment to hybrid processes, the evaluation of organic micropollutant removal: A review, Water Research. 111 (2017) 297–317. https://doi.org/10.1016/j.watres.2017.01.005.

C. LI, X. LI, X. DU, T. TONG, T.Y. CATH, J. LEE, Antiwetting and antifouling janus membrane for desalination of saline oily wastewater by membrane distillation, ACS Applied Materials & Interfaces. 11 (2019) 18456–18465. https://doi.org/10.1021/acsami.9b04212.

C. LIU, L. CHEN, L. ZHU, Fouling mechanism of hydrophobic polytetrafluoroethylene (PTFE) membrane by differently charged organics during direct contact membrane distillation (DCMD) process: An especial interest in the feed properties, Journal of Membrane Science. 548 (2018) 125–135. https://doi.org/10.1016/j.memsci.2017.11.011.

C. LIU, L. CHEN, L. ZHU, Z. WU, Q. HU, M. PAN, The effect of feed temperature on biofouling development on the MD membrane and its relationship with membrane performance: An especial attention to the microbial community succession, Journal of Membrane Science. 573 (2019) 377–392. https://doi.org/10.1016/j.memsci.2018.12.003.

C. LIU, L. ZHU, L. Chen, Biofouling phenomenon of direct contact membrane distillation (DCMD) under two typical operating modes: Open-loop mode and closed-loop mode, Journal of Membrane Science. 601 (2020a) 117952. https://doi.org/10.1016/j.memsci.2020.117952.

C. LIU, L. ZHU, L. Chen, Effect of salt and metal accumulation on performance of membrane distillation system and microbial community succession in membrane biofilms, Water Research. 177 (2020b) 115805. https://doi.org/10.1016/j.watres.2020.115805.

C. LIU, L. ZHU, L. CHEN, Mechanism of biofilm formation on a hydrophobic polytetrafluoroethylene membrane during the purification of surface water using direct contact membrane distillation (DCMD), with especial interest in the feed properties, Biofouling. 36 (2020c) 14-31. https://doi.org/10.1080/08927014.2019.1710136.

C. MARCONNET, A. HOUARI, D. SEYER, M. DJAFER, G. CORITON, V. HEIM, P. DI MARTINO, Membrane biofouling control by UV irradiation, Desalination. 276 (2011) 75–81. https://doi.org/10.1016/j.desal.2011.03.016.

C. SCHIRALDI, M. DE ROSA, Mesophilic Organisms, in: Drioli E., Giorno L. (Eds.), Encyclopedia of Membranes, Springer, Berlin, Heidelberg, 2014. https://doi.org/10.1007/978-3-642-40872-4_1610-2.

C.F. COUTO, A.V. SANTOS, M.C.S. AMARAL, L.C. LANGE, L.H. DE ANDRADE, A.F.S. FOUREAUX, B.S. FERNANDES, Assessing potential of nanofiltration, reverse osmosis and membrane distillation drinking water treatment for pharmaceutically active compounds (PhACs) removal, Journal of Water Process Engineering. 33 (2020) 101029. https://doi.org/10.1016/j.jwpe.2019.101029.

C.-H. CHEN, Y. FU, D.-W. GAO, Membrane biofouling process correlated to the microbial community succession in an A/O MBR, Bioresource Technology. 197 (2015) 185–192. https://doi.org/10.1016/j.biortech.2015.08.092.

C.H. NAHM, K. KIM, S. MIN, H. LEE, D. CHAE, K. LEE, K.-H. CHOO, C.-K. LEE, I. KOYUNCU, P.-K. PARK, Quorum sensing: an emerging link between temperature and membrane biofouling in membrane bioreactors, Biofouling. 35 (2019) 443–453. https://doi.org/10.1080/08927014.2019.1611789.

C.V. MANALO, M. OHNO, S. NISHIMOTO, T. OKUDA, S. NAKAI, W. NISHIJIMA, Long-term pilot plant study using direct chlorination for biofouling control of a chlorine-resistant polyamide reverse osmosis membrane, Desalination and Water Treatment. 138 (2019) 57-67. https://doi.org/10.5004/dwt.2019.23319.

D. GONZÁLEZ, J. AMIGO, F. SUÁREZ, Membrane distillation: Perspectives for sustainable and improved desalination, Renewable and Sustainable Energy Reviews. 80 (2017) 238–259. https://doi.org/10.1016/j.rser.2017.05.078.

D. KIM, S. JUNG, J. SOHN, H. KIM, S. LEE, Biocide application for controlling biofouling of SWRO membranes — An overview, Desalination. 238 (2009) 43–52. https://doi.org/10.1016/j.desal.2008.01.034.

D. KWON, W. BAE, J. KIM, Hybrid forward osmosis/membrane distillation integrated with anaerobic fluidized bed bioreactor for advanced wastewater treatment, Journal of Hazardous Materials. 404 (2021) 124160. https://doi.org/10.1016/j.jhazmat.2020.124160.

D. SAEKI, Y. NAGASHIMA, I. SAWADA, H. MATSUYAMA, Effect of hydrophobicity of polymer materials used for water purification membranes on biofilm formation dynamics, Colloids Surfaces A: Physicochemical Engineering Aspects. 506 (2016) 622-628. https://doi.org/10.1016/j.colsurfa.2016.07.036.

D. WOLDEMARIAM, A. KULLAB, U. FORTKAMP, J. MAGNER, H. ROYEN, A. Martin, Membrane distillation pilot plant trials with pharmaceutical residues and energy demand analysis, Chemical Engineering Journal. 306 (2016) 471–483. https://doi.org/10.1016/j.cej.2016.07.082.

D.M. WARSINGER, A. SERVI, S. VAN BELLEGHEM, J. GONZALEZ, J. SWAMINATHAN, J. KHARRAZ, H.W. CHUNG, H.A. ARAFAT, K.K. GLEASON, J.H. LIENHARD V, Combining air recharging and membrane superhydrophobicity for fouling prevention in membrane distillation, Journal of Membrane Science. 505 (2016) 241–252. https://doi.org/10.1016/j.memsci.2016.01.018.

D.M. WARSINGER, J. SWAMINATHAN, E. GUILLEN-BURRIEZA, H.A. ARAFAT, J.H. LIENHARD V, Scaling and fouling in membrane distillation for desalination applications: A review, Desalination. 356 (2014) 294–313. https://doi.org/10.1016/j.desal.2014.06.031.

D.M. WARSINGER, J. V. GONZALEZ, S. M. VAN BELLEGHEM, A. SERVI, J. SWAMINATHAN, H.W. CHUNG, J.H. LIENHARD, The combined effect of air layers and membrane superhydrophobicity on biofouling in membrane distillation, Proceedings of the American Water Works Association Annual Conference and Exposition, Anaheim, CA, USA (2015).

E. ARCHER, B. PETRIE, B. KASPRZYK-HORDERN, G.M. WOLFAARDT, The fate of pharmaceuticals and personal care products (PPCPs), endocrine disrupting contaminants (EDCs), metabolites and illicit drugs in a WWTW and environmental waters, Chemosphere. 174 (2017) 437–446. https://doi.org/10.1016/j.chemosphere.2017.01.101.

E. BAR-ZEEV, I. BERMAN-FRANK, O. GIRSHEVITZ, T. BERMAN, Revised paradigm of aquatic biofilm formation facilitated by microgel transparent exopolymer particles, Proceedings of the National Academy of Sciences. 109 (2012) 9119–9124. https://doi.org/10.1073/pnas.1203708109.

E. BAR-ZEEV, U. PASSOW, S.R.-V. CASTRILLO, M. ELIMELECH, Transparent Exopolymer Particles: From Aquatic Environments and Engineered Systems to Membrane Biofouling, Environtal Science & Technology. 49 (2015) 691–707. https://doi.org/10.1021/es5041738.

E. DRIOLI, A. ALI, F. MACEDONIO, Membrane distillation: Recent developments and perspectives, Desalination. 356 (2015) 56–84. https://doi.org/10.1016/j.desal.2014.10.028.

E. DRIOLI, Y. WU, Membrane distillation: An experimental study, Desalination. 53 (1985) 339–346. https://doi.org/10.1016/0011-9164(85)85071-2.

E. GUILLEN-BURRIEZA, A. RUIZ-AGUIRRE, G. ZARAGOZA, H.A. ARAFAT, Membrane fouling and cleaning in long term plant-scale membrane distillation operations, Journal of Membrane Science. 468 (2014) 360–372. https://doi.org/10.1016/j.memsci.2014.05.064.

E. LYAUTEY, C.R. JACKSON, J. CAYROU, J.-L. ROLS, F. GARABÉTIAAN, Bacterial community succession in natural river biofilm Assemblages, Microbial Ecology. 50 (2005) 589–601. https://doi.org/10.1007/s00248-005-5032-9.

E.W. TOW, D.M. WARSINGER, A.M. TRUEWORTHY, J. SWAMINATHAN, G.P. THIEL, S.M. ZUBAIR, A.S. MYERSON, J.H.LIENHARD, Comparison of fouling propensity between

reverse osmosis, forward osmosis, and membrane distillation, Journal of Membrane Science. 556 (2018) 352–364. https://doi.org/10.1016/j.memsci.2018.03.065.

F. AHMED, B.S. LAILA, V. KOCHKODAN, N. HILAL, R. HASHAIKEH, Electrically conductive polymeric membranes for fouling prevention and detection: A review, Desalination. 391 (2016) 1–15. https://doi.org/10.1016/j.desal.2016.01.030.

F. MACEDONIO, E. DRIOLI, Chapter 5 - Membrane distillation development, in: C. M. Galanakis, E. Agrafioti (Eds.), Sustainable Water and Wastewater Processing, Elsevier, Amsterdam, 2019, 133-159. https://doi.org/10.1016/B978-0-12-816170-8.00005-3.

G. LI, L. LU, Modeling and performance analysis of a fully solar-powered stand-alone sweeping gas membrane distillation desalination system for island and coastal households, Energy Conversion. Management. 205 (2020) 112375. https://doi.org/10.1016/j.enconman.2019.112375.

G. MATAFONOVA, V. BATOEV, Recent advances in application of UV light-emitting diodes for degrading organic pollutants in water through advanced oxidation processes: A review, Water Research. 132 (2018) 177–189. https://doi.org/10.1016/j.watres.2017.12.079.

G. NAIDU, S. JEONG, S. VIGNESWARAN, T.-M. HWANG, Y.-J. CHOI, S.-H. KIM, A review on fouling of membrane distillation, Desalination and Water Treatment. 57 (2015) 10052–10076. https://doi.org/10.1080/19443994.2015.1040271.

G. ZARAGOZA, J.A. ANDRÉS-MAÑAS, A. Ruiz-Aguirre, Commercial scale membrane distillation for solar desalination, Npj Clean Water. 1 (2018) 20-25. https://doi.org/10.1038/s41545-018-0020-z.

G.C. KNIGHT, R.S. NICOL, T.A. MCMEEKIN, Temperature step changes: a novel approach to control biofilms of Streptococcus thermophilus in a pilot plant-scale cheese-milk pasteurisation plant, International Journal of Food Microbiology. 93 (2004) 305–318. https://doi.org/10.1016/j.ijfoodmicro.2003.11.013.

G.E. BATLEY, J.K. KIRBY, M.J. MCLAUGHLIN, Fate and risks of nanomaterials in aquatic and terrestrial environments, Accounts of Chemical Research. 46 (2013) 854–862. https://doi.org/10.1021/ar2003368.

G.W. MEINDERSMA, C.M. GUIJT, A.B. DE HAAN, Desalination and water recycling by air gap membrane distillation, Desalination. 187 (2006) 291–301. https://doi.org/10.1016/j.desal.2005.04.088.

H. ZHANG, R. LAMB, J. LEWIS, Engineering nanoscale roughness on hydrophobic surface — preliminary assessment of fouling behaviour, Science and Technology of Advanced Materials. 6 (2005) 236-239. https://doi.org/10.1016/j.stam.2005.03.003.

H.C. DUONG, P. COOPER, B. NELEMANS, T.Y. CATH, L.D. NGHIEM, Evaluating energy consumption of air gap membrane distillation for seawater desalination at pilot scale level, Separation and Purification Technology. 166 (2016) 55–62. https://doi.org/10.1016/j.seppur.2016.04.014.

H.-C. FLEMMING, J. WINGENDER, The biofilm matrix, Nature Reviews Microbiology. 8 (2010) 623–633. https://doi.org/10.1038/nrmicro2415.

J. GUO, D.Y.S. YAN, F.L.-Y. LAM, B.J. DEKA, X. LV, Y.H. NG, A.K. An, Self-cleaning BiOBr/Ag photocatalytic membrane for membrane regeneration under visible light in membrane distillation, Chemical Engineering Journal. 378 (2019) 122137. https://doi.org/10.1016/j.cej.2019.122137.

J. GUO, L. FORTUNATO, B.J. DEKA, S. JEONG, A.K. An, Elucidating the fouling mechanism in pharmaceutical wastewater treatment by membrane distillation, Desalination. 475 (2020) 114148. https://doi.org/10.1016/j.desal.2019.114148.

J. Guo, M.U. Farid, E.-J. Lee, D.Y.-S. Yan, S. Jeong, A.K. An, Fouling behavior of negatively charged PVDF membrane in membrane distillation for removal of antibiotics from wastewater, Journal of Membrane Science. 551 (2018) 12–19. https://doi.org/10.1016/j.memsci.2018.01.016.

J. KIM, M. SHIN, W. SONG, S. PARK, J. RYU, J. JUNG, S. CHOI, Y. YU, J. KWEON, J.-H. LEE, Application of quorum sensing inhibitors for improving anti-biofouling of polyamide reverse osmosis membranes: Direct injection versus surface modification, Separation and Purification Technology. 255 (2021) 117736. https://doi.org/10.1016/j.seppur.2020.117736.

J. MANSOURI, S. HARRISSON, V. CHEN, Strategies for controlling biofouling in membrane filtration systems: challenges and opportunities, Journal of Materials Chemistry. 20 (2010) 4567–4586. https://doi.org/10.1039/b926440j.

J.A. ANDRÉS-MAÑAS, A. RUIZ-AGUIRRE, F.G. ACIÉN, G. ZARAGOZA, Performance increase of membrane distillation pilot scale modules operating in vacuum-enhanced air-gap configuration, Desalination. 475 (2020) 114202. https://doi.org/10.1016/j.desal.2019.114202.

J.E. GONZÁLEZ, N.D. KESHAVAN, Messing with bacterial quorum sensing, Microbiology and Molecular Biology Reviews. 70 (2006) 859–875. https://doi.org/10.1128/MMBR.00002-06.

J.P. KIRKPATRICK, L.V. MCINTIRE, W.G. CHARACKLIS, Mass and heat transfer in a circular tube with biofouling, Water Research. 14 (1980) 117-127. https://doi.org/10.1016/0043-1354(80)90227-4.

J.S. BAKER, L.Y. DUDLEY, Biofouling in membrane systems - A review, Desalination. 118 (1998) 81–89. https://doi.org/10.1016/S0011-9164(98)00091-5.

J.S. VROUWENVELDER, D. VAN DER KOOIJ, Diagnosis, prediction and prevention of biofouling of NF and RO membranes, Desalination. 139 (2001) 65–71. https://doi.org/10.1016/S0011-9164(01)00295-8.

J.W. CHEW, W.B. KRANTZ, A.G. FANE, Effect of a macromolecular- or bio-fouling layer on membrane distillation, Journal of Membrane Science. 456 (2014) 66–76. https://doi.org/10.1016/j.memsci.2014.01.025.

K. BESEMER, Biodiversity, community structure and function of biofilms in stream ecosystems, Research in Microbiol. 166 (2015) 774–781. https://doi.org/10.1016/j.resmic.2015.05.006.

K. HORI, S. MATSUMOTO, Bacterial adhesion: From mechanism to control, Biochemical Engineering Journal. 48 (2010) 424–434. https://doi.org/10.1016/j.bej.2009.11.014.

K. MOPPER, J. ZHOU, K.S. RAMANA, U. PASSOW, H.G. DAMJ, D.T. DRAPEAUS, The role of surface-active carbohydrates in the flocculation of a diatom bloom in a mesocosm, Deep Sea Research Part II: Topical Studies in Oceanography. 42 (1995) 47–73. https://doi.org/10.1016/0967-0645(95)00004-A.

K. SONG, M. MOHSENI, F. TAGHIPOUR, Application of ultraviolet light-emitting diodes (UV-LEDs) for water disinfection: A review, Water Research. 94 (2016) 341–349. https://doi.org/10.1016/j.watres.2016.03.003.

K.J. LU, J. ZUO, J. CHANG, H.N. KUAN, T.-S. CHUNG, Omniphobic hollow-fiber membranes for vacuum membrane distillation, Environmental Science & Technology. 52 (2018) 4472–4480. https://doi.org/10.1021/acs.est.8b00766.

K.-J. LU, J. ZUO, T.-S. CHUNG, Tri-bore PVDF hollow fibers with a super-hydrophobic coating for membrane distillation, Journal of Membrane Science. 514 (2016) 165–175. https://doi.org/10.1016/j.memsci.2016.04.058.

K.-J. LU, Y. CHEN, T.-S. CHUNG, Design of omniphobic interfaces for membrane distillation - A review, Water Research. 162 (2019) 64–77. https://doi.org/10.1016/j.watres.2019.06.056.

K.R. ZODROW, E. BAR-ZEEV, M.J. GIANNETTO, M. ELIMELECH, Biofouling and Microbial Communities in Membrane Distillation and Reverse Osmosis, Environmental Science & Technology. 48 (2014) 13155–13164. https://doi.org/10.1021/es503051t.

K.W. LAWSON, D.R. LLOYD, Membrane distillation, Journal of Membrane Science 124 (1997) 1–25. https://doi.org/10.1016/S0376-7388(96)00236-0.

L. CHEN, Y. WANG, Z. CHEN, Z. CAI, The fouling layer development on MD membrane for water treatments: An especial focus on the biofouling progress, Chemosphere. 264 (2021) 128458. https://doi.org/10.1016/j.chemosphere.2020.128458.

L. EYKENS, I. HITSOV, K. DE SITTER, C. DOTREMONT, L. PINOY, B. VAN DER BRUGGEN, Direct contact and air gap membrane distillation: Differences and similarities between lab and pilot scale, Desalination. 422 (2017) 91–100. https://doi.org/10.1016/j.desal.2017.08.018.

L. EYKENS, K. DE SITTER, C. DOTREMONT, L. PINOY, B. VAN DER BRUGGEN, How to optimize the membrane properties for membrane distillation: A review, Industrial & Engineering Chemistry Research. 55 (2016) 9333–9343. https://doi.org/10.1021/acs.iecr.6b02226.

L. JIANG, L. CHEN, L. ZHU, Electrically conductive membranes for anti-biofouling in membrane distillation with two novel operation modes: Capacitor mode and resistor mode, Water Research. 161 (2019) 297–307. https://doi.org/10.1016/j.watres.2019.06.015.

L. JIANG, L. CHEN, L. ZHU, Fouling process of membrane distillation for seawater desalination: An especial focus on the thermal-effect and concentrating-effect during biofouling, Desalination. 485 (2020) 114457. https://doi.org/10.1016/j.desal.2020.114457.

L.A. DE WEGER, C.I. VAN DER VLUGT, A.H. WIJFJES, P.A. BAKKER, B. SCHIPPERS, B. LUGTENBERG, Flagella of a plant-growth-stimulating pseudomonas fluorescens strain are required for colonization of potato roots, Journal of Bacteriology. 169 (1987) 2769–2773. https://doi.org/10.1128/jb.169.6.2769-2773.1987.

L.D. TIJING, Y.C. WOO, J.-S. CHOI, S. LEE, S.-H. KIM, H. K. SHON, Fouling and its control in membrane distillation - A review, Journal of Membrane Science. 475 (2015) 215-244. https://doi.org/10.1016/j.memsci.2014.09.042.

L.F. MELO, T.R. BOTT, Biofouling in water systems, Experimental Thermal and Fluid Science. 14 (1997) 375–381. https://doi.org/10.1016/S0894-1777(96)00139-2.

L.M. CAMACHO, L. DUMÉE, J. ZHANG, J. LI, M. DUKE, J. GOMEZ, S. GRAY, Advances in membrane distillation for water desalination and purification applications, Water. 5 (2013) 94–196. https://doi.org/10.3390/w5010094.

L.N. NTHUNYA, L. GUTIERREZ, E.N. NXUMALO, A.R. VERLIEFDE, S.D. MHLANGA, M.S. ONYANGO, f-MWCNTs/AgNPs-coated superhydrophobic PVDF nanofibre membrane for organic, colloidal, and biofouling mitigation in direct contact membrane distillation, Journal of Environmental Chemical Engineering. 8 (2020) 103654. https://doi.org/10.1016/j.jece.2020.103654.

L.N. NTHUNYA, L. GUTIERREZ, L. LAPEIRE, K. VERBEKEN, N. ZAOURI, E.N. NXUMALO, B.B. MAMBA, A.R. VERLIEFDE, S.D. MHLANGA, Fouling-resistant PVDF nanofibre membranes for the desalination of brackish water in membrane distillation, Separation and Purification Technology. 228 (2019) 115793. https://doi.org/10.1016/j.seppur.2019.115793.

L.N. NTHUNYA, L. GUTIERREZ, N. KHUMALO, S. DERESE, B.B. MAMBA, A.R. VERLIEFDE, S.D. MHLANGA, Superhydrophobic PVDF nanofibre membranes coated with an organic fouling resistant hydrophilic active layer for direct-contact membrane distillation, Colloids and Surfaces A: Physicochemical and Engineering Aspects. 575 (2019) 363–372. https://doi.org/10.1016/j.colsurfa.2019.05.031.

L.N. WEI, C.Z. SHI, C.X. LUO, C.Y. HU, Y.H. MENG, Phloretin inhibits biofilm formation by affecting quorum sensing under different temperature, LWT. 131 (2020) 109668. https://doi.org/10.1016/j.lwt.2020.109668.

M. AL-ABRI, B. AL-GHAFRI, T. BORA, S. DOBRETSOV, J. DUTTA, S. CASTELLETTO, L. ROSA, A. BORETTI, Chlorination disadvantages and alternative routes for biofouling control in reverse osmosis desalination, Npj Clean Water. 2 (2019) 2. https://doi.org/10.1038/s41545-018-0024-8.

M. ESSALHI, M. KHAYET, 10 - Fundamentals of membrane distillation, in: A. Basile, A. Figoli, M. Khayet (Eds.), Pervaporation, Vapour Permeation and Membrane Distillation, Woodhead Publishing, Oxford, 2015, 277-316 https://doi.org/10.1016/B978-1-78242-246-4.00010-6.

M. ESSALHI, M. KHAYET, Self-sustained webs of polyvinylidene fluoride electrospun nano-fibers: Effects of polymer concentration and desalination by direct contact membrane distillation, Journal of Membrane Science. 454 (2014) 133–143. https://doi.org/10.1016/j.memsci.2013.11.056.

M. GRYTA, Calcium sulphate scaling in membrane distillation process, Chemical Papers. 63 (2009) 146–151. https://doi.org/10.2478/s11696-008-0095-y.

M. GRYTA, Effect of iron oxides scaling on the MD process performance, Desalination. 216 (2007) 88–102. https://doi.org/10.1016/j.desal.2007.01.002.

M. GRYTA, Fouling in direct contact membrane distillation process, Journal of Membrane Science. 325 (2008) 383–394. https://doi.org/10.1016/j.memsci.2008.08.001.

M. GRYTA, Long-term performance of membrane distillation process, Journal of Membrane Science. 265 (2005) 153–159. https://doi.org/10.1016/j.memsci.2005.04.049.

M. GRYTA, The assessment of microorganism growth in the membrane distillation system, Desalination. 142 (2002) 79–88. https://doi.org/10.1016/S0011-9164(01)00427-1.

M. HERMANSSON, The DLVO theory in microbial adhesion, Colloids Surfaces B: Biointerfaces. 14 (1999) 105–119. https://doi.org/10.1016/S0927-7765(99)00029-6.

M. KRIVOROT, A. KUSHMARO, Y. OREN, J. GILRON, Factors affecting biofilm formation and biofouling in membrane distillation of seawater, Journal of Membrane Science. 376 (2011) 15–24. https://doi.org/10.1016/j.memsci.2011.01.061.

M. LAQBAQBI, M.C. GARCÍA-PAYO, M. KHAYET, J. EL KHARRAZ, M. CHAOUCH, Application of direct contact membrane distillation for textile wastewater treatment and fouling study, Separation and Purification Technology. 209 (2019) 815–825. https://doi.org/10.1016/j.seppur.2018.09.031.

M. MARGULIES, M. EGHOLM, W.E. ALTMAN, S. ATTIYA, J.S. BADER, L.A. BEMBEN, J. BERKA, M.S. BRAVERMAN, Y.-J. CHEN, Z. CHEN, S.B. DEWELL, L. DU, J.M. FIERRO, X. V GOMES, B.C. GODWIN, W. HE, S. HELGESEN, C.H. HO, G.P. IRZYK, S.C. JANDO, M.L.I. ALENQUER, T.P. JARVIE, K.B. JIRAGE, J.-B. KIM, J.R. KNIGHT, J.R. LANZA, J.H. LEAMON, S.M. LEFKOWITZ, M. LEI, J. LI, K.L. LOHMAN, H. LU, V.B. MAKHIJANI, K.E. MCDADE, M.P. MCKENNA, E.W. MYERS, E. NICKERSON, J.R. NOBILE, R. PLANT, B.P. PUC, M.T. RONAN, G.T. ROTH, G.J. SARKIS, J.F. SIMONS, J.W. SIMPSON, M. SRINIVASAN, K.R. TARTARO, A. TOMASZ, K.A. VOGT, G.A. VOLKMER, S.H. WANG, Y. WANG, M.P. WEINER, P. YU, R.F. BEGLEY, J.M. ROTHBERG, Genome sequencing in microfabricated high-density picolitre reactors, Nature. 437 (2005) 376–380. https://doi.org/10.1038/nature03959.

M. PASMORE, P. TODD, B. PFIEFER, M. RHODES, C.N. BOWMAN, Effect of Polymer Surface Properties on the Reversibility of Attachment of Pseudomonas aeruginosa in the Early Stages of Biofilm Development, Biofouling. 18 (2002) 65-71. https://doi.org/10.1080/08927010290017743.

M. REZAEI, D.M. WARSINGER, J.H. LIENHARD V, M.C. DUKE, T. MATSUURA, W.M. SAMHABER, Wetting phenomena in membrane distillation: Mechanisms, reversal, and prevention, Water Research. 139 (2018) 329-352. https://doi.org/10.1016/j.watres.2018.03.058.

M.A. HAMMAMI, J.G. CROISSANT, L. FRANCIS, S.K. ALSAIARI, D.H. ANJUM, N. GHA, N.M. KHASHAB, Engineering hydrophobic organosilica nanoparticle-doped nanofibers for enhanced and fouling resistant membrane distillation, ACS Applied Materials & Interfaces. 9 (2017) 1737–1745. https://doi.org/10.1021/acsami.6b11167.

M.A. SHANNON, P.W. BOHN, M. ELIMELECH, J.G. GEORGIADIS, B.J. MARIN, A.M. MAYES, Science and technology for water purification in the coming decades, Nature. 452 (2008) 301–310. https://doi.org/10.1038/nature06599.

M.C. VAN LOOSDRECHT, J. LYKLEMA, W. NORDE, G. SCHRAA, A.J. ZEHNDER, The role of bacterial cell wall hydrophobicity in adhesion, Applied Environmental Microbiology. 53 (1987) 1893–1897. https://doi.org/10.1128/AEM.53.8.1893-1897.1987

M.E. FINDELY, Vaporization through porous membranes, Industrial & Engineering Chemistry Process Design and Development. 6 (1967) 226–230. https://doi.org/10.1021/i260022a013.

M.J. VIEIRA, L.F. MELO, M.M. PINHEIRO, Biofilm formation: Hydrodynamic effects on internal diffusion and structure, Biofouling. 7 (1993) 67–80. https://doi.org/10.1080/08927019309386244.

M.M.A. SHIRAZI, A. KARGARI, A.F. ISMAIL, T. MATSUURA, Computational Fluid Dynamic (CFD) opportunities applied to the membrane distillation process: State-of-the-art and perspectives, Desalination. 377 (2016) 73–90. https://doi.org/10.1016/j.desal.2015.09.010.

M.O. BARBOSA, N.F.F. MOREIRA, A.R. RIBEIRO, M.F.R. PEREIRA, A.M.T. SILVA, Occurrence and removal of organic micropollutants: An overview of the watch list of EU Decision 2015/495, Water Research. 94 (2016) 257–279. https://doi.org/10.1016/j.watres.2016.02.047.

M.R. CHOUDHURY, N. ANWAR, D. JASSBY, M.S. RAHAMAN, Fouling and wetting in the membrane distillation driven wastewater reclamation process – A review, Advances in Colloid and Interface Science. 269 (2019) 370–399. https://doi.org/10.1016/j.cis.2019.04.008.

N. DIZGE, E. SHAULSKY, V. KARANIKOLA, Electrospun cellulose nanofibers for superhydrophobic and oleophobic membranes, Journal of Membrane Science. 590 (2019) 117271. https://doi.org/10.1016/j.memsci.2019.117271.

N. DOW, J.V. GARCÍA, L. NIADOO, N. MILNE, J. ZHANG, S. GRAY, M. DUKE, Demonstration of membrane distillation on textile waste water: assessment of long term performance, membrane cleaning and waste heat integration, Environmental Science: Water Research & Technology. 3 (2017) 433–449. https://doi.org/10.1039/c6ew00290k.

N.A. WEERASEKARA, K.-H. CHOO, C.-H. LEE, Biofouling control: Bacterial quorum quenching versus chlorination in membrane bioreactors, Water Research. 103 (2016) 293–301. https://doi.org/10.1016/j.watres.2016.07.049.

N.G.P. CHEW, Y. ZHANG, K. GOH, J.S. HO, R. XU, R. WANG, Hierarchically structured Janus membrane surfaces for enhanced membrane distillation performance, ACS Appled Materials & Interfaces. 11 (2019) 25524–25534. https://doi.org/10.1021/acsami.9b05967.

N.P. IVLEVA, P. KUBRYK, R. NIESSNER. Raman microspectroscopy, surface-enhanced Raman scattering microspectroscopy, and stable-isotope Raman microspectroscopy for biofilm characterization. Analytical and bioanalytical chemistry, 409(18) (2017) 4353-4375.

N.R. MADDELA, B. SHENG, S. YUAN, Z. ZHOU, R. VILLAMAR-TORRES, F. MENG, Roles of quorum sensing in biological wastewater treatment: A critical review, Chemosphere. 221 (2019) 616–629. https://doi.org/10.1016/j.chemosphere.2019.01.064.

O. HABIMANA, A.J.C. CORREIA-SEMIÃO, E. CASEY, The role of cell-surface interactions in bacterial initial adhesion and consequent biofilm formation of nanofiltration/reverse osmosis membranes Journal of Membrane Science. 454 (2014) 82–96. https://doi.org/10.1016/j.memsci.2013.11.043.

P. Biniaz, N.T. Ardekani, M.A. Makarem, M.R. Rahimpour, Water and wastewater treatment systems by novel integrated membrane distillation (MD), ChemEngineering. 3 (2019) 8. https://doi.org/10.3390/chemengineering3010008.

P. ZHANG, P. KNÖTIG, S. GRAY, M. DUKE, Scale reduction and cleaning techniques during direct contact membrane distillation of seawater reverse osmosis brine, Desalination. 374 (2015) 20–30. https://doi.org/10.1016/j.desal.2015.07.005.

P.S. GOH, A.K. ZULHAIRUN, A.F. ISMAIL, N. HILAL, Contemporary antibiofouling modifications of reverse osmosis desalination membrane: A review, Desalination. 468 (2019) 114072. https://doi.org/10.1016/j.desal.2019.114072.

R. P. SCHWARZENBACH, B. I. ESCHER, K. FENNER, T. B. HOFSTETTER, C. A. JOHNSON, U. VON GUNTEN, B. WEHRLI, The challenge of micropollutants in aquatic systems, Science. 313 (2006) 1072–1077. https://doi.org/10.1126/science.1127291.

R. Wang, D. Liang, X. Liu, W. Fan, S. Meng, W. Cai, Effect of magnesium ion on polysaccharide fouling, Chemical Engineering Journal. 379 (2020) 122351. https://doi.org/10.1016/j.cej.2019.122351.

S. DOBRETSOV, M. TEPLITSKI, M. BAYER, S. GUNASEKERA, P. PROKSCH, V.J. PAUL, Inhibition of marine biofouling by bacterial quorum sensing inhibitors, Biofouling. 27 (2011) 893-905. https://doi.org/10.1080/08927014.2011.609616.

S. DOBRETSOV, M. TEPLITSKI, V. PAUL, Mini-review: quorum sensing in the marine environment and its relationship to biofouling, Biofouling. 25 (2009) 413-427. https://doi.org/10.1080/08927010902853516.

S. GOH, J. ZHANG, Y. LIU, A.G. FANE, Fouling and wetting in membrane distillation (MD) and MD-bioreactor (MDBR) for wastewater reclamation, Desalination. 323 (2013) 39–47. https://doi.org/10.1016/j.desal.2012.12.001.

S. GOH, Q. ZHANG, J. ZHANG, D. MCDOUGALD, W.B. KRANTZ, Y. LIU, A.G. FANE, Impact of a biofouling layer on the vapor pressure driving force and performance of a membrane distillation process, Journal of Membrane Science. 438 (2013) 140–152. https://doi.org/10.1016/j.memsci.2013.03.023.

S. KALLA, S. UPADHYAYA, K. SINGH, Principles and advancements of air gap membrane distillation, Reviews in Chemical Engineering. 35 (2019) 817–859. https://doi.org/10.1515/revce-2017-0112.

S. LEAPER, A. ABDEL-KARIM, T.A. GAD-ALLAH, P. GORGOJO, Air-gap membrane distillation as a one-step process for textile wastewater treatment, Chemical Engineering Journal. 360 (2019) 1330–1340. https://doi.org/10.1016/j.cej.2018.10.209.

S. LEE, K. LEE, W.M. WAN, Y. CHOI, Comparison of membrane permeability and a fouling mechanism by pre-ozonation followed by membrane filtration and residual ozone in membrane cells, Desalination. 178 (2005) 287–294. https://doi.org/10.1016/j.desal.2004.11.040.

S. MENG, Y. LIU, Transparent exopolymer particles (TEP)-associated membrane fouling at different Na+ concentrations, Water Research. 111 (2017) 52–58. https://doi.org/10.1016/j.watres.2016.12.044.

S. SRISURICHAN, R. JIRARATANANON, A.G. FANE, Mass transfer mechanisms and transport resistances in direct contact membrane distillation process, Journal of Membrane Science. 277 (2006) 186–194. https://doi.org/10.1016/j.memsci.2005.10.028.

S. SUDHAKARAN, S. K. MAENG, G. AMY, Hybridization of natural systems with advanced treatment processes for organic micropollutant removals: New concepts in multi-barrier treatment, Chemosphere. 92 (2013) 731–737. https://doi.org/10.1016/j.chemosphere.2013.04.021.

S. WOODCOCK, W.T. SLOAN, Biofilm community succession: a neutral perspective, Microbiology. 163 (2017) 664–668. https://doi.org/10.1099/mic.0.000472.

S. ZOU, Y.-N. WANG, F. WICAKSANA, T. AUNG, P. CHUEN, Y. WONG, A.G. FANE, C.Y. TANG, Direct microscopic observation of forward osmosis membrane fouling by microalgae: Critical flux and the role of operational conditions, Journal of Membrane Science. 436 (2013) 174–185. https://doi.org/10.1016/j.memsci.2013.02.030.

S.B. SADR GHAYENI, P.J. BEATSON, R.P. SCHNEIDER, A.G. FANE, Adhesion of waste water bacteria to reverse osmosis membranes, Journal of Membrane Science. 138 (1998) 29–42. https://doi.org/10.1016/S0376-7388(97)00196-8.

S.-I. ANDERSSON, N. KJELLANDER, B. RODESJO, Design and field tests of a new membrane distillation desalination process, Desalination. 56 (1985) 345–354. https://doi.org/10.1016/0011-9164(85)85037-2.

S.S. RAY, R. DANGAYACH, Y.-N. KWON, Surface engineering for anti-wetting and antibacterial membrane for enhanced and fouling resistant membrane distillation performance, Chemical Engineering Journal. 405 (2021) 126702. https://doi.org/10.1016/j.cej.2020.126702.

T. HARIF, H. ELIFANTZ, E. MARGALIT, M. HERZBERG, T. LICHI, D. MINZ, The effect of UV pre-treatment on biofouling of BWRO membranes: A field study, Desalination and Water Treatment. 31 (2011) 151–163. https://doi.org/10.5004/dwt.2011.2377.

T. NGUYEN, F.A. RODDICK, L. FAN, Biofouling of water treatment membranes: A review of the underlying causes, monitoring techniques and control measures, Membranes. 2 (2012) 804–840. https://doi.org/10.3390/membranes2040804.

T. TERNES, A. JOSS, J. OEHLMANN, Occurrence, fate, removal and assessment of emerging contaminants in water in the water cycle (from wastewater to drinking water), Water Research. 72 (2015) 1–2. https://doi.org/10.1016/j.watres.2015.02.055.

T.-H KHAING, J. LI, Y. LI, N. WAI, F. WONG, Feasibility study on petrochemical wastewater treatment and reuse using a novel submerged membrane distillation bioreactor, Separation and Purification Technology. 74 (2010) 138–143. https://doi.org/10.1016/j.seppur.2010.05.016.

T.R. GARRET, M. BHAKOO, Z. ZHANG, Bacterial adhesion and biofilms on surfaces, Progress in Natural Science. 18 (2008) 1049–1056. https://doi.org/10.1016/j.pnsc.2008.04.001.

U. PASSOW, Transparent exopolymer particles (TEP) in aquatic environments, Progress in Oceanography. 55 (2002) 287–333. https://doi.org/10.1016/S0079-6611(02)00138-6.

V. LUND, K. ORMEROD, The influence of disinfection processes on biofilm formation in water distribution systems, Water Research. 29 (1995) 1013–1021. https://doi.org/10.1016/0043-1354(94)00280-K.

V. NAGARAJ, L. SKILLMAN, D. LI, G. HO, Review – Bacteria and their extracellular polymeric substances causing biofouling on seawater reverse osmosis desalination membranes, Journal of Environmental Management. 223 (2018) 586–599. https://doi.org/10.1016/j.jenvman.2018.05.088.

W. LI, Y. CHEN, L. YAO, X. REN, Y. LI, L. DENG, Fe3O4/PVDF-HFP photothermal membrane with in-situ heating for sustainable, stable and efficient pilot-scale solar-driven membrane distillation, Desalination. 478 (2020) 114288. https://doi.org/10.1016/j.desal.2019.114288.

W. LUO, H.V. PHAN, G. LI, F.I. HAI, W. E. PRICE, M. ELIMELECH, L.D. NGHIEM, An Osmotic Membrane Bioreactor − Membrane Distillation System for Simultaneous Wastewater Reuse and Seawater Desalination: Performance and Implications, Environmental Science & Technology. 51 (2017) 14311–14320. https://doi.org/10.1021/acs.est.7b02567.

W. MA, Y. DING, M. ZHANG, S. GAO, Y. LI, C. HUANG, G. FU, Nature-inspired chemistry toward hierarchical superhydrophobic, antibacterial and biocompatible nanofibrous membranes for effective UV-shielding, self-cleaning and oil-water separation, Journal of Hazardous Materials. 384 (2020) 121476. https://doi.org/10.1016/j.jhazmat.2019.121476.

W. M. EDGAR. Studies of the role of calcium in plaque formation and cohesion. Journal of dentistry, 7(2) (1979) 174-179. https://doi.org/10.1016/0300-5712(79)90014-9.

W. QIN, Z. XIE, D. NG, Y. YE, X. JI, S. GRAY, J. ZHANG, Comparison of colloidal silica involved fouling behavior in three membrane distillation configurations using PTFE membrane, Water Research. 130 (2018) 343–352. https://doi.org/10.1016/j.watres.2017.12.002.

W. SUWAILEH, D. JOHNSON, D. JONES, N. HILAL, An integrated fertilizer driven forward osmosis- renewables powered membrane distillation system for brackish water desalination: A combined experimental and theoretical approach, Desalination. 471 (2019) 114126. https://doi.org/10.1016/j.desal.2019.114126.

W. WANG, X. DU, H. VAHABI, S. ZHAO, Y. YIN, A.K. KOTA, T. TONG, Trade-off in membrane distillation with monolithic omniphobic membranes, Nature Communications. 10 (2019) 3220. https://doi.org/10.1038/s41467-019-11209-6.

W. YU, D. ZHANG, N.J.D. Graham, Membrane fouling by extracellular polymeric substances after ozone pre-treatment: Variation of nano-particles size, Water Research. 120 (2017) 146–155. https://doi.org/10.1016/j.watres.2017.04.080.

W.G. CHARACKLIS, J.D. BRYERS, Fouling biofilm development : A process analysis, Biotechnology and. Bioengineering. 102 (2009) 309–347. https://doi.org/10.1002/bit.22227.

W.G. CHARCKLIS, K.E. COOKSEY, Biofilms and microbial fouling, Advances in Applied Microbiology. 29 (1983) 93-138. https://doi.org/10.1016/S0065-2164(08)70355-1.

World Health Organization (WHO), United Nations Children's Fund (UNICEF), Progress on Drinking Water, Sanitation and Hygiene: 2017 Update and SDG Baselines, Geneva (2017).

W.J. LEE, Z.C. NG, S.K. HUBADILLAH, P.S. GOH, W.J. LAU, M.H.D. OTHMAN, A.F. ISMAIL, N. HILAL, Fouling mitigation in forward osmosis and membrane distillation for desalination, Desalination 480 (2020) 114338. https://doi.org/10.1016/j.desal.2020.114338.

W.M. DUNNE, Bacterial adhesion: Seen any good biofilms lately?, Clinical Microbiology Reviews. 15 (2002) 155–166. https://doi.org/10.1128/CMR.15.2.155-166.2002.

X. AN, Y. HU, N. WANG, Z. ZHOU, Z. LIU, Continuous juice concentration by integrating forward osmosis with membrane distillation using potassium sorbate preservative as a draw solute, Journal of Membrane Science. 573 (2019) 192–199. https://doi.org/10.1016/j.memsci.2018.12.010.

X. LI, Y. ZHANG, J. CAO, X. WANG, Z. CUI, S. ZHOU, M. LI, E. DRIOLI, Z. WANG, S. ZHAO, Enhanced fouling and wetting resistance of composite Hyflon AD / poly(vinylidene fluoride) membrane in vacuum membrane distillation, Separation and Purification Technology. 211 (2019) 135–140. https://doi.org/10.1016/j.seppur.2018.09.071.

Y. GU, J. HUANG, G. ZENG, Y. SHI, Y. HU, B. TANG, J. ZHOUA, W. XU, L. SHI, Quorum quenching activity of indigenous quorum quenching bacteria and its potential application in mitigation of membrane biofouling, Journal of Chemical Technology & Biotechnology. 93 (2018) 1394–1400. https://doi.org/10.1002/jctb.5507.

Y. XIONG, Y. LIU, Biological control of microbial attachment: a promising alternative for mitigating membrane biofouling, Applied Microbiology Biotechnology. 86 (2010) 825–837. https://doi.org/10.1007/s00253-010-2463-0.

Y. XU, J. MA, D. LIU, H. XU, F. CUI, W. WANG, Origami system for efficient solar driven distillation in emergency water supply, Chemical Engineering Journal. 356 (2019) 869–876. https://doi.org/10.1016/j.cej.2018.09.070.

Y. ZHANG, P. ZHAO, J. LI, D. HOU, J. WANG, H. LIU, A hybrid process combining homogeneous catalytic ozonation and membrane distillation for wastewater treatment, Chemosphere. 160 (2016) 134–140. https://doi.org/10.1016/j.chemosphere.2016.06.070.

Y.N. SLAVIN, J. ASNIS, U.O. HÄFELI, H. BACH, Metal nanoparticles: understanding the mechanisms behind antibacterial activity, Journal of Nanobiotechnology. 15 (2017) 65. https://doi.org/10.1186/s12951-017-0308-z.

Z. WANG, S. LIN, Membrane fouling and wetting in membrane distillation and their mitigation by novel membranes with special wettability, Water Research. 112 (2017) 38–47. https://doi.org/10.1016/j.watres.2017.01.022.

Z. ZHANG, M. CHEN, J. LI, B. ZHAO, L. WANG, Significance of transparent exopolymer particles derived from aquatic algae in membrane fouling, Arabian Journal of Chemistry. 13 (2020) 4577–4585. https://doi.org/10.1016/j.arabjc.2019.10.004.

Z.D. HENDREN, J. BRANT, M.R. WIESNER, Surface modification of nanostructured ceramic membranes for direct contact membrane distillation, Journal of Membrane Science. 331 (2009) 1–10. https://doi.org/10.1016/j.memsci.2008.11.038.

Z.-Q. DONG, X.-H. MA, Z.-L. XU, Z.-Y. GU, Superhydrophobic modification of PVDF-SiO2 electrospun nanofiber membranes for vacuum membrane distillation, RSC Advances. 5 (2015) 67962-67970. https://doi.org/10.1039/C5RA10575G.

CHAPTER 5

Final Considerations

1 DISSERTATION OVERVIEW, MAIN CONCLUSIONS, AND RECOMMENDATIONS

This study developed and evaluated the performance of a new hybrid module for membrane distillation with UV irradiation by a LED-UV, whose main objective is the mitigation of membrane fouling. Chapter 2 presented the evaluation of the performance of the hybrid MD-LED-UV module in the post-treatment of wastewater from anaerobic treatment. The hybrid system suffered a more abrupt drop in flux, this was attributed to changes in organic matter characteristics, which led to pore blockage. A lower initial removal of COD in the hybrid system corroborates the formation of volatile products through photolysis. However, the instantaneous removal of COD increased until reaching values close to that of MD. However, considering other parameters, the performance of both tests was very similar.

It was possible to verify the lesser extent of fouling in the MD-LED-UV compared to MD tests. The fouling formed in the hybrid system had a greater hydrophilic character and a lower concentration of proteins composing the SMP/EPS, being less adhered to the membrane surface and easily removed mechanically. The antifouling action of a higher turbulence condition in MD modules was also evidenced.

In chapter 3, the slighter removal of COD during the LED test raised questions about whether the hybrid system may perform worse, allowing the permeation of pollutants, such as micropollutants, or whether the results found are due to the matrix rich in organic matter (and its degradation by photolysis) and microorganisms. Thus, chapter 3 brought the comparative study of the MD and the MD-LED-UV system performance in removing EE2. Although membrane surface degradation was observed, similar performance was observed in the two systems in terms of flux, conductivity, temperatures, polarization, and EE2 removal. Above 99% for both systems, the estrogenic effect removals prove the hybrid system's efficiency. Since the performance was not impaired by the coupling of LED-UV and MD in a non-turbid matrix and without forming a fouling layer, together with the removal of conductivity and other parameters evaluated in the wastewater tests, the lower MD-KED-UV rejection to COD needs to be further investigated.

In chapter 4, there is a comprehensive review of biofouling in MD, which clarifies that the high MD temperatures lead to microbial community succession, and these selected bacteria can

colonize the membrane surface. Besides, the high temperature and concentration in MD concentrate do not prevent biofouling during long-term operation. Although biofilms are composed of fewer living microorganisms in these conditions, the stress of the bacterial community leads to more cell lysis and, consequently releases more intracellular products, which can lead to more severe fouling and scaling. Thus, it opens the horizon for studies concerning biofilm mitigation in MD and demonstrates that it is worth deeply evaluating the hybrid module developed to mitigate biofouling. Accordingly, the coupling with LED can be promising when tartar feed with greater fouling potential, like post-treatment of secondary wastewater from anaerobic treatment.

Therefore, for future studies, it is recommended:

- to evaluate the formation of volatile by-products through photolysis in the hybrid system;

- to assess the toxicity of the currents after irradiation;

- to carry out the genetic sequencing of the microorganisms found in the biofouling MD in order to understand the effect of radiation on the bacterial community;

- to optimize the dose of UV radiation so that with the lowest energy expenditure, better performance and mitigation of the biofilm are obtained simultaneously;

- to conduct a test turning the LED on only after the fouling layer is established;

- to perform tests for a long time and temporarily collect samples from the membrane to understand how UV changes the dynamics of biofouling formation.

- to perform the recovery of ammonia and integrate the process with renewable energy sources to obtain an economically and environmentally attractive operation.